FACHHOCHSCHUL - MASTERSTUDIENGANG

AUTOMATISIERUNGSTECHNIK

A Cost Effective Battery Sizing Strategy for Residential PV Systems using a Physical Battery Lifetime Model in a High Penetration Environment

submitted as a Master Thesis

to obtain the academic degree

Master of Science in Engineering

by

Andreas AICHHORN

December 2011

Assistance of the Master Thesis by

Prof.(FH) DI. Dr. Peter Zeller (Fachhochschule Wels)
Dr. Hui Li, M.S. B.E.E. (Florida State University)

Contents

Acknowledgment

I want to show my gratitude to my adviser, Dr. Peter Zeller, at my home university, the Upper Austria University of Applied Sciences / Campus Wels, for initiating contact to the Center for Advanced Power Systems and the support during my research.

I am also deeply grateful to Dr. Steinar Dale, the Director of the Center for Advanced Power Systems at Florida State University, where I did the research for this Master Thesis, for the excellent opportunity to conduct research with this department. I also want to show my gratitude to my adviser from the Florida State University, Dr. Hui Li, for the guidance during my stay. I wish to express my warm and sincere thanks to my colleagues Yan Zhou and Michael Greenleaf for their collaboration. I also want to thank the rest of my group at the Center for Advanced Power Systems.

Further, I want to thank the Austrian Marshallplan Foundation as I did the research for this Master Thesis as a scholar from the Austrian Marshallplan Foundation.

To my parents, Jutta Maria and Rudolf Kurt, I owe my deepest gratitude for their dedication and support during my undergraduate and graduate studies that provided me the foundation for my career.

I also want to express my deepest gratefulness to Allyssa Kilanowski for her support and sympathy during my work on this thesis.

This work is supported by National Science Foundation under Grant ECCS-1001415.

Campus Wels

I hereby declare that this thesis is the result and sole effort of original research, without any outside assistance. No additional sources of information were used other than those expressly cited herein, and the work in hand corresponds with that submitted for approval by my thesis advisor.
I certify that the work presented in this thesis has not been submitted, either in whole or in part, for a degree at this or any other university or published in any form.

.....
Andreas Aichhorn

Wels, 01.12.2011

Kurzfassung

Die Anzahl an privaten Photovoltaik (PV) Anlagen steigt stetig. Ein wichtiger Aspekt dieser Anlagen ist, dass diese durch den stetigen Zuwachs die Netzspannung und dadurch auch die Netzqualität durch Umwelteinflüsse negativ beeinflussen können. Wenn kein Energiemanagement System in einem Haushalt mit PV Anlage realisiert ist, speist diese Anlage überschüssige Energie ins Netz ein. Bei zunehmender Anzahl dieser Anlagen in der gleichen Region, kann dies beispielsweise um die Mittagszeit zu Spannungserhöhungen im Energienetz führen. Bei wolkigen Wetterbedingungen kann sich die erzeugte Leistung durchaus im Minutenbereich von der Spitzenleistung auf null Watt ändern. Im schlimmsten Fall trifft diese Situation auf alle PV Anlagen in der gleichen Region zu, z.B. verursacht durch eine großflächige Bewölkung, und die Energie für die Endverbraucher, die im Normalfall von der PV Anlage bezogen wird, muss dann vom Energienetz bereitgestellt werden was die Netzspannung und somit auch die Netzqualität beeinflussen kann. Diese Arbeit beschäftigt sich mit PV Anlagen, die zusätzlich einen Batterie beinhalten um einerseits den Einfluss der Photovoltaik Anlagen aufgrund von Umwelteinflüssen auf das Energienetz zu reduzieren und man sich andererseits als Netzverbraucher mit einer PV Anlage unabhängiger vom Energiemarkt machen kann. In dieser Diplomarbeit wird die Profitabilität einer Batterie in Kombination mit einer PV Anlage berechnet, basierend auf zwei unterschiedlichen Abrechnungssystemen der Energieversorgungsunternehmen, Time of Use und Real Time Pricing. Der verwendete Batterietyp für die Berechnung ist eine LiFePO4 Batterie. Die Berechnung zielt auf die optimale Wirtschaftlichkeit des Gesamtsystems wobei die Batteriegröße (Kapazität und maximale Lade- / Entladeleistung) die veränderliche Variable in dem Berechnungssystem ist. Mit Real Time Pricing wurde keine finanzielle Ersparnis durch die Batterie erreicht, wohingegen mit Time of Use ein positiver Profit erzielt werden kann.

Abstract

The number of residential photovoltaic (PV) systems is increasing steadily. An important aspect of these systems is that with a rising penetration level the grid voltage can be influenced which also affects the power quality due to environmental conditions. If no energy management system in a household in combination with a PV system is implemented then this system feeds the surplus power into the grid. A rise in the penetration level of PV systems in the same region may cause for example an increase in the line voltage without using an energy management system. In cloudy weather conditions, the power generated may change in the minute range of the peak power down to zero watts. In the worst case, this situation applies to all PV systems in the same region, e.g. caused by a large cloud, and the energy for the end user, which is normally obtained by the PV system, has then to be provided by the energy grid which may effect the line voltage and therefore the grid quality. This work deals with PV systems, which include an additional battery to reduce the influence of PV systems due to environmental influences on the energy grid and to be more independent as a consumer from the electrical energy price development. In this thesis, the profitability of a battery in combination with a PV system is calculated based on two different utility rating systems a time of use and real time pricing. The battery type used in this study is a LiFePO4 battery. The calculation result outputs the most cost effective battery size (capacity and maximum charge / discharge power). With the real time pricing utility rate, no positive profit was achieved using the battery, whereas applying the time of use rate, a positive profit was achieved.

Chapter 1

Introduction

The electrical energy demand is growing year by year. Figure 1.1 shows the development of the energy consumption from 1949 to 2009, classified by the end-use sector.

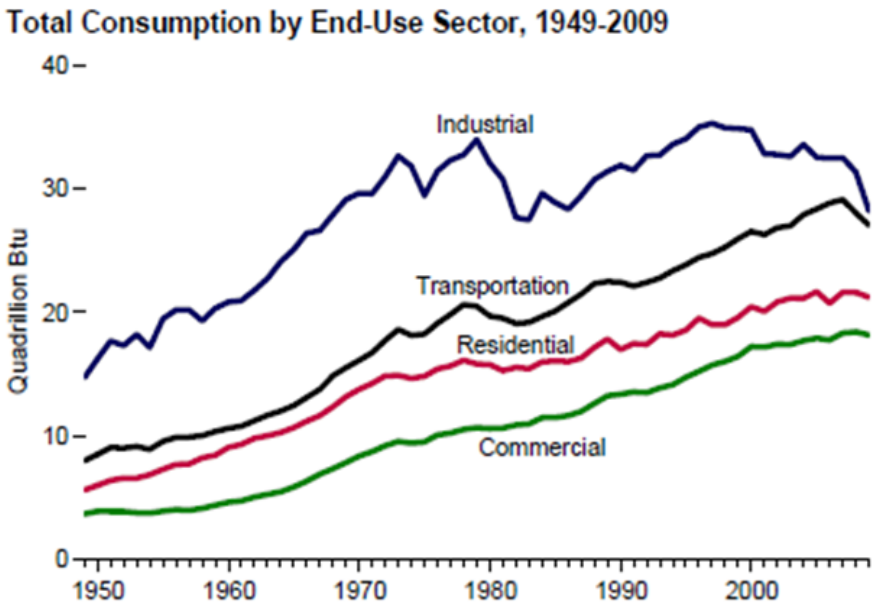

Figure 1.1: Energy consumption development, divided by end-use sector [1]

In the last 20 years, the industrial demand has been decreasing. However, the residential, commercial, and transportation sectors have been rising since this time. Approaches to meet the rising energy demand are either to install extra power plants or to reduce the demand by energy efficiency methods. The extra power plants can be centralized or distributed realized, centralized with high power generating plants

or distributed directly at the consumer. In order to reduce the complexity of this work, only distributed renewable energy systems should be considered. Common renewable energy sources for this application would be photovoltaic (PV) systems or wind turbines. This work considers just PV systems as distributed renewable energy sources (DRES) as it is found in most of the literature [3, 6, 7] and it is more practical to install it at a residential house. In addition to global considerations, other benefits can be gained out of the system like independence from the energy market. Figure 1.2 shows the development of the electricity price since 1973. It is clearly visible that the price is rising steadily. By installing of PV systems as DRES, the consumer gained more independence from the market price as most of the used energy is produced with the PV cell.

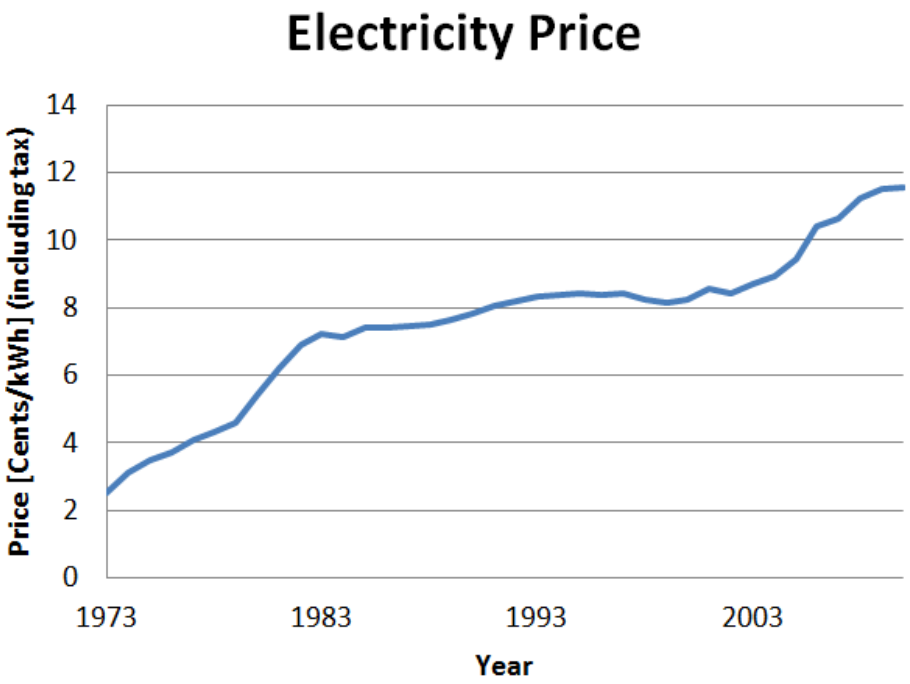

Figure 1.2: Electricity price development [22]

It has to be considered that the output power of photovoltaic systems is influenced by environmental factors. Equation 1.1 [6] shows the output power as a function of the irradiation of the sun and the air temperature.

$$P_{PV} = (-0.006825\, T_{ambient} + 1.171)\, P_{incl}\, P_{fc} \frac{P_{global}}{P_{isoref}}\, P_{max\,ref} \tag{1.1}$$

$T_{ambient}$ ... surrounding air temperature of the PV cell [°C]

P_{incl} ... inclination correction; a value between 0 and 1

P_{fc} ... longitudinal correction; a value between 0 and 1

P_{global} ... global solar irradiation $\left[\frac{W}{m^2}\right]$

$P_{ref\,iso}$ ... reference solar irradiation $\left[1000\,\frac{W}{m^2}\right]$

$P_{ref\,max}$ ... maximum output power of the PV array at $1,000\,\frac{W}{m^2}$ and 25 °C

A variation in the irradiation influences the grid as the PV generator's output power is changing. In situations with a low power output from the DRES, the grid has to provide the necessary energy for the consumer loads. If the PV power exceeds the consumer demand, the PV power will be fed into the grid.

In principle, there are two different irradiation changes, fast and slow. A fast change can be caused by changing cloud situations, where the output power drops in a time range of some 10 seconds. The slow change is caused by a position change of the sun. Figure 1.3, 1.4 and 1.5 shows the output power for different irradiation scenarios. The output power profiles of Figure 1.3 to Figure 1.5 originate from the same photovoltaic system on the same location but the seasons are different which is the reason for the different peak power values. Figure 1.3 is a day in March, whereas Figures 1.4 and 1.5 are power profiles from May. In the case of Figure 1.6 it is a day in January. The ideal conditions are full sun during the day (Figure 1.3). On sunny days with intermittent clouds it is possible for the output power of the PV to decrease from nominal power to almost 0 Watt in a very short time (Figure 1.4), which influences the line voltage through a change in the direction of the power flow. Changing power flow directions and power fluctuations caused by changing irradiation situations cause changing voltage drops on the power line. Consequently, in situations of low grid integration serious problems with a varying line voltage may occur. Therefore, a throughout cloudy day as it is shown in Figure 1.5 influences the behavior of the grid voltage through a fluctuation between producing power and using it from the grid. These effects may cause serious energy quality problems, which rises with a rise in the penetration level of PV systems. It is also possible that there is a rather low power generation for the whole day in the case of Figure 1.6. The measured peak power on this day is $1.1\,kW$, which is just 10 % of the power peak value before and after that day. All mentioned scenarios must be considered in order to keep the grid quality within given standards independent from the environmental conditions.

As mentioned above, if the power of the PV generator exceeds the load power in a system without an energy storage device, energy is fed into the grid. Depending on the power and the penetration level[1] in this area, a voltage rise appears through that reverse power flow. The utility is responsible to keep the line voltage in a specified range. Counteractions such as reducing the power generation of grid power plants have to be initiated in order to meet the energy quality standards.

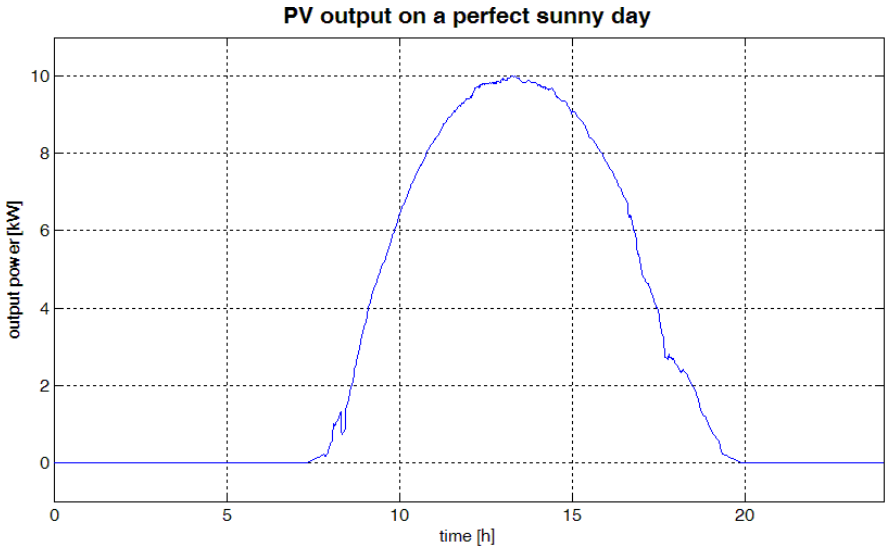

Figure 1.3: PV output power profile on a sunny day [24]

[1] *„When PV penetration reaches high enough levels (e.g., 5 to 20% of total generation) however, the intermittent nature of PV generation can start to have noticeable negative effects on the entire grid.“* [7].

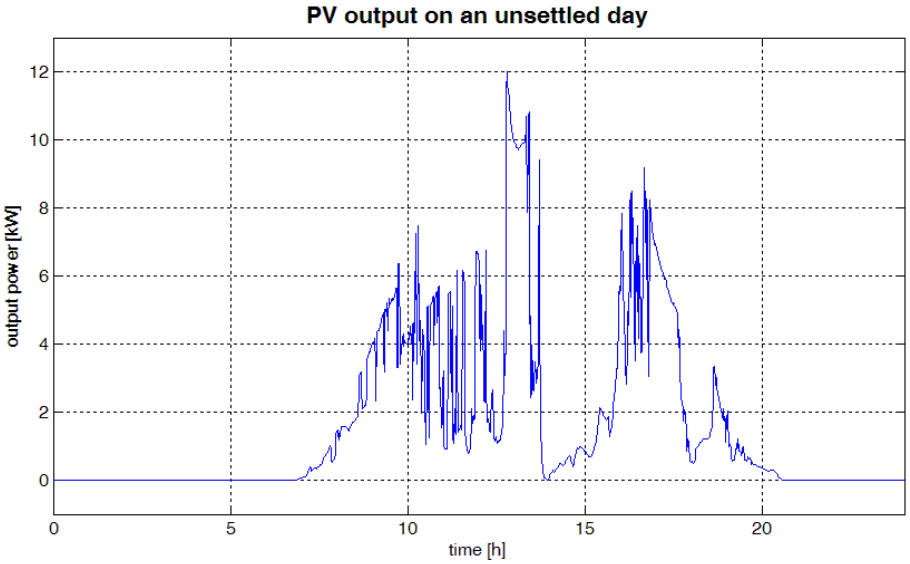

Figure 1.4: PV output power profile on an unsettled day [24]

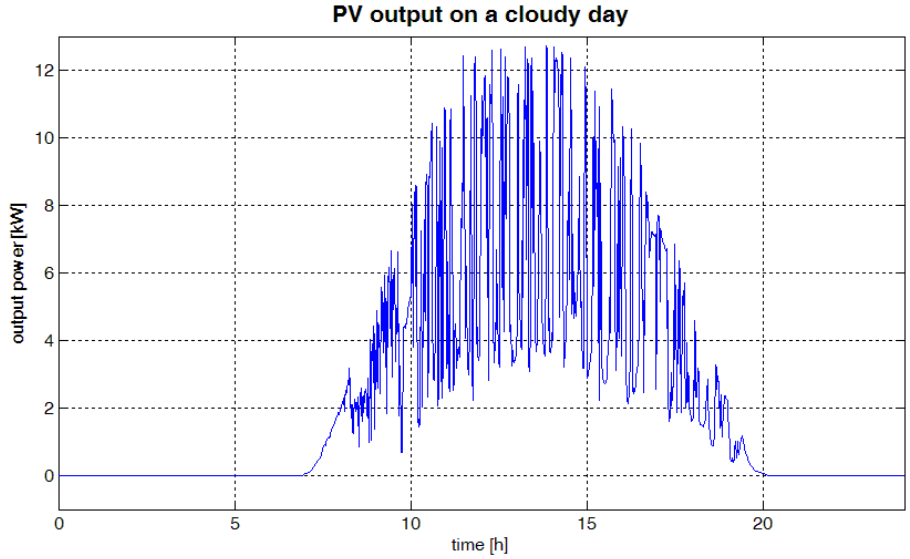

Figure 1.5: PV output power profile on a cloudy day [24]

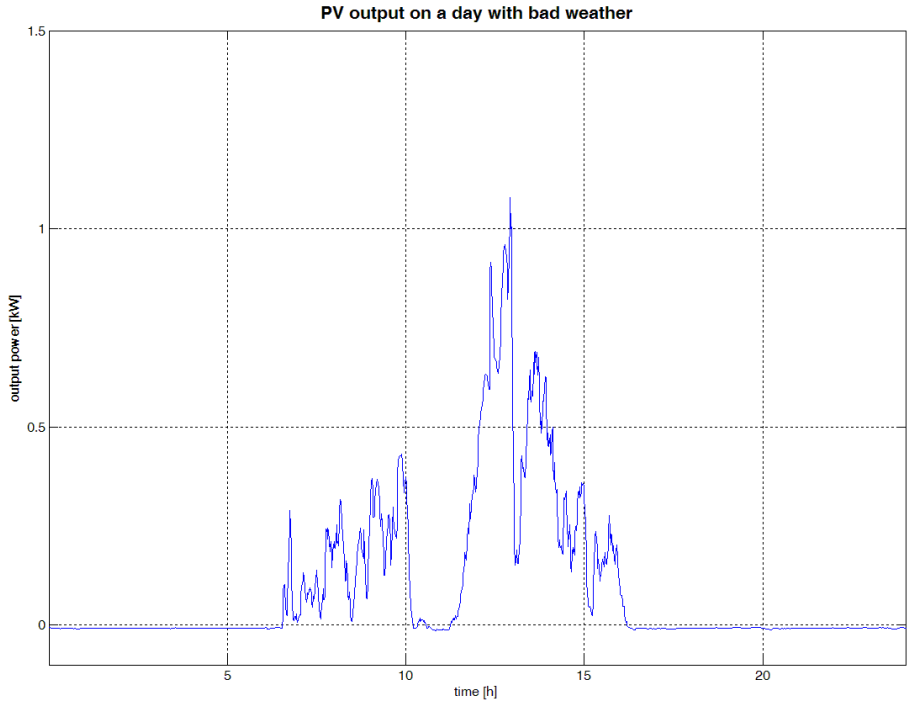

Figure 1.6: PV output power profile on a cloudy day [24]

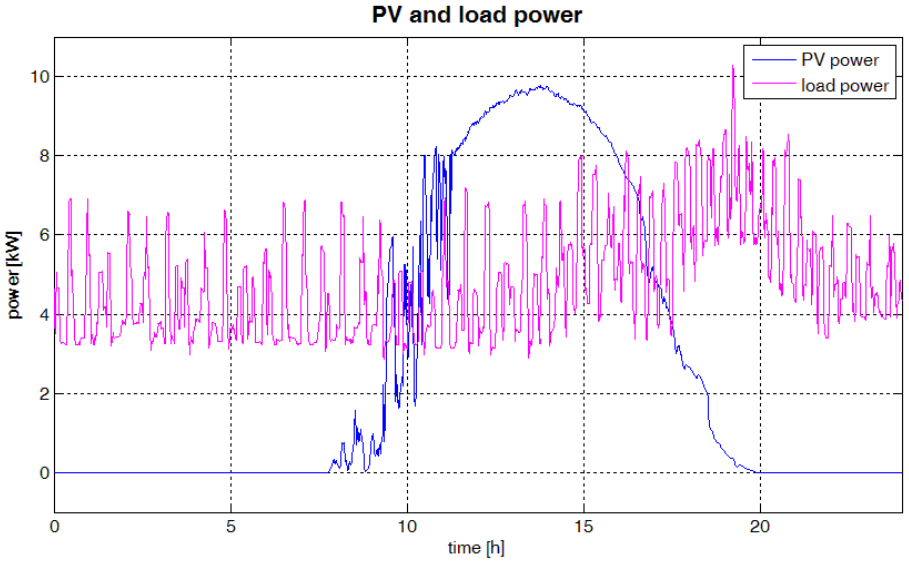

Figure 1.7: PV power and load power profile [24]

As an example a detailed situation of PV power generation and consumer demand for one residential application is given in Figure 1.7. The peak load of the consumer is at $7:15\,pm$, whereas the PV power peak is at $1:30\,pm$. The load power profile, shown in Figure 1.7, has an average base load of $4.5\,kW$, which is higher

than the PV power during the night. The PV power exceeds the load power from $9:30\,am$ to $5\,pm$. After this time the load power rises and reaches its maximum value of $10.27\,kW$. The peak power of the PV system is $9.75\,kW$ in this specific case. Therefore, most time of the day the power demand is not met by the PV power generation. Consequently, a continuous power feed in and consumption interrelation with the grid or with any storage device will appear.

There is a necessity for power management including some energy storage capacity. The energy storage system in combination with a power management system helps to stabilize the grid voltage. In the case of residential energy storage, a power management system may provide a back up function. An energy storage system can be provided by the utility or by the customer. Possible solutions from the utility side are:

- apply batteries at substations
- adopt the power from power plants
- apply pumped storage power stations

The most common way to compensate for the power mismatch from the customer side is to integrate a secondary battery (in the following just mentioned as battery) into the home grid system.

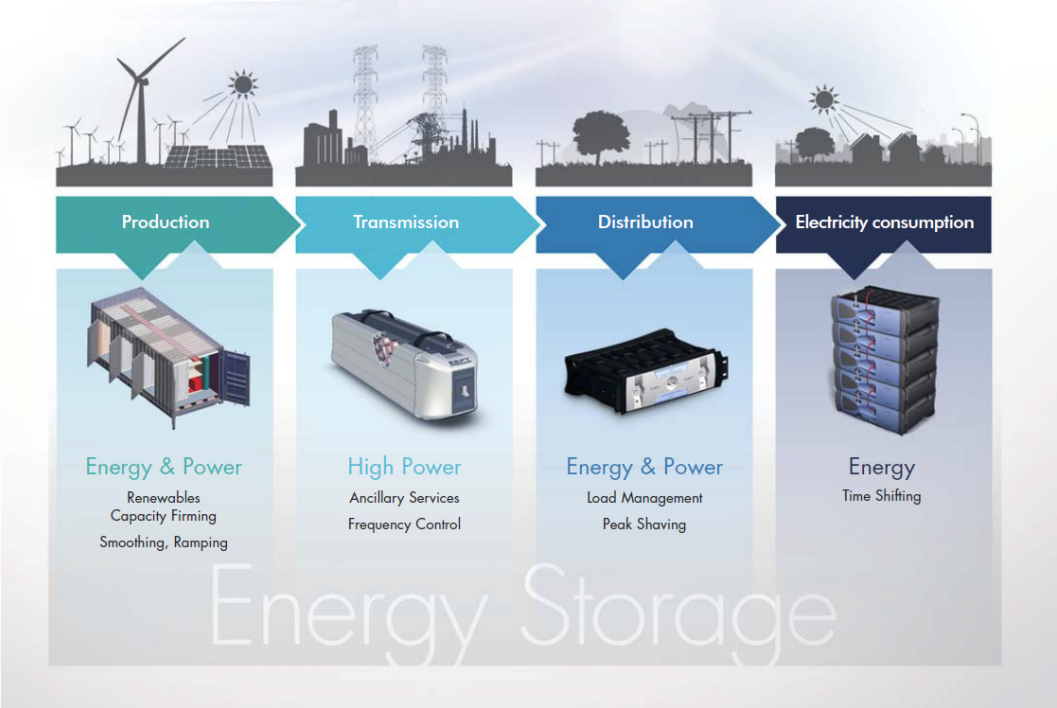

Figure 1.8: Different application area of battery energy storage systems [28]

It has to be emphasized that storage of electrical energy may be applied at every grid level and not at user level only. Figure 1.8 shows examples for further applications of electrical energy storage from the production to the consumer level. In this work the close focus is on the customer side only.

Using a photovoltaic generator in combination with an energy storage unit can solve the power mismatch problem, as outlined in Figure 1.7.

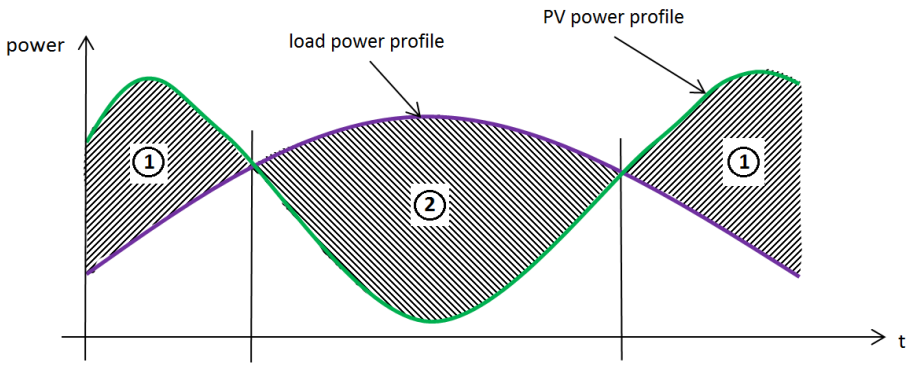

Figure 1.9: Qualitative diagram of a PV and a load power profile

Figure 1.9 shows qualitatively a PV and a load power profile. The green graph is

the PV power profile and the purple graph is the load power profile. Without using a battery, the shaded area is either the power which has to be taken from the grid (indicated by "2") or which has to be fed into the grid (indicated by "1"). Figure 1.10 shows this scenario.

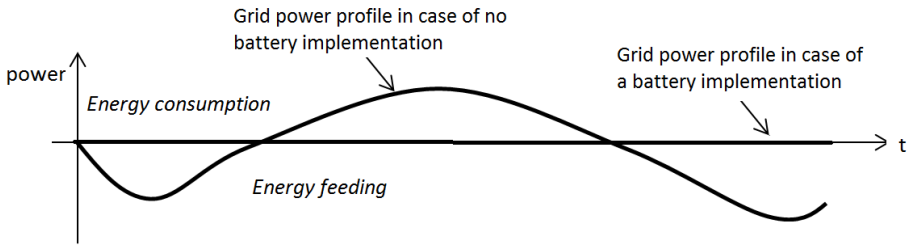

Figure 1.10: Grid power profile without a battery

The energy storage demand may be covered by either the grid or any battery. In an ideal case, using a PV system in combination with a battery causes the power exchange with the grid to equal zero (indicated in Figure 1.10 by "*Grid power profile in case of a battery implementation*").

Such an operation of balanced energy management (no energy exchange with the grid) can be realized with small battery stacks for short time intervals. Long term balanced energy management requires huge energy battery systems and high investment costs consequently.

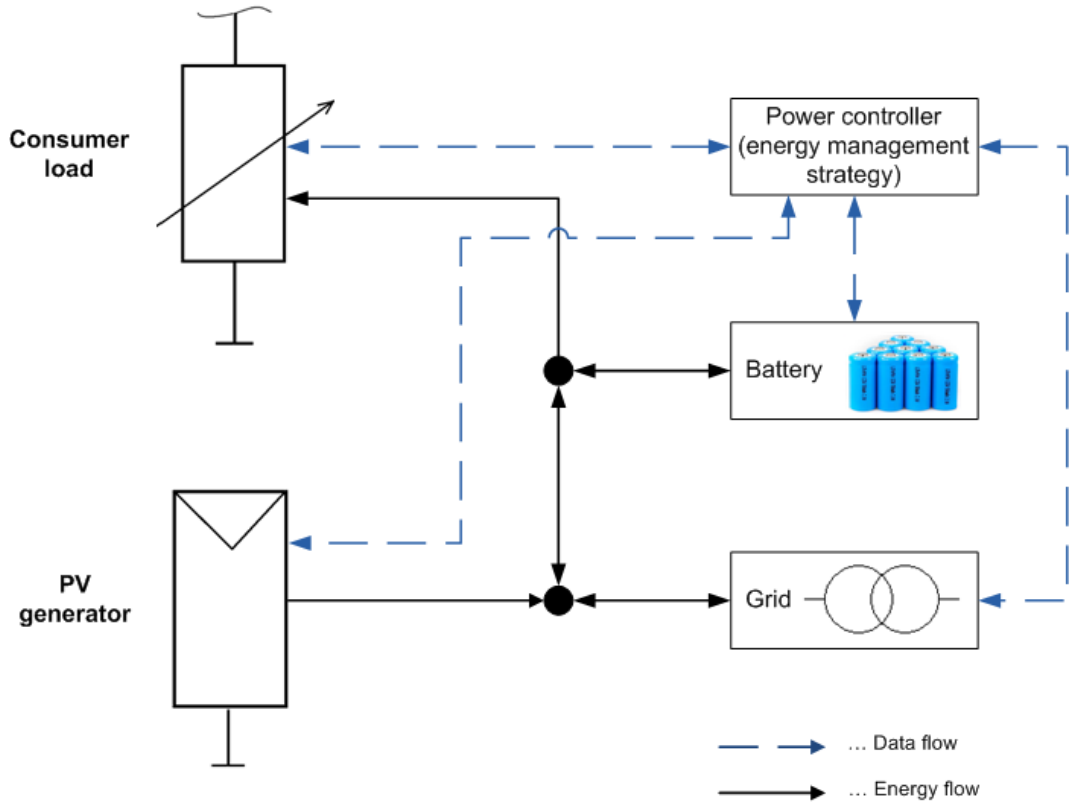

Figure 1.11: Structure of a residential PV system with a battery energy storage system

A basic microgrid[2] system, using a battery as an electrical energy storage is shown in Figure 1.11. The structure shows a grid connected system, using a PV as DRES and a battery as energy storage, which is controlled by a power controller. This controller algorithm decides whether the battery has to be charged or discharged. The power controller influences the power flow based on energy balance aspects. Additionally, if the momentary energy costs are considered, a cost optimization may be achieved. If energy costs are low, the battery could be charged and if energy costs are high, energy from the battery may be fed into the grid.

Based on energy cost considerations strategies may be applied. Typical strategies may be:

- Peak shaving

  The peak shaving mode is used for demand charge ratings which means that

[2] *"A microgrid is defined as a distribution system with distributed energy sources, storage devices, and controllable loads, that may generally operate connected to the main power grid but is capable of operating as an island".* [8], page 217

the energy costs are based on the peak value of the power used. Therefore, the focus of this operation mode is to reduce the peak load to a specified value either with the PV generator or the energy storage. To lower the peak value used from the grid a control algorithm is used. It depends on the utility whether demand billing can be applied just a commercial customer or also for residential customer as well. Typically, this mode is just for commercial consumer.

- Load shifting
  Load shifting uses energy storage to meet the energy demand at expensive energy rates with the storage. It is similar to the peak shaving mode, but the main objective is different. This application considers the rates from the utility to decide the source of the used energy.

- Demand response
  This mode considers the utility energy rates and applied to high power devices which are flexible in the time of use, for example a storage water heater. This is a typical device for demand response because it does not matter at which time a customer's water is heated (it is assumed that amount of stored hot water in the tank reaches for at least a whole day). It is necessary for the application of demand response to have information from the current utility rate. There has to be a communication in between the utility and the customer to get current electricity rates.

- Outage protection
  In the case of a power blackout, energy is fed from the ESS during the off time. Therefore the microgrid has to be disconnected from the grid and changes to islanding mode. [3] describes a method of sizing the energy storage according to outage statistics using a Monte Carlo simulation based on the time and duration of outage events.

- Grid power quality control
  If the grid voltage or the frequency reaches a value out of the specified limits, the system changes from grid connected to islanding mode and the battery covers the energy consumption as described in the outage protection mode.

To increase the cost efficiency of a residential house, an energy management strategy (EMS), which is based on a combination of the previously mentioned operation

modes, must be investigated as each mode has a different objective. The new operation mode, developed for this model, will be based on load shifting and demand response as both modes have a similar focus. Peak shaving is also indirectly discussed, but not directly focused on, because the objective is to keep the high rated energy use from the grid as low as possible which meets the definition of peak shaving indirectly, as there is no specific value for the allowed peak power. The other options mentioned above such as outage protection are additional modes which are possible to apply, however the implementation of these functions is not considered in this work.

There are lots of possibilities to store electrical energy for residential applications such as:

- pumped storage power plants
- batteries
- super capacitors
- fuel cells

The pumped storage power plants are just possible to use in individual cases such as a farm in the mountains.

Batteries are used for both sides, the utility and the consumer side as they are available from small capacities.

Super capacitors have some advantages compared to batteries, such as a higher life cycles and a higher efficiency with almost $\eta \approx 100\,\%$ [10]. The biggest disadvantage of supercapacitors is that the self discharge over time is rather high. It reaches a value of more than $10\,\%$ of its stored capacity if there is no load connected for 1 day. Furthermore, the cost per Wh is about 10 times higher and the specific energy is at least 20 times lower compared to a Li-Ion battery.

Fuel cells would also be a possible technology to store energy but it is not a fully developed technology as there is still some research needed on this topic. Only expensive prototypes are available.

As a conclusion of the considerations above, the battery is the most proper energy storage with respect to financial and technical aspect. The following paragraph shows the state of the art of battery energy storage systems (BESS), which is derived

from the references [10-12]. The most common way of storing electrical energy in the residential sector is using a battery.

The most common battery technologies which are available on the market are discussed below.

- Lead-Acid
  The Lead-Acid battery is the most commonly used battery type in the industrial field. The cathode electrode is lead dioxide, whereas the anode consists of lead. The applied electrolyte is a sulfuric acid. Reasons for using this old type of battery is the low capital cost and the high efficiency (Table 1.1).

Advantages	Disadvantages
Cost effective	Low energy density
Good roundtrip efficiency	High maintenance
Low self-discharge	Low cycle lifetime
Mature technology	Low calendar lifetime
	Environmentally hazardous materials

Table 1.1: Qualitative characteristics of Lead-Acid batteries

- Lithium-Ion (Li-Ion)
  The cathode of a Li-Ion battery is a lithiated metal oxide. The anode is made of graphitic carbon. The used electrolyte is composed of a lithium salt. The main advantage of this technology is that it has a higher energy density compared to older technologies, like the Lead-Acid battery or the Nickel-Cadmium battery. The price of Li-Ion batteries was very high at the time of introducing this technology. The price decreased after the first five years by a factor of three which is shown in Figure 1.12. The increased energy density of this technology is also shown in this figure.

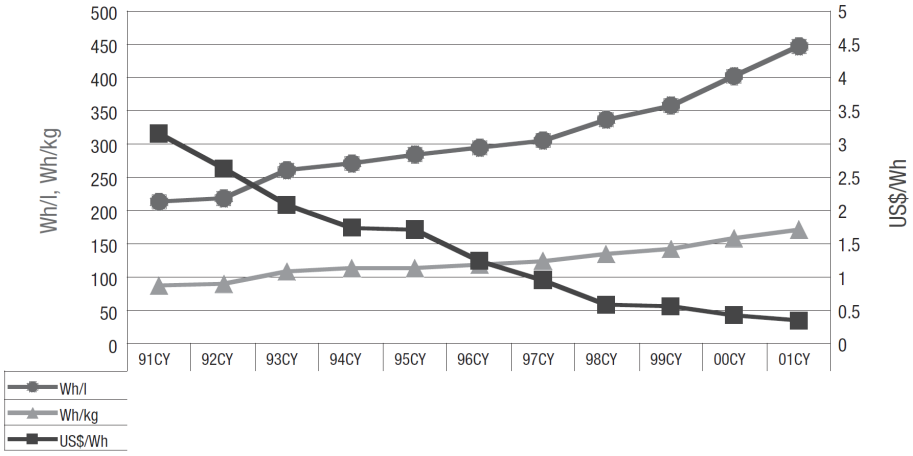

Figure 1.12: The development of the price and the energy density of Li-Ion batteries [33]

Table 1.2 shows the main attributes in summary.

Advantages	Disadvantages
Excellent efficiency	High cost
High energy density	Low cycle lifetime
	Safety concerns (explosion, fire)

Table 1.2: Qualitative characteristics of Li-Ion batteries

The main application of this battery type is in mobile electronic devices and hybrid electric vehicles.

- Lithium-Iron-Phosphate (LiFePO4)
  The LiFePO4 battery is based on the Li-Ion battery technology. The cathode is made of a LiFePO4 material, and the anode is made of graphite. The applied electrolyte is a polymer. This particular kind of Li-Ion Battery is the safest and cheapest development compared to other ones, like LiCoO2 or Li4Ti5O12, according to [15]. A résumé of the most important characteristic of this battery type is shown in Table 1.3.

Advantages	Disadvantages
Safer than traditional Li-Ion Batteries	High price for the batteries
High power density	Low conductivity (not usable for high power applications)
Lower cost than traditional Li-Ion Batteries	
High temperature range	
Environmental friendly material used	
Very stable voltage in a certain band	
Cheap raw material used	
High energy density	

Table 1.3: Qualitative characteristics of LiFePO4 batteries

The current application area of this battery type is for full electric vehicles because of the high energy density, as well as for the mass to volume ratio. It is an important characteristic for cars to keep weight low to achieve high energy density.

As a summary, the energy density of the most common battery types used is shown in Figure 1.13 and the comparison of the mentioned battery technologies is shown in Table 1.4. In this table the technologies are rated with the symbols: -, o, and + from bad to good.

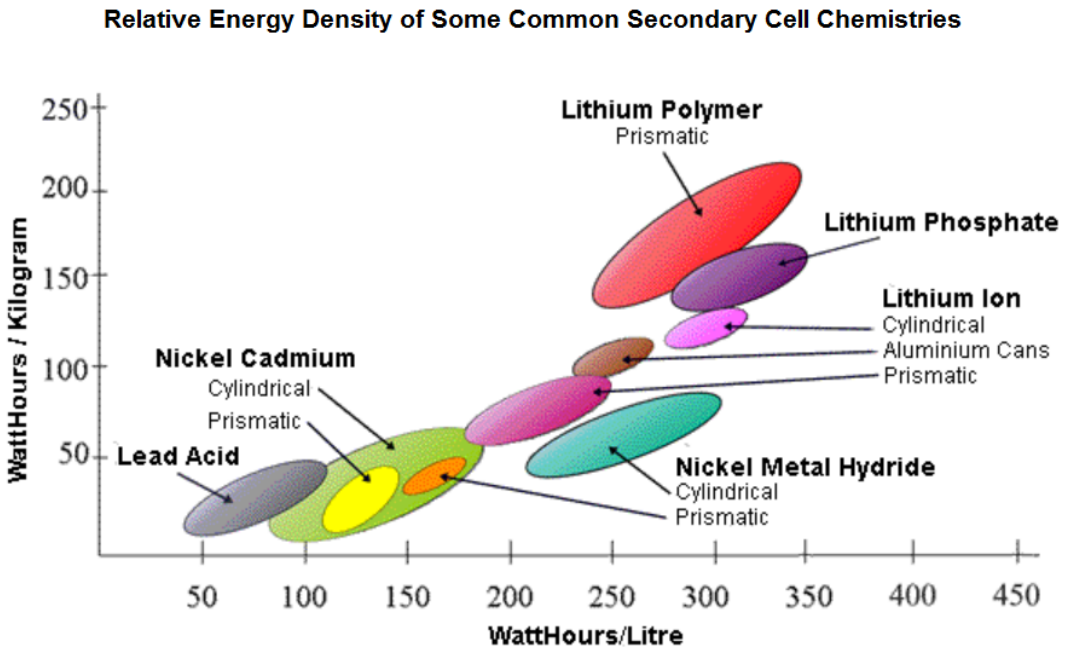

Figure 1.13: Energy density of common battery technologies [34]

	Lead-Acid	Li-Ion	LiFePO4
Price / capacity	+	o	-
Energy density	-	o	+
Safety concerns	o	-	+
Cycle lifetime	-	o	+
Charge / discharge efficiency	-	o	+

Table 1.4: Comparison of Lead-Acid, Li-Ion, and LiFePO4 batteries

LiFePO4 batteries are considered in this study because this technology will succeed in the market. This technology is still expensive, but it is reasonable to assume that the price will drop within the next five years. This assumption is based on the price development of the Li-Ion batteries (Figure 1.12), where the market price reached one third of its initial price within the first five years. In addition, the cost for raw materials for LiFePO4 is cheaper than for traditional Li-Ion, which further supports the assumption that the price of the LiFePO4 battery technology will drop. A second criteria for the LiFePO4 battery is the energy density. For example, it is important for electric vehicles to have the lowest weight possible to increase the reachable distance. Energy density is also important for residential PV applications. Two important factors, size and weight, have to be considered. Larger batteries take

up more space in a home, so a small battery is optimal. Additionally, battery weight must be controlled because residential floors have a limited specific load.

Profit is gained in this system by controlled charging or discharging of the battery. It can either be charged from the grid if the electricity price is cheap or from the PV if there is surplus energy available. Therefore, the utility rate has a big influence on the economic efficiency. There are, in practice, three different rating systems available:

- flat rate
- time of use (TOU)
- real time pricing (RTP)

First, flat rate pricing means that the price for electricity is independent of the time of usage. It may differ from summer to winter but it does not change from daytime to nighttime. This is still a common accounting method, but it will loose its importance considering the introduction of smart grids[3].

Second, the time of use rate is an electricity pricing rate with at least two different prices per day. Usually there is an on peak and an off peak price. Also a semi peak price is sometimes applied, depending on the utility. Some States already have this rate introduced:

- New York
- Arizona
- Nevada
- Oregon
- Florida
- California

The utility in Berkeley, California, Pacific, Gas, and Electric Company (PG&E), is a good example of an established TOU rating system. Considering economic aspects

[3]In this specific case, a Smart Grid is a microgrid with an energy management strategy to control the DES and the BESS to increase the cost efficiency.

with this rating, a PV power profile is compared with the applied price rate (Figure 1.14). The correlation between the generated electrical power and price rate is very high. Therefore, if the produced PV power will be feeding into the grid, either a high financial benefit can be gained or the energy demand can be covered by the PV cell to bypass expensive electricity rates.

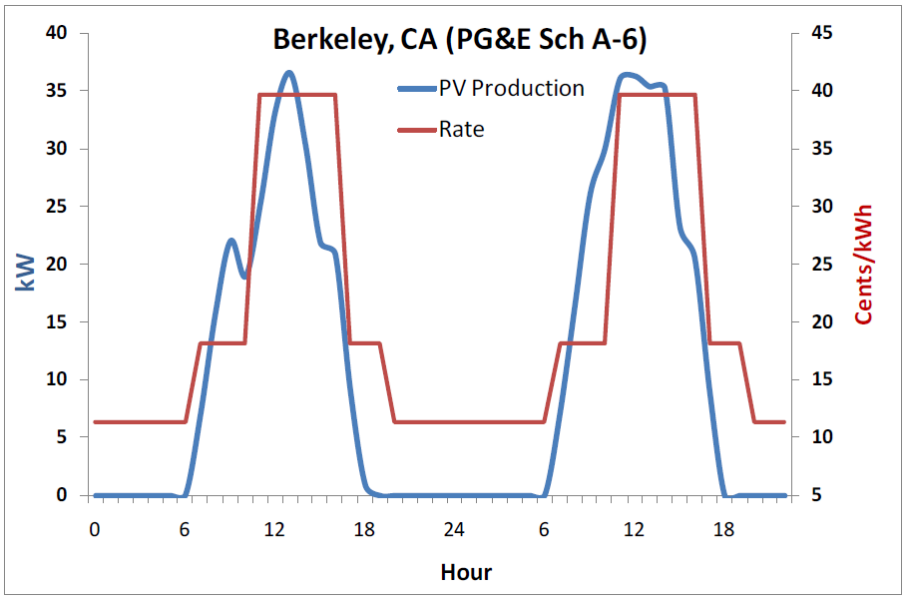

Figure 1.14: Comparison of the TOU rate structure with the PV power profile from PG&E (based on [9])

In Tallahassee, Florida, the TOU rate program started on the 1st November, 2010 and is still a pilot project, which is open to 2,000 customers [25] at the moment. Figure 1.15 shows the correlation of a PV power profile and the applied TOU rate from Tallahassee. As the on peak of this TOU rate is between 7am and 7pm, the correlation with the PV profile is very good.

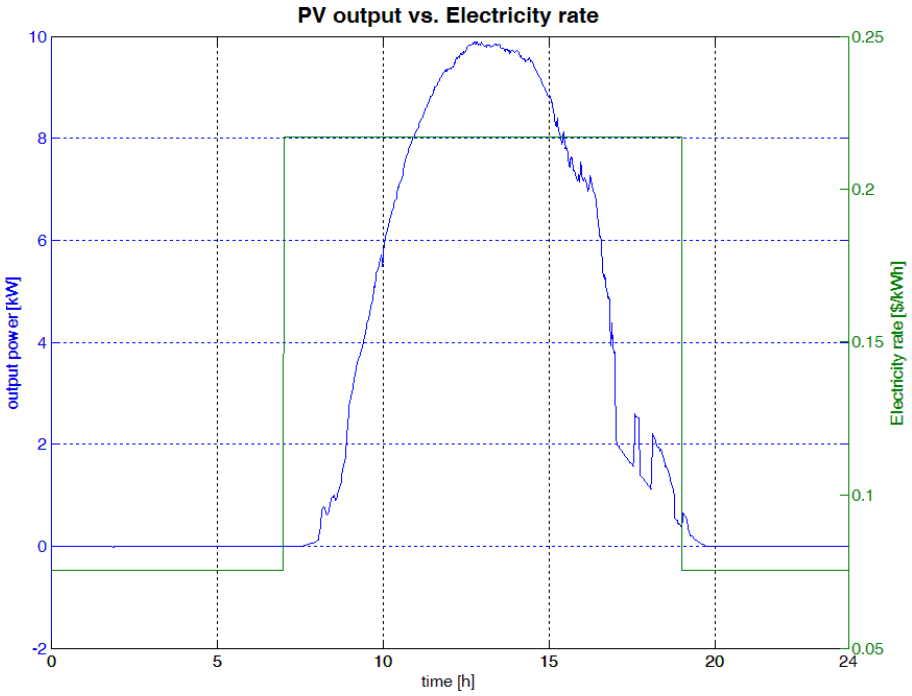

Figure 1.15: The applied TOU rate compared with the used PV power profile [24, 25]

The last rating system which should be discussed is real time pricing (RTP). In this system, the electricity price changes hourly and is based on the current energy market price. RTP is only available in Illinois and Southern California available, as it is still a new rating system. The utility company in Southern California, EDISON, provides the RTP rate just for industrial usage. ComEd, a utility company from Illinois, provides this rating for the residential customer. Therefore the rating from Illinois is used in this research, as the treated application area is the residential home. The correlation of any day with the PV power profile is shown Figure 1.16.

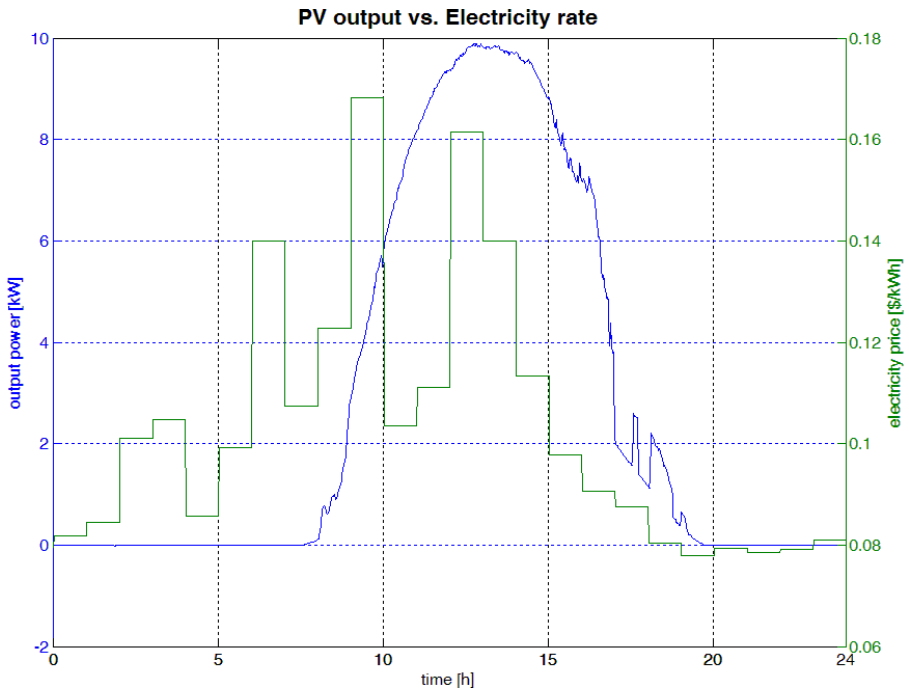

Figure 1.16: The applied TOU rate compared with the used PV power profile [24, 26]

The correlation between the PV power profile and the electricity price rate is not as high as with the TOU rate.

ComEd provides one day ahead predictions for the electricity price of the next 24 hours. They also provide the previous electricity rates (real price rates and predicted ones) at their homepage [26]. Figure 1.17 shows the real electricity price, blue line, compared to the predicted one, magenta line. There is a big difference in between these rates, e.g. around noon, which makes it difficult to create an optimum power management to gain the highest profit out of such a system.

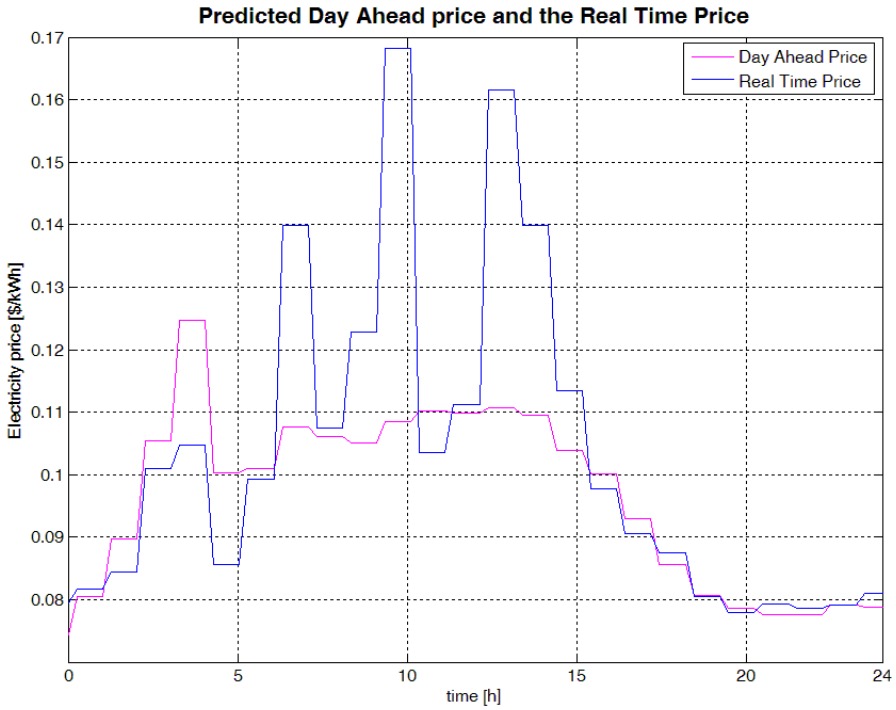

Figure 1.17: Comparison of the day ahead price and the real time price [26]

For the profitability it is important to consider both possibilities for the customer, using electrical energy from the grid or feeding electrical energy into the grid (e.g. PV surplus power). As an example, Tallahassee utility has a 1:1 quote for the feed in, which means that the amount of money that can be gained by feeding into the grid equals to the cost of using electricity from the grid.

Chapter 2

Scientific question

In summary, there is a steady rising energy demand which has to be covered by proper systems. Battery storage combined with photovoltaic systems is a possible approach to solving these demand issues. These system controlled by power management can assure the grid quality due to a rise in penetration level of DRES. These systems are a popular topic in the literature [3, 4, 5]. Previous work [2] on the optimization of electricity usage of a commercial building uses a battery for storage, however there is no DRES considered in this specific application. Peak load shifting is used to enlarge the benefit of such a system. An important point is that for this calculation no battery model is used and therefore the calculated lifetime of the battery is just an estimation as well. Additionally, the load profile used [2] in is estimated. A similar study [3] examines an industrial usage of a PV system. In that paper the objective is to calculate the optimal battery size for outage situations so there is enough energy to bypass such a situation. An energy management strategy is included which focuses on the peak load shift. A main part in this cost function is the outage cost which is calculated by using probabilistic methods. The simulation data is based on real data, like in this thesis. Other research deals with a stand alone system which uses PV and Wind power as DRES [4]. In this study, the optimum battery size depends on having a high autonomy level. This sizing technique calculates the optimum size of all components of the system. Here, the simulation data is based on average data and the battery is considered to be ideal. A lifetime model for the battery is the basis of the sizing [5]. The main objective is not to increase the economic value.

This thesis focuses on finding the most cost effective battery size for a residential house which consists of a PV system in combination with a BESS. The input data

is based on real data profiles and not average values. The battery model used is a physical based battery lifetime model of the new battery technology LiFePO4. This combination was not found in the literature and therefore not investigated yet. This approach combines the mentioned factors and presents a solution for how to size a battery focusing on the cost efficiency.

Chapter 3

Proposed battery sizing strategy

This chapter describes the proposed battery sizing strategy. First, the strategy is generally explained (Section 3.1). Second, the functions applied are explained in detail in Sections 3.2 - 3.5). Last, the implementation in the simulation programmer is explained (Section 3.6).

3.1 General

Figure 3.1 shows the general structure of the proposed battery sizing strategy.

First, the simulation loads all the simulation data required. Then, the first considered battery size is set and the variable for the state of health is set to one (the initial value). The outer loop of the simulation (Figure 3.1) stands for the different considered battery sizes. Then, the inner for loop applies the lifetime simulation of the particular specified battery size which consists of the energy management strategy and the battery model. The EMS calculates the required charge / discharge power which is the input value for the battery model. The battery feedbacks the actual state of charge (SOC) and state of health (SOH) to the EMS. The loop is then executed as often as the battery is not treated as broken. If the battery life is over, the cost calculation is accomplished to get the profitability of the battery size used. After that, the next considered battery size is set. After the simulation of all predefined battery sizes the optimum battery size is calculated out of the economic values. Figure 3.2 shows an example of a surface plot of the simulation results for the cost efficiency. A second result of the simulation is the lifetime of the battery.

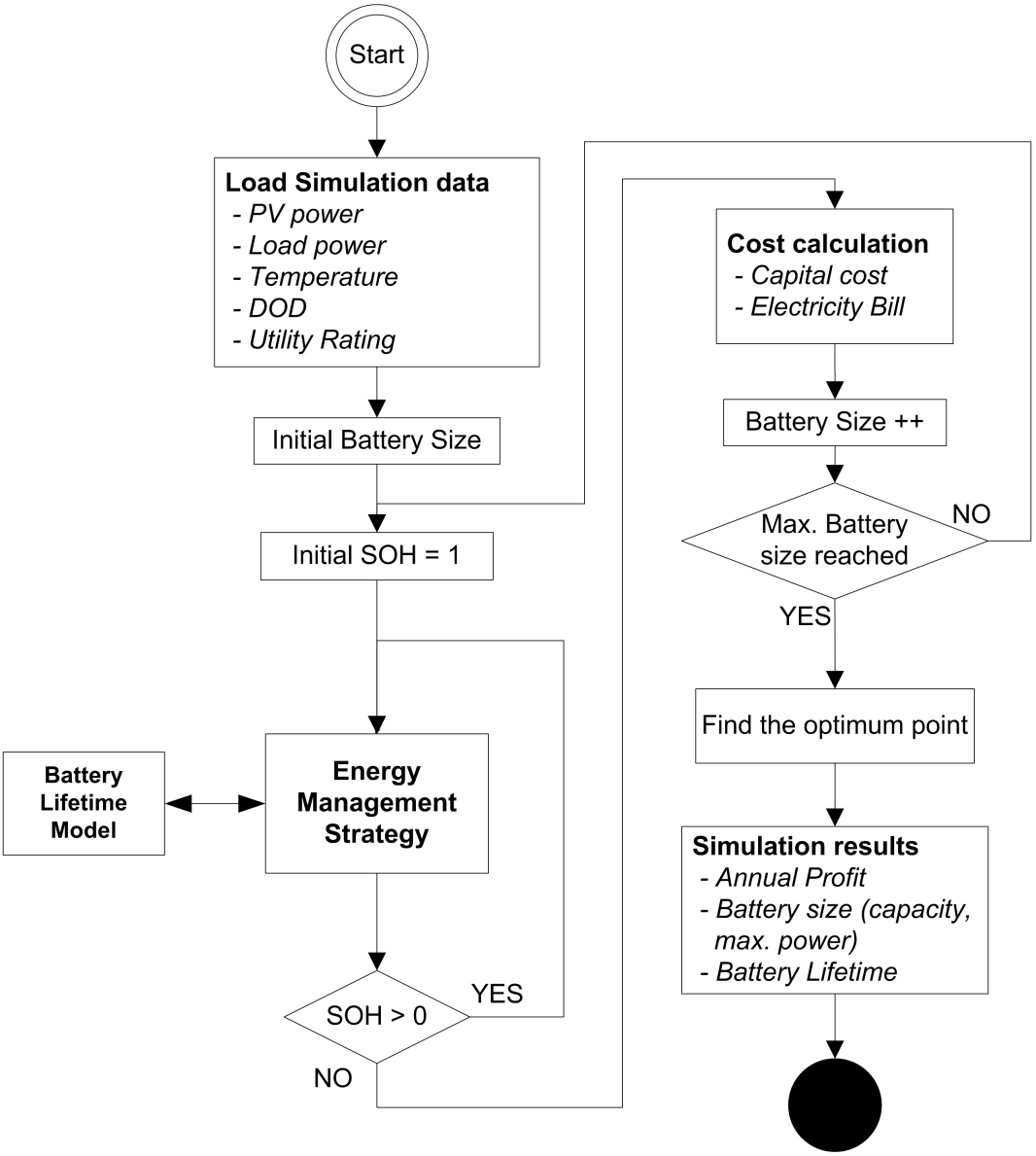

Figure 3.1: Flowchart of the whole simulation

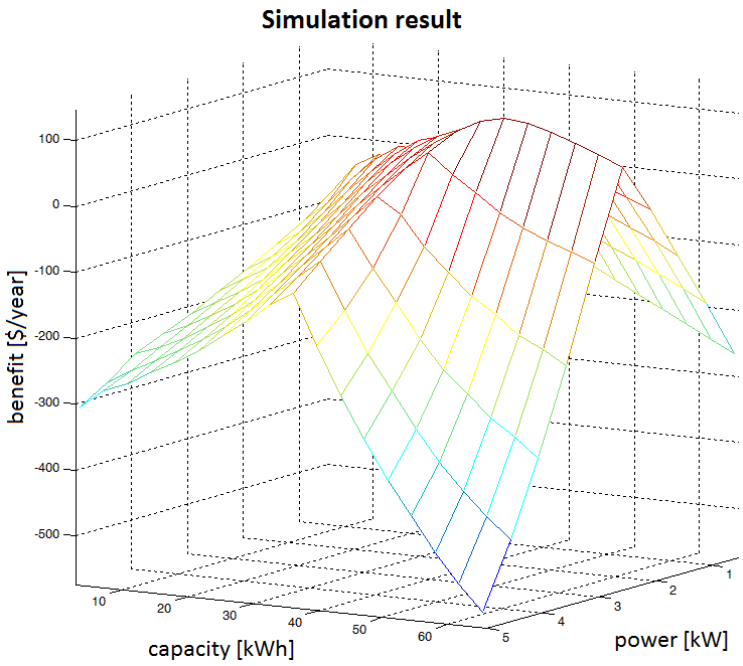

Figure 3.2: Simulation result

The input / control data used and the developed / applied functions are explained in detail in the Sections 3.2 - 3.5.

The timestep of the simulation is an important criteria for the accuracy. This simulation is designed to run with small timesteps compared to the whole simulation time in order to get a response from the battery model which is realistic concerning the battery stress. The simulation time depends, in principle, on the battery life which is about 10 years or longer (depending on the use, chemistry, etc. ...). The timestep of the simulation is set to 15 minutes, which is a compromise between a high accuracy with a very low timestep and a rather high timestep which would result in an average of a few hours. The selected value is also appropriate to the time constant of the operating time of residential loads. Figure 3.3 and 3.4 show the load profiles of a residential house of two days. Figure 3.3 shows the daily load profile with a timestep of 1 minutes and Figure 3.4 illustrates the profile with a timestep of 15 minutes. The profiles are not identical, but the trend is the same. Therefore, the simplification does not lead to a result which is as accurate as with the original load profile but it is a good compromise to reach shorter durations of the simulation and still have a lifelike load profile.

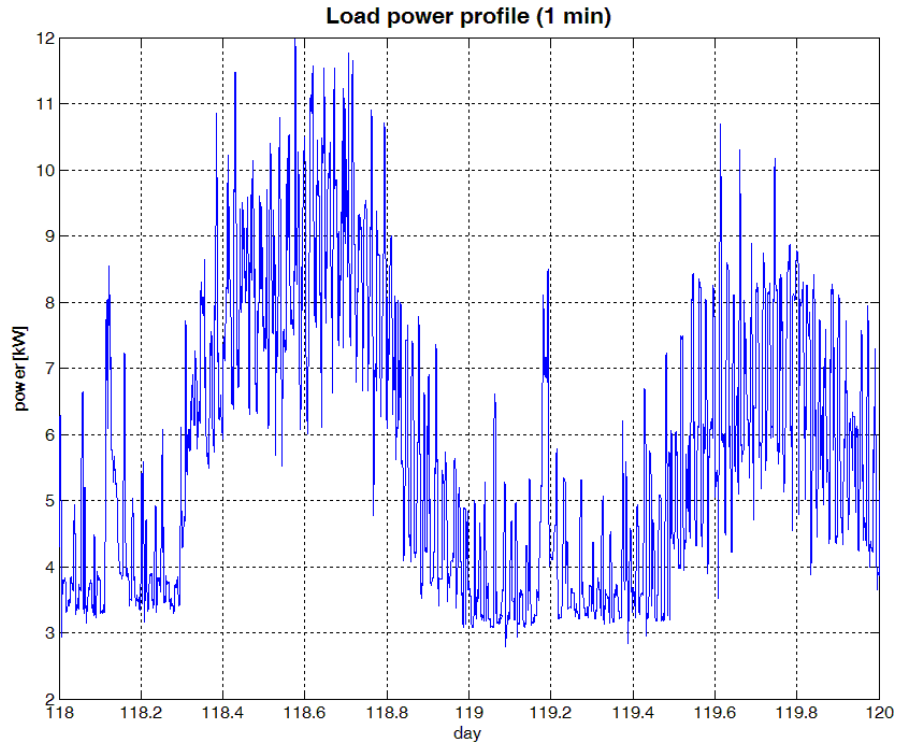

Figure 3.3: Load power profile / 1 minute [24]

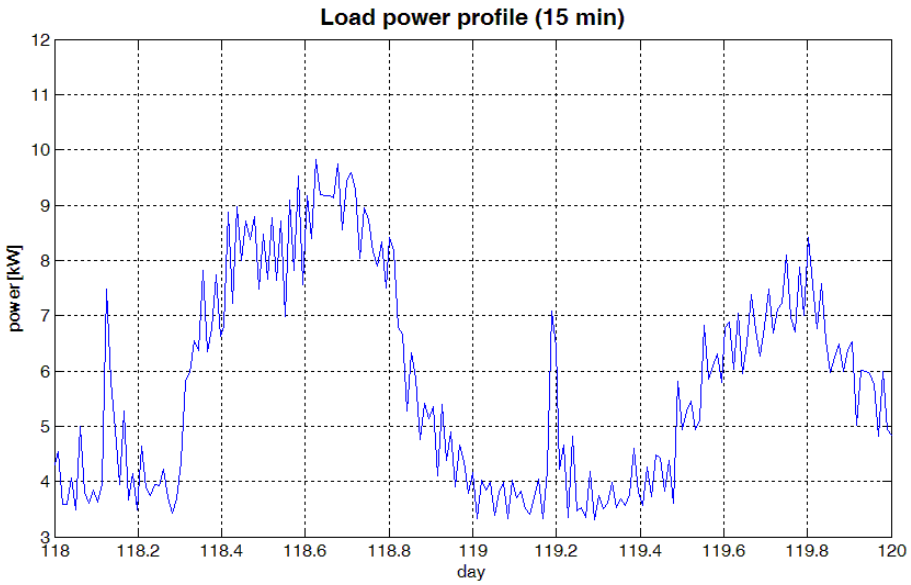

Figure 3.4: Load power profile / 15 minutes [24]

3.2 I/O data and control parameter

3.2.1 Input data

The required input data is the customer load power profile, the PV power profile, the temperature profile, and the electricity price. As it is mentioned above, the sampling time of the simulation is 15 minutes, which is also required for the input data. The requirement for the input data is to have the data profiles for a whole year to consider the seasonal differences. Since the length of the simulation equals to the battery life, which is usually longer than 1 year and the requirements for the input data is to have annual data, the used input data is equal to every year.

The electricity price is a further input parameter. It is not necessary to have this data in a timestep of 15 minutes available as it just changes a few times a day. For example, the TOU rate from Tallahassee Utility has just two different prices. Alternatively, the real time pricing rate has a different electricity price every hour which leads to a timestep of this time interval.

3.2.2 Control parameters

The control parameters are independent from the individual user and from surrounding conditions except the utility rating type as the different rating systems are not everywhere available. The control parameters are:

- depth of discharge (DOD)
- battery capacity
- charge / discharge power limit for the battery
- utility rating type

The DOD defines the lower and upper limits of the battery's state of charge. The capacity and the charge / discharge power limit specifies the battery size. The last control parameter, the utility rating type, gives the current electricity price and feed in tariff.

3.2.3 Output data

The output data of the simulation covers the gained profit from all simulated battery sizes, with the information of the most profitable size.

3.3 Energy management strategy

The energy management strategy is the power management in the residential microgrid. The functionality basically consists of load shaving and demand response. The main purpose of the EMS is focused on reaching the lowest cost for the customer. For example, if a temporary cloudy condition is present (Figure 1.4), during peak times, when electricity is expensive, the required electricity is taken from the battery in order to save money.

The energy management strategy decides about the operation mode:

- unoperated mode
- charging mode
- discharging mode

and the amount of charge / discharge power of the battery.

In the unoperated mode the charge / discharge power of the BESS is zero. The other 2 control modes use the BESS for the charge or discharge operation. If the system is in charging mode, the battery can either be charged from the PV panel or from the grid. If the energy storage system is in discharge mode, the battery supports the load demand. Figure 3.5 shows the structure of the developed EMS.

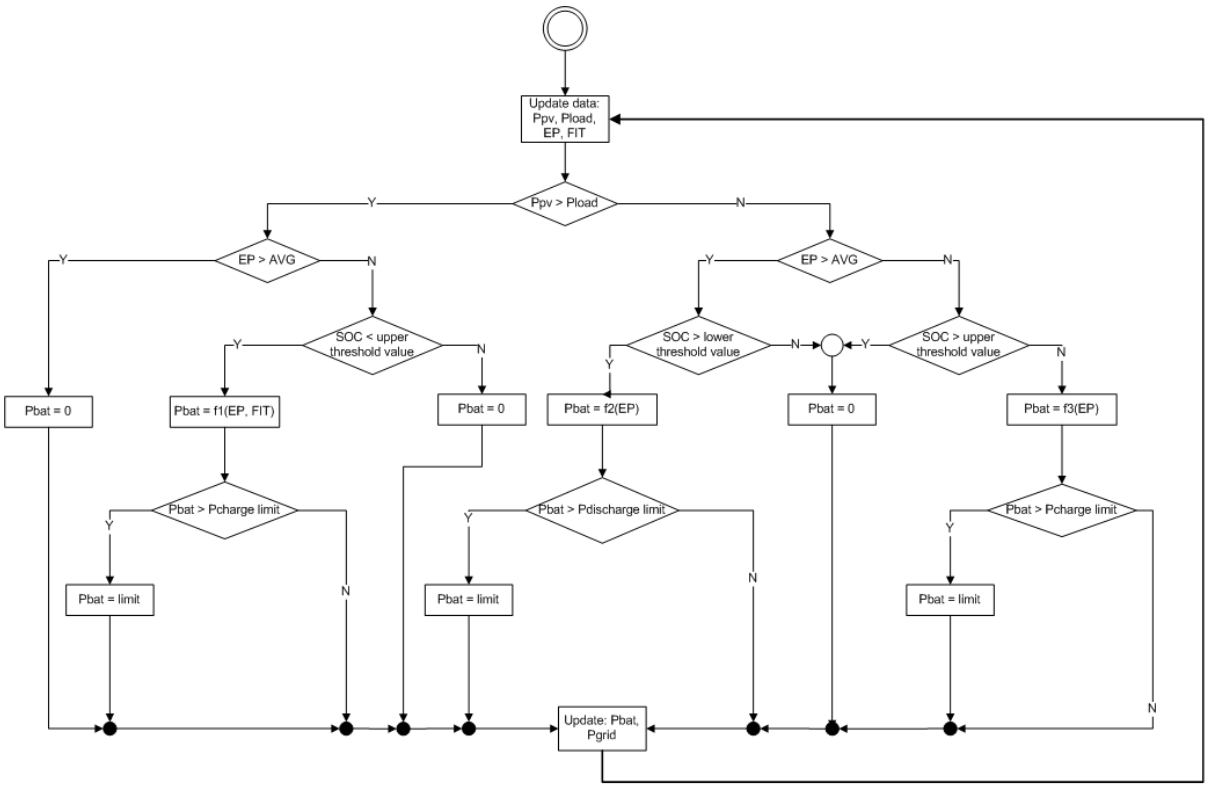

Figure 3.5: Structure of the energy management strategy

3.3.1 General functionality of the strategy

The first action in the strategy initiates / updates the PV power profile, the load power profile and the pricing data (electricity price (EP) and the feed in tariff (FIT)). The following step demonstrates the basic transition in this strategy, which is the relation between the PV and the load power. If the PV power exceeds the load power, the left branch of of the strategy is applied. In this case, the battery is charged based on the current electricity price. If the price is higher than the calculated average price (the calculation of the average EP is explained in the following paragraph), the PV surplus is fed into the grid. If the EP is high, the FIT is also high and therefore the benefit for the electrical energy cost increases. If the actual EP is lower than the calculated average price, energy is stored in the battery. The amount of charging power depends on the current price (the used charge function f_1 and its development is explained in detail in the last paragraph of this section) to optimize the usage of the energy storage system. It is volitional to charge the battery with cheap energy or with energy from the PV (if it is not worth feeding it into the grid, because of a low FIT). If the stored amount of energy reaches the specified upper threshold level

of the SOC, the battery is set to the unoperated mode. The bottom action in the structure updates the current calculated battery and grid power.

If the load power exceeds the PV power, all 3 operation modes are considered which is shown in the right branch of the diagram in Figure 3.5. The battery is either used to support the load demand or to gain from cheap electrical energy through charging the battery. At a PV surplus power, the battery is treated as storing the energy, if the electricity price is low. Therefore, the left branch of the EMS structure is just an adapted copy of the right branch excluding battery discharging. The charge and discharge functions f_2 and f_3 are explained in detail in the last paragraph of this chapter, as well as the function f_1.

Positive values for the battery power stands for discharging and negative ones are for charging, as it is treated in the calculation of the sum of the power in the point of common coupling. Also the grid power is positive if the power flow is from the grid to the microgrid and vice versa.

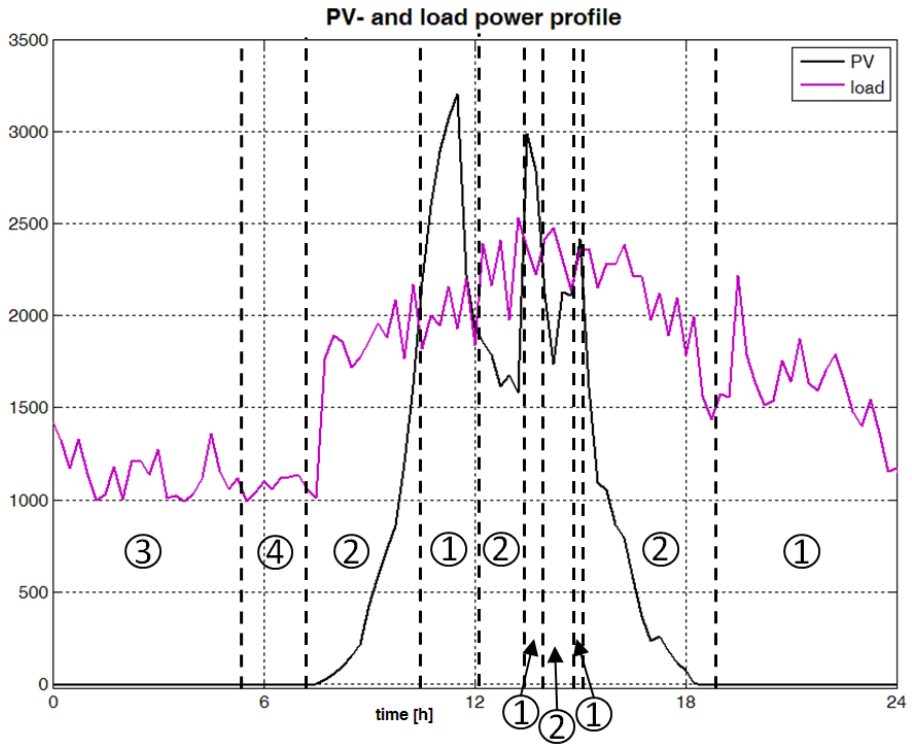

Figure 3.6: Load and PV power profile of a sample day (based on [24])

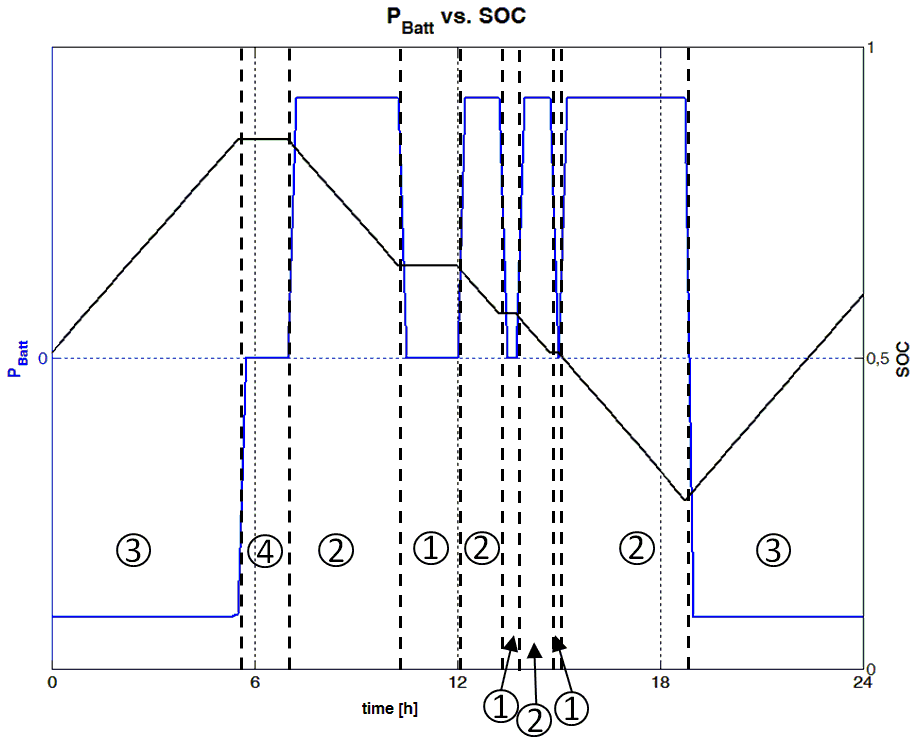

Figure 3.7: Charge / discharge power and the SOC of the battery

Figure 3.6 and 3.7 illustrates the result of the developed EMS for one day. The utility rate used is a TOU rate with two different prices between 7 am (on peak (OP)) and 7 pm (off peak (FP)). In this particular day, four different cases from the strategy occur, which are marked in the figures. The occurred cases are described below:

- **Case 1:** The PV power exceeds the load power and the electricity price exceeds its average. In this case the battery is neither charged nor discharged. The PV surplus power is fed into the grid.
- **Case 2:** The load power exceeds the PV power and the electricity price exceeds its average. In this case the battery is discharged to support the load.
- **Case 3:** The load power exceeds the PV power and the electricity price is smaller than its average value. In this case the battery is charged as the electricity price is low.
- **Case 4:** The same as case 3, but with the difference that the battery is fully charged and therefore, there is no action on the battery.

3.3.2 Calculating the average electricity price

It is important to consider the calculation of the average EP because this value influences the result of the strategy a lot. The different methods, which are considered to calculate the average value, are: mean, median and the average value between the OP and the FP price. For the TOU rate it does not make a difference which method is used for calculating the average price, because there are just 2 different values, on peak and off peak for the same duration of time (12 hours on peak - from 7am to 7pm and 12 hours off peak - from 7pm to 7am), which is shown in Figure 3.8. Figure 3.9 demonstrates the resulting average values when Real Time Pricing is applied.

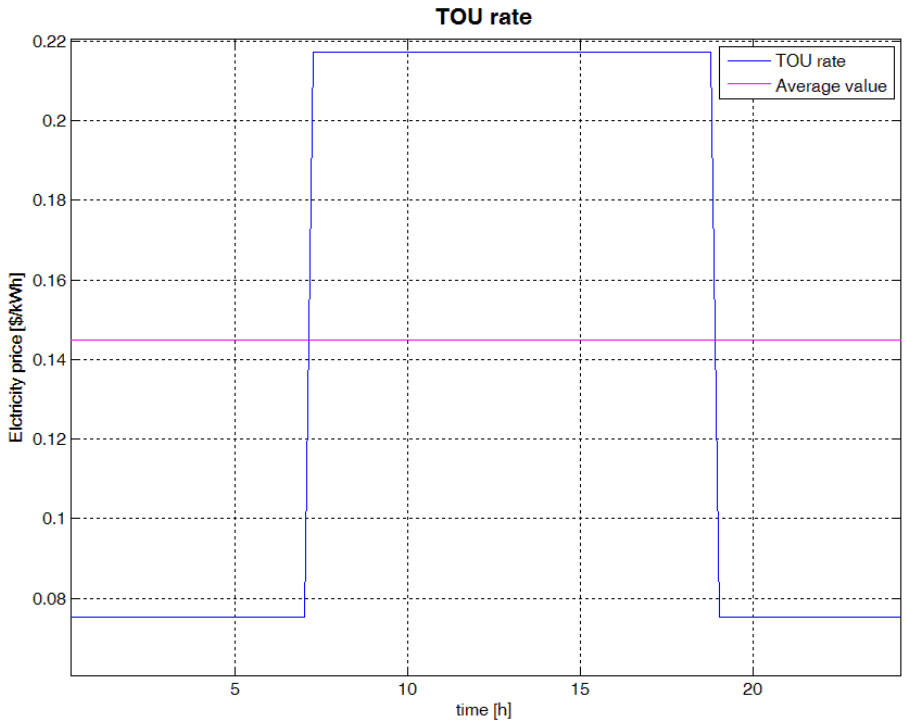

Figure 3.8: Average price for the TOU rating (based on [24])

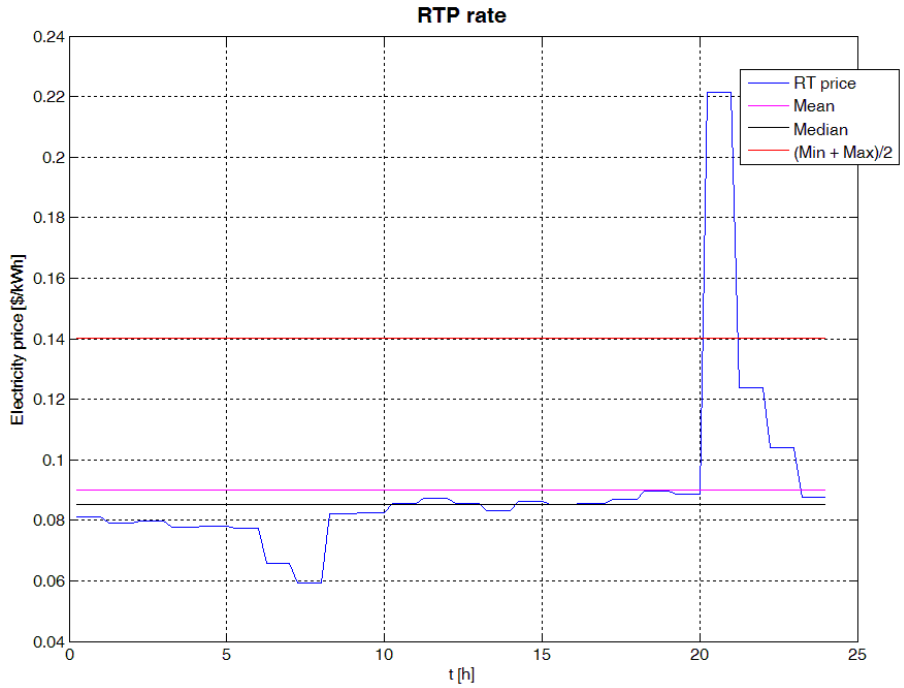

Figure 3.9: Average price for the RTP rating (based on [26])

It is clearly visible that the different methods make a big difference in the result. It can be derived from Figure 3.9 that the peaks of the RTP rating are just present for a short period of time. For the particular day in Figure 3.9, the high peak is only present for 3.25 h and the low peak is also only available for 2.25 h. The electricity price in between the peaks fluctuates around the median in a small range. The simulation result[1] for the RTP rate without using a charge function (the considered average value is taken as threshold value and the applied charge/discharge power equals the power limit). The gained profit for the different calculation of the average value is shown in Table 3.1.

Method	Profit [$]
Median	90.62
Mean	**93.70**
$\frac{OP+FP}{2}$	90.02

Table 3.1: Different approaches to calculate the average value (day ahead price)

It shows that the mean value as average value achieves the highest profit, which is chosen for the calculation in further simulations. As it is mentioned in the intro-

[1]Simulation setting: 1 year simulation, $W = 14.52kWh$, $P_{limit} = 2kW$

duction, the predicted real time price is available $24\,h$ ahead - which is used for the calculation of the average value, because the real price is not available ahead and the aim of this work is to make the whole simulation as lifelike and applicable as possible. It has to be emphasized that the average value is recalculated daily as the price is different for every day. Figure 1.17 shows the differences between the predicted and the real time price. While the RTP is not applicable, it is important to demonstrate the difference in results by running the simulation using the RTP for calculating average price. Table 3.2 shows the results, which are better than the ones shown in Figure 3.1. So a major problem with using the RTP rating is the realization of the control with the imprecise day ahead price.

Method	Profit [$]
Median	118.34
Mean	**126.48**
$\frac{OP+FP}{2}$	93.61

Table 3.2: Different approaches to calculate the average value (real price)

3.3.3 Creating the charge function

Figure 3.10 shows the basic charge/discharge functions f_1, f_2 and f_3. The terms EP_{min} and EP_{max} stand for the minimum and the maximum electricity price. The EP is the electricity price, the FIT is the feed in tariff, and the avg stands for the calculated average electricity price.

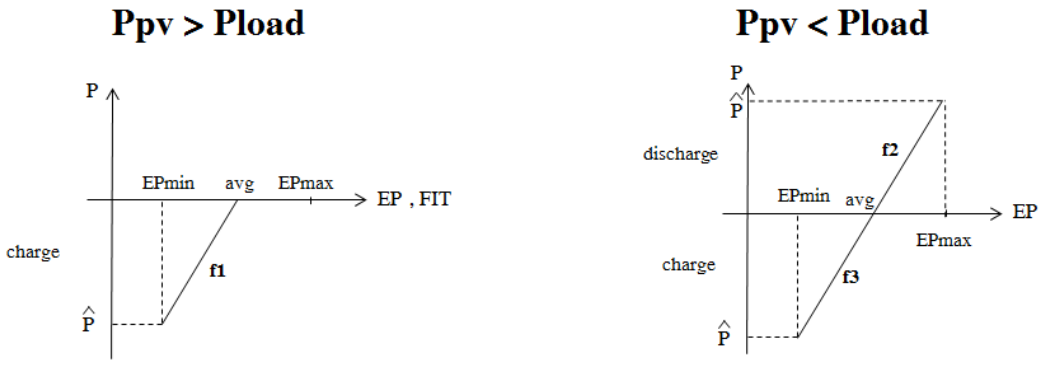

Figure 3.10: Basic charge function

As the charge function only has an influence on the RTP rating, the results in this section belong to this rating type. The reason for separating the functions for the

case $P_{PV} < P_{load}$ into the two functions f_2 and f_3 is due to the fact that the function is defined by the average and the power limit (charge or discharge) as a point of reference. This results in 2 different curves as the average price does not have to be in the center between OP and FP.

The result of implementing this basic function leads to a profit of 89.91 $\$$[2], which is a worse result than only implementing the limit values above or below the threshold for charging/discharging. A main characteristic of the RTP, as mentioned previously, is that the peak values are not present for a long time period and the price fluctuations in between have a rather low amplitude. So the power limit is reached for a short time period and therefore, it leads to a rather low revenue of the BESS. To improve the charge function, the relation between the power limit and the related electricity price is applied at a lower value than the on peak or off peak price. The function is adapted until the profit reaches a maximum, which is shown in Figure 3.11.

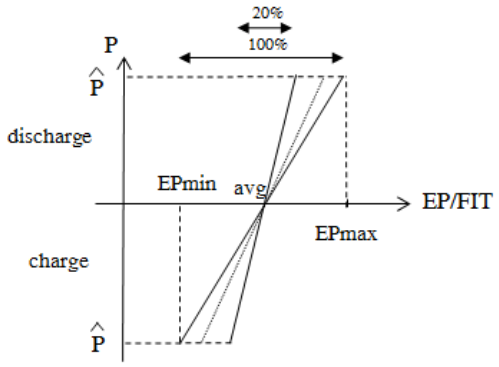

Figure 3.11: Improved charge function

Table 3.3 shows the profit resulting from different adjustment factors to squeeze the charge curve, according to Figure 3.11. The applied variation factor is between $30\,\% - 100\,\%$.

[2]Simulation setting: 1 year simulation, $W = 14.52kWh$, $P_{limit} = 2kW$

Adjustment factor	Profit
100%	89,91
90%	90,98
80%	92,15
70%	93,18
60%	94,09
50%	**94,30**
40%	94,22
30%	89,96

Table 3.3: Different settings on the charge function

For this specific application the charge function reaches the most efficient operating point by using an adjustment factor of 50%.

3.4 Physical based battery lifetime model

This section is written according to the References [11, 16, 15, 17]. The battery model is the core component of this system as it defines the length of the simulation through the implemented lifetime and the available capacity. It's functionality during the simulation is to process charge and discharge actions, which originate from the energy management strategy. The resulting state of charge and state of health are returned to the energy management strategy. The basic interface of the model is shown in Figure 3.12.

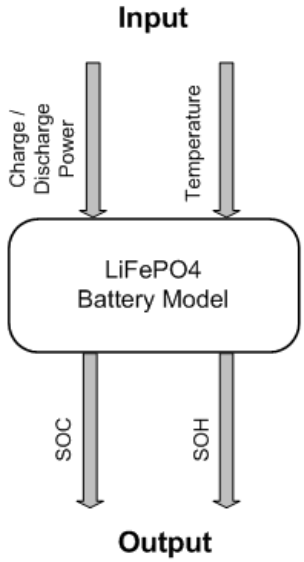

Figure 3.12: Interface of the battery model

The first input is the applied power and the second is the ambient air temperature profile of the battery.

The battery model used is based on the physical parameters according to the equivalent circuit model, shown in Figure 3.13. The chosen battery technology is a Lithium-Iron-Phosphate battery (see Introduction, Chapter 1). The values used for the physical parameters are based on measurements and approximations.

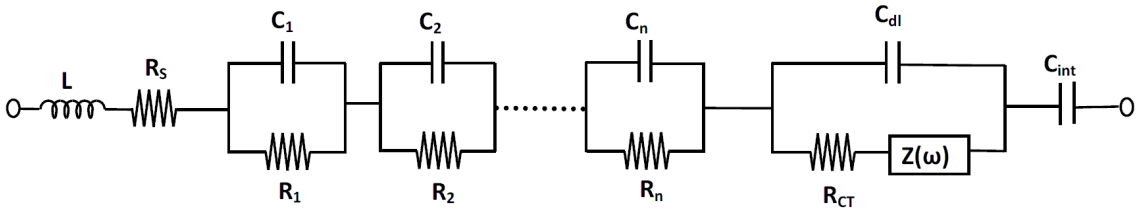

Figure 3.13: Equivalent circuit model [11]

The battery cell used for the measurement is the cell APR18650 CYLINDRICAL from A123 systems [30]. The data sheet related to this battery is shown in the Appendix in Section A.3.

The elements of the battery model are defined in the following paragraph. The inductance L stands for the inductivity caused by the winding from the cylindrical shape. Since there are no dynamics considered in this simulation and the time step for the simulation is 15 minutes long this part of the circuit model is not

considered. R_S is the ohmic conductive and wiring resistance. The $R_n||C_n$ circuits represent the solid electrolyte interphase film which is a covering layer in between the anode (negative electrode) and the electrolyte. This layer will develop if the voltage on a single cell drops below $1\,V$. The series connection of $R\,||\,C$ circuits can be modeled with 1, $2\,or\,n$ elements. Increasing elements in the series connection increases model accuracy, but also increases complexity. A series connection with 3 elements are chosen as a compromise. The parallel connection of C_{dl} and R_{CT} stand for the charge transfer kinetics. R_{CT} is the charge transfer resistance, which from the mathematical point of view is modeled as ohmic resistance, but it has non ohmic resistance. The capacitance of the charge transfer kinetics C_{DL} is the double layer capacitance – occurring between the electrolyte and both electrodes.

The element, which is connected in series to the charge transfer resistance, is the Warburg impedance $Z(\omega)$. This is the nonlinear diffusion at a low frequency.

The capacity C_{int} is the intercalation capacitance, which is caused by ions intercalating into the electrode matrix.

These parameters are measured and calculated by the use of an electrochemical impedance spectroscopy (EIS). This method is usually applied for the characterization of electrode processes and complex interfaces [18]. The output of this measuring technique is the complex impedance with the frequency as parameter (nyquist plot).

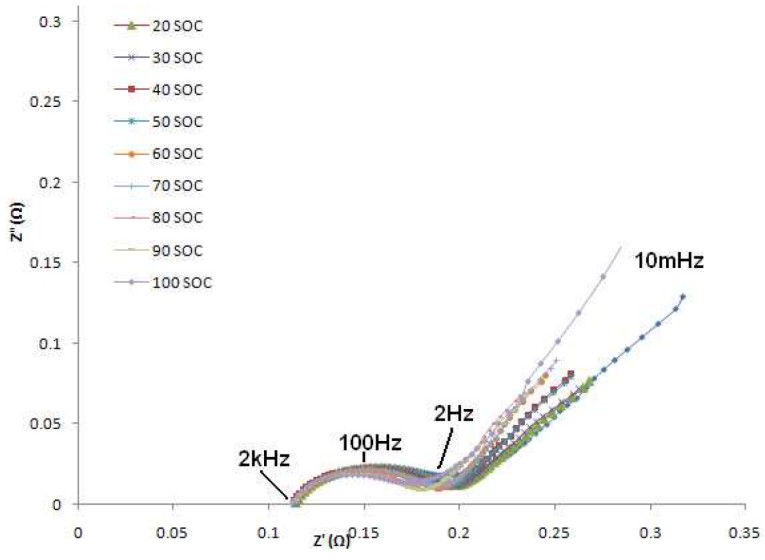

Figure 3.14: Measurement result of the electrochemical impedance spectroscopy [11]

The result from the EIS on the LiFePO4 battery is shown in Figure 3.14. This dia-

gram includes several graphs, where each one stands for a different state of charge. It is applied from 20 % - 100 % in steps of 10 %. The frequency range of the EIS is applied between $10\,mHz$ and $2\,kHz$. The x-axis ($Z'(\omega)$) shows the real impedance, whereas the y-axis displays the negative imaginary axis ($Z''(\omega)$). Figure 3.15 illustrates how the physical parameters are derived out of the impedance plot.

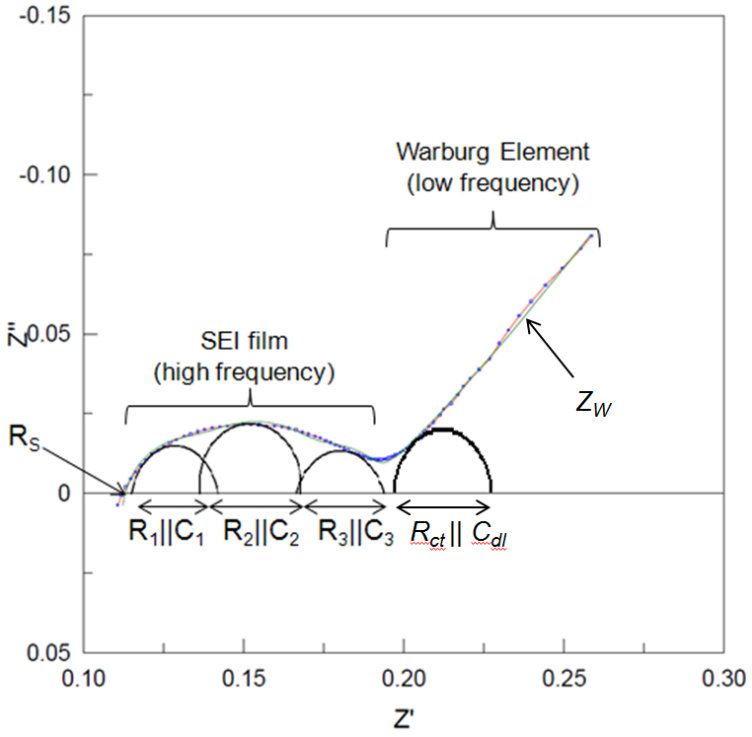

Figure 3.15: Parameter determination

The ohmic resistance, R_S, equals the value at the intersection of the graph with the x-axis. The values for $R_n||C_n$ are determined by placing circles under the elliptical shape, since a circle in the nyquist plot equals a parallel connection of an ohmic resistor and a capacity. The same method is applied for the charge transfer kinetics right beyond the elliptical shape, as it is also shown in Figure 3.15. The Warburg impedance, $Z(\omega)$, is derived in the small frequency range (at the right side of the nyquist plot) at the point where the function can be treated as linear and $Z(\omega)$ can be calculated from the slope. But in practice, this function is not linear and would not cross the x-axis if only the Warburg impedance would be plotted. The parameter C_{int}, the intercalation capacitance, is responsible for the turn and this function would never cross the x-axis.

The resulting values for each considered state of charge is shown in Table 3.4.

SOC	100%	90%	80%	70%	60%	50%	40%	30%	20%	10%	0%
Rs(Ω)	0.106	0.11	0.11	0.11	0.11	0.11	0.11	0.11	0.109	0.11	0.11
R1(Ω)	0.011	0.01	0.01	0.01	0.01	0.01	0.01	0.01	0.009	0.01	0.04
C1(F)	8.412	9.72	11.2	9.59	7.62	5.05	5.12	5.77	5.825	8.08	3.92
R2(Ω)	0.021	0.02	0.02	0.02	0.02	0.02	0.02	0.02	0.022	0.02	0.02
C2(F)	0.01	0.01	0.01	0.01	0.01	0.01	0.01	0.01	0.01	0.01	0.01
R3(Ω)	0.015	0.02	0.02	0.02	0.02	0.02	0.02	0.03	0.025	0.02	0.05
C3(F)	0.542	0.34	0.39	0.35	0.31	0.25	0.26	0.26	0.267	0.41	0.45
Rct(Ω)	0.025	0.03	0.03	0.03	0.03	0.27	0.03	0.03	0.028	0.03	0.03
Cdl(F)	0.053	0.04	0.05	0.05	0.05	0.04	0.04	0.04	0.046	0.05	0.09
W-R(W)	0.562	0.35	0.18	0.22	0.22	0.34	0.33	0.26	0.512	0.42	3.63
W-T	234.9	314	104	101	110	193	185	117	379.4	99.5	279
W-P	0.5	0.5	0.5	0.5	0.5	0.5	0.5	0.5	0.5	0.5	0.5
Cint(Ω)	264	1446	728	501	600	1361	1190	2428	10767	913	21

Table 3.4: Parameter values of the battery model [11]

In order to get the component values according Table 3.4 for continuous and not discrete state of charges the measured values are approximated with a linear function as it is shown in Figure 3.16, which represents the fit for the resistance R_S.

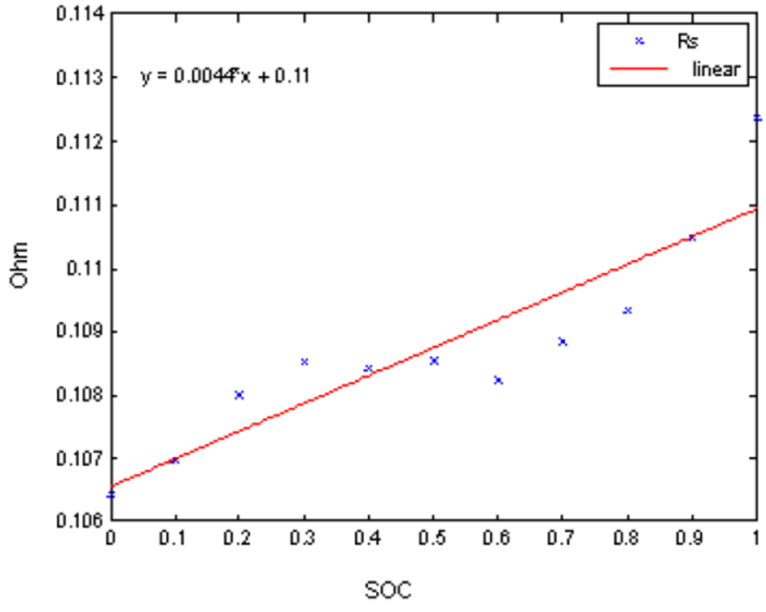

Figure 3.16: Parameter estimation, R_S as an example [11]

To verify the accuracy of the model, the simulated and the measured discharging

curves are compared in Figure 3.17. The left graph shows the discharge curve at a $1\,C$-rate[3]. The right graph discharges with a current of $\frac{1}{2}\,C$-rate. In conclusion a lower discharge current makes the model more accurate.

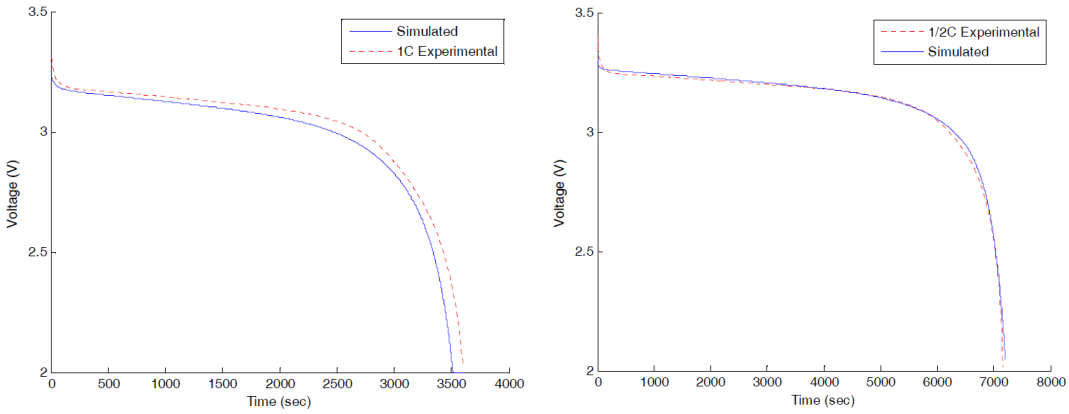

Figure 3.17: Discharge Simulation; left 1 C rate, right 0.5 C rate [11]

The battery model is used in the simulation to calculate the current state of charge and state of health, based on the charge/discharge power.

- ***SOC***
  The calculation of the actual SOC is a function based on the parameters, mentioned in the Equation 3.1.

$$SOC_i = f\left(physical\,parameters,\, OCV_i,\, p_i,\, SOC_{i-1}\right) \tag{3.1}$$

  $physical\,parameters$ ... derived parameters according to 3.13
  OCV_i ... actual open circuit voltage
  p_i ... actual charge / discharge power
  SOC_{i-1} ... previous state of charge
  A detailed description for the calculation of the state of charge can be found in [11].

- ***SOH***
  This output value is a major part of this battery model, because it defines the available capacity and the end of life of the battery. This value is also known as the irreversible capacity loss or the irreversible self discharge, which

[3]C-rate: Definition of the charge/discharge current based on the capacity of the battery divided by one second.

equals the lost capacity. It is split into 2 different specifications. First, the cyclation based state of health (SOH_C) and second the irreversible capacity loss caused by the calendrical aging (SOH_t). In general, the end of life of the battery is reached as soon as its capacity in a fully charged state reaches less than 80% of the initial capacity. This specific value is recommended from the manufacturer and also mentioned in the literature [15].
In general, the effect of the aging causes an increase of the internal resistance and therefore an increase in the power loss. Usually, the aging mechanism of Li-Ion batteries takes place at the barrier layer between the anode and the cathode with the electrolyte. The main cause of aging is the creation of a covering layer on the electrodes, which is known as the SEI-film[4]. Table 3.5 shows the main characteristics including the cause and effect of the different types of the SOH, which is created according to Reference [15].

SOH	Initiator	Cause	Effect	Result
SOH_c	- High amount of cyclation - High SOC	Volume change and SEI creation cause a change through a parasitic reaction	- Increase of the internal resistance - Over voltage	Capacity- and Power loss
SOH_t	- High temperature - High SOC	- Decomposition of the electrolyte (SEI) - Decrease in the reachable surface because of the gain of the SEI-film	- Increase of the internal resistance - Lithium loss	Power loss

Table 3.5: Cause and effect of the aging of Lithium-Ion batteries

In the following paragraphs are the cyclation based state of health and the calendrical aging described.

- Cyclation based capacity loss : SOH_c
  The cyclation based capacity loss, SOH_c, is based on counting the amount of transferred charge. To calculate this value the specification from the manufacturer is taken into account. There is a big dependency between the charge / discharge current and the ambient temperature on the lifetime of the battery.

[4]SEI-film: Through a reaction from the active material with the electrolyte, respectively through decomposing the electrolyte, a covering layer is built up at the anode. [15].

Figure 3.18 shows a graph from the data sheet of the manufacturer A123 but for a different cell (ANR26650) and not the considered one (APR18650). The difference in cell types is just the capacity.

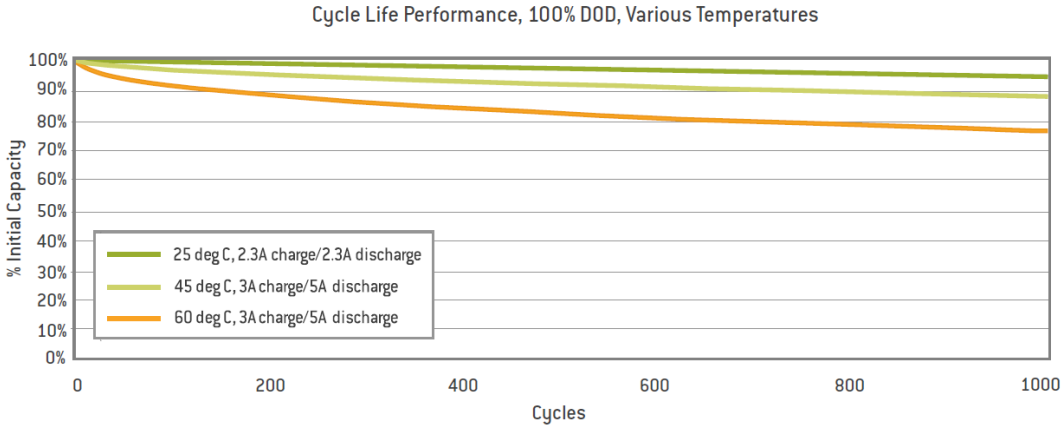

Figure 3.18: Lifetime prediction for different parameters [30]

The characteristics of these two battery types are the same and therefore, the lifetime is also the same. The displayed data shows the dependency between the lifetime and the applied charge / discharge current, and average temperature. The higher the temperature and the C-rate, the lower the lifetime.
The assumed amount of cycles for the cyclation based state of health is taken from the manufacturer [30] with a $2\,C$-rate for discharging and a $1\,C$-rate for charging at room temperature. This data is assumed to be average for the whole simulation and is the basis for SOH_C. In this case the aimed $80\,\%$ mark is reached after $2,000\,cycles$, considering a depth of discharge of $100\,\%$. Figure 3.19 illustrates the available amount of coulombs for the considered condition which reveals a capacity of $220\,Ah$ to transfer.

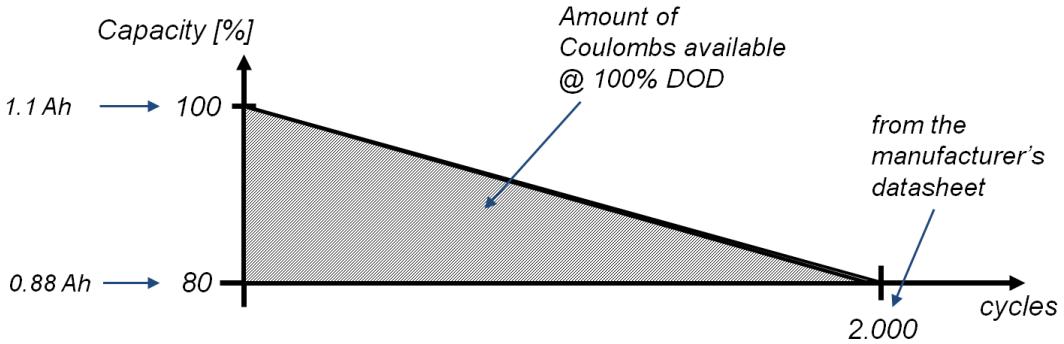

Figure 3.19: Calculation of the SOH_c

As the capacity also decreases with the calendrical aging, the battery can not reach the specified $2,000\,cycles$ with the SOH_C. Therefore, a linear function to model the trend of SOH_C has to be investigated.
The ambient air temperature also influences the cyclation based capacity loss. This influence is indirectly considered because it affects the terminal voltage and through a considered constant charge / discharge power, the current changes. The changes in current influences the amount of coulombs which are transferred from / to the battery. Thus, there is an indirect relationship between the temperature and the SOH_C.

- Calendrical aging: SOH_t
  This effect applies stronger on Lithium-Ion batteries than for other chemistries and it only occurs if the battery is in an unoperated state. The three main influence factors for this effect are temperature, current SOC, and the unoperated time. The measurement data which is taken to implement this aging effect originates from a Master Thesis from the University of Munich, Germany [15]. This thesis presents a measurement based model for calendrical aging of LiFePO4 batteries. The battery cell type used for the measurements is the cell *APR18650* from *A123 Systems*, which is the same type as it is used in this research. The measurement value, taken from that research, is shown in Table 3.6.

Temp. [°C] \ SOC [%]	10	33	55	78	100
0					$7,121.10^{-5}$
10		$4,783.10^{-5}$		$1,0153.10^{-4}$	$5,377.10^{-5}$
20			$1,131.10^{-4}$		$1,9432.10^{-4}$
30		$1,1535.10^{-4}$		$2,8608.10^{-4}$	$4,8602.10^{-4}$
40	$3,74.10^{-4}$		$3,548.10^{-4}$		$9,2203.10^{-4}$
50		$6,709.10^{-4}$		$1,1082.10^{-3}$	$1,4955.10^{-3}$
60	$9,4.10^{-4}$		$1,669.10^{-3}$		$2,1996.10^{-3}$

Table 3.6: Measurement data for the SOH_t (based on [15])

The measurement data is just available for 5 different SOC and 6 different temperature values. To get the capacity loss, for every SOC and temperature, a polynomial function is fit into this data. Figure 3.20 shows the measurement data including the polynomial fit. For this specific application a function of the third order was taken to fit the trend of the SOH_t. The y-axis shows the decrease in the SOH_t per day and the x-axis shows the temperature in $[°C]$.

Each curve stands for a different average SOC value. The appropriate black graph represents the particular fit, which is calculated with the least square method (LMS) [21].

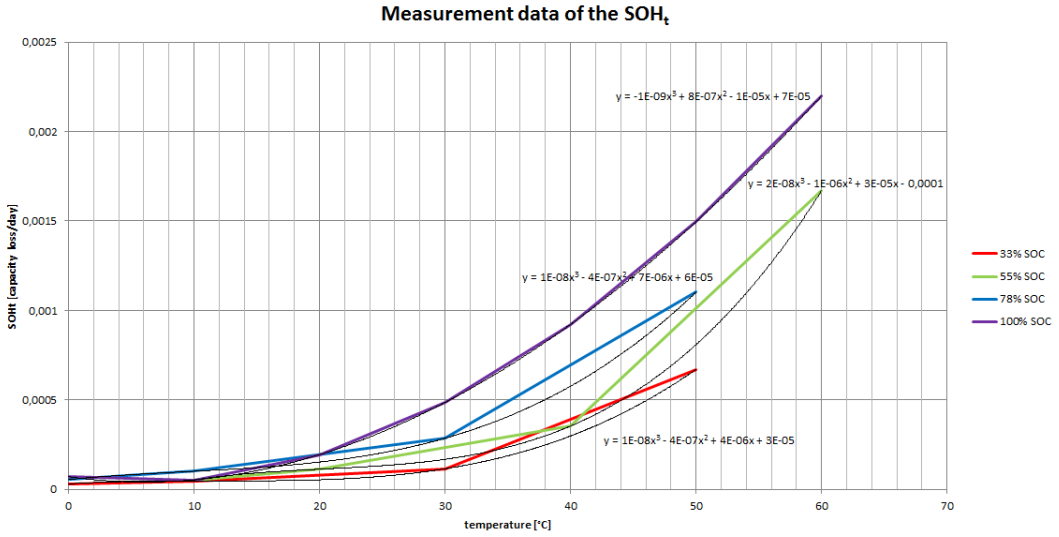

Figure 3.20: Measurement data of the SOH_t depending of the temperature and the average SOC

The general function for calculating the SOH_t, depending on the temperature and the average SOC, is a third order polynomial function (Equation 3.2).

$$SOH_t = a \,.\, T^3 + b \,.\, T^2 + c \,.\, T + d \tag{3.2}$$

The measurement data is fit to a polynomial function to obtain the parameters a, b, c and d. For each SOC value, different parameters are calculated, as the capacity loss is a two dimensional function $f(T, SOC)$. To be able to get a general function of these parameters, another fit is applied through the different parameters of the polynomial function. In this case, the parameters are dependent on the SOC, whereas the basic function depends on the temperature. The function used to fit these parameters is also a third order polynomial function. Therefore, the required SOH_t is calculated in two steps. First, the parameters a, b, c and d are calculated, based on the current SOC. Second, the SOH_t is calculated with these parameters based on the temperature. The result shows the decrease in the state of health of the battery for a whole day. As the time step of this simulation is set to 15 minutes, the resulting value for the SOH_t is also down scaled to this time base.

As this aging only appears if the battery is in an unoperated state, the function for accumulating the calendrical aging is only called when the charge / discharge power is $P = 0\,W$. MATLAB® uses a double precision (64 bit) floating point data type by default. It is important not to compare a floating point number with a specific value on equity, because the floating point data type has a limited accuracy, which may cause a wrong result if it is compared with an integer value for example. To avoid this kind of error the battery is treated to be in an unoperated state as the charge / discharge power is lower than 0.5 % of its power limit.

As the irreversible capacity loss of SOH_c and SOH_t is independent of each other, both can not be in affect at the same time. The resulting SOH of the battery is calculated by summing the individual parts (Equation 3.3).

$$\Delta SOH = \Delta SOH_c + \Delta SOH_t \tag{3.3}$$

An indicator of an efficient usage of the battery is the difference between the calendrical and the cyclation based aging. The higher the calendrical aging compared to the cyclation based aging, the lower the usage efficiency is.

3.5 Cost calculation

The cost function calculates the reachable profit of the whole system, which is the criteria for the resulting battery size. This function consists of the annual revenue of the battery storage system (Equation 3.4).

$$B_{total} = \sum_{i=1}^{lifetime} (R_{Annual}\ f(i)) - C_{Capital} \tag{3.4}$$

R_{Annual} ... Annual revenue of the BESS

$f(i)$ ... Decrease of the revenue caused by the capacity loss through aging

$C_{Capital}$ ... Initial cost of the energy storage system (battery + inverter)

B_{total} ... Overall benefit

The annual revenue of the BESS is defined in Equation 3.5.

$$R_{Annual} = b_{WB} - b_B \tag{3.5}$$

b_{WB} ... Annual electrical energy cost without a BESS

b_B ... Annual electrical energy cost with a BESS

The proposed sizing algorithm contains a lot of data and takes a long time to run the simulation. To avoid lengthy simulations, only a few years are modeled and fit to a function to the trend line of the calculated state of health to predict the lifetime and the change in the annual profit. A function has to be defined to apply this approach.
The graph in Figure 3.21 shows the SOH after a 3 year simulation. (Note: Every simulation in this section relies on a basic energy management strategy, uses $2,000$ battery cells which are equal to $7.26\,kWh$, and a power limit of $2\,kW$). The blue line shows the simulated data and the red line shows the fitted linear function. The SOH fluctuates around the linear fit but its average value is very close to the simulation result.

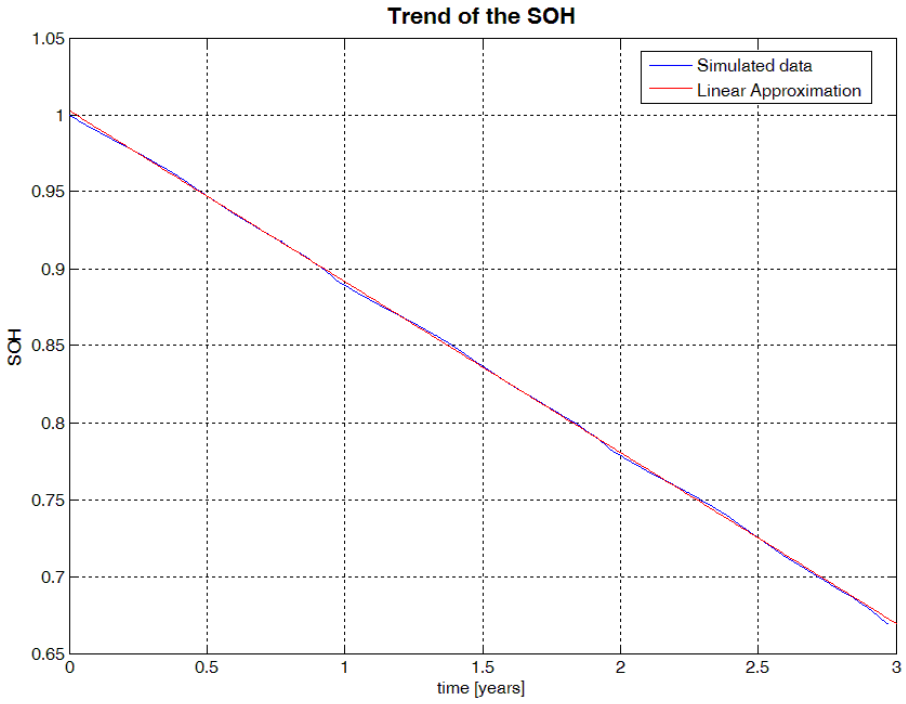

Figure 3.21: Comparison of the simulation result and the approximated result

To use this similarity, a linear function has to be defined which is applied to the cost function (Equation 3.6). For the cost function, it is only necessary to simulate values for one year because the decrease in the SOH is treated as linear which leads to a constant share of the annual capital cost. ΔSOH stands for the annual change of the SOH. The annual revenue is also treated to be linear.

$$B_{Annual} = R_{Annual} - C_{capital} \,.\, \Delta SOH \tag{3.6}$$

The simulation runs for a whole battery lifetime to verify the linear assumption, which is the red curve in Figure 3.22. This diagram shows the result between the middle of the 8th year and the end of life which is close to the 10th simulation year. For comparison, a quadratic fit is also applied to the simulated data, which is the green graph in the diagram. The result is different than expected. The behavior of the state of health over the whole lifetime has a quadratic characteristic.

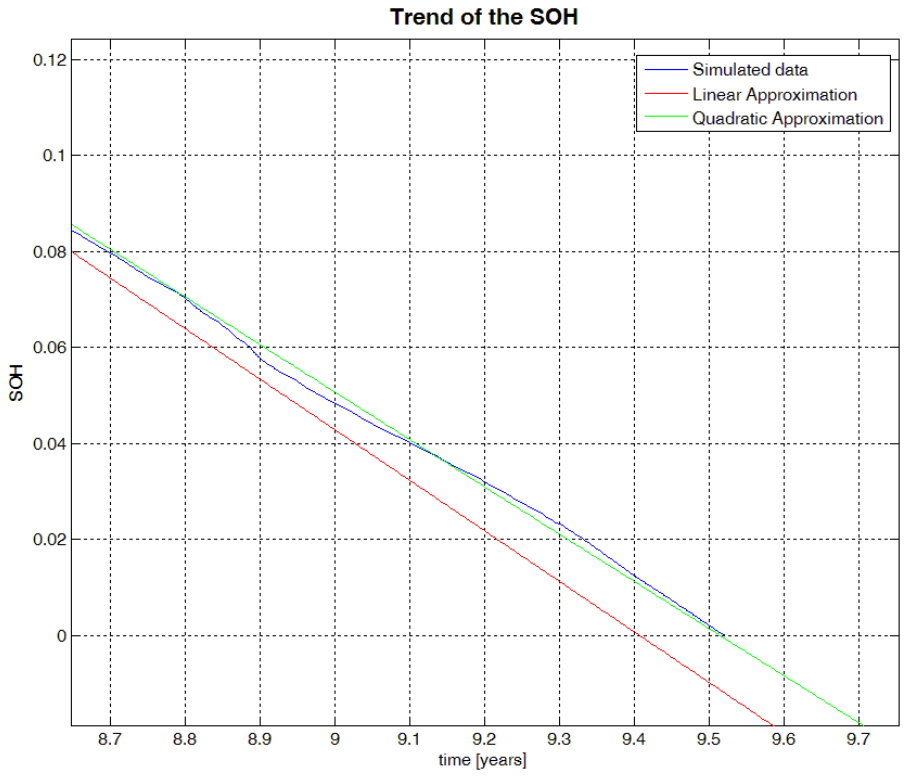

Figure 3.22: Comparison of the simulation result and an approximation with a linear and a quadratic approach for the whole battery life

Therefore, it is assumed to calculate the SOH with a quadratic fit, based on a three year simulation. To verify this approach, the simulation is executed again for the

whole lifetime and the predicted SOH is based on the three year simulation. Figure 3.23 displays the result of the simulation.

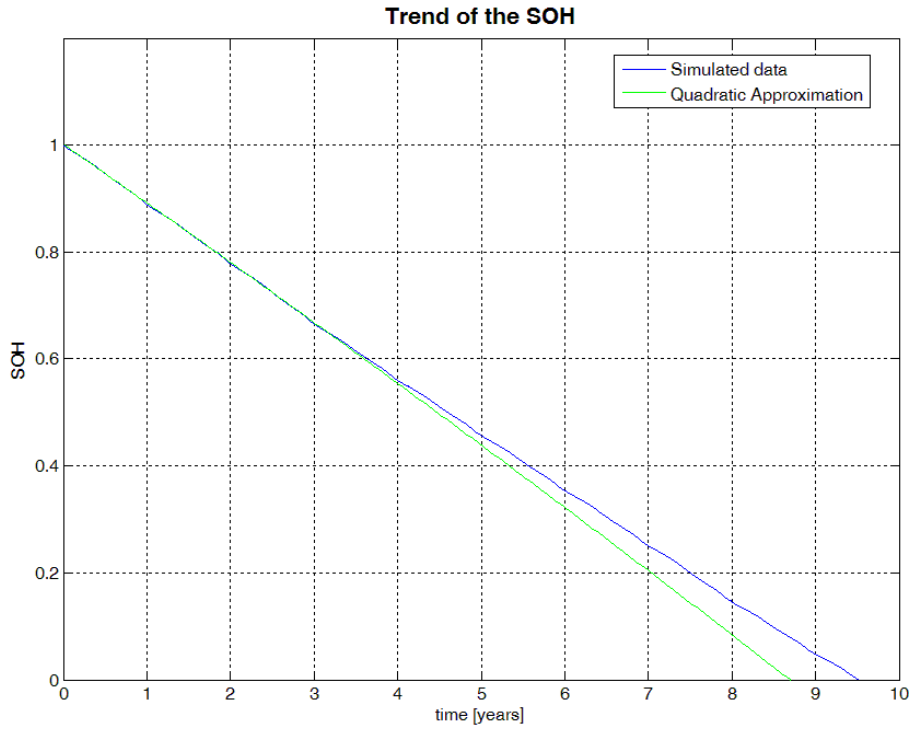

Figure 3.23: Comparison of the lifetime estimation with the whole life simulation

The whole life simulation outputs a lifetime of 9.52 $years$. The predicted lifetime (based on the three year simulation) resulted in a lifetime of 8.69 $years$, which leads to an error of 8.72 % (Figure 3.23) which is too inaccurate to apply it in the simulation.

Hence, the simulation has to be run till the battery is dead to achieve an accurate result. Furthermore, Equation 3.7 is used to calculate the whole benefit of the system for the entire battery lifetime.

$$B_{total} = \sum_{i=1}^{lifetime} (R(i)_{Annual}) - C_{Capital} \tag{3.7}$$

For different simulation settings, e.g. different capacities of the battery, the resulting lifetime of the battery differs. Therefore, to calculate the most cost effective battery size it is important not just to compare the overall benefit of the system. The significant criterion is the calculated average annual benefit of the system, shown in Equation 3.8, which is applied in the simulation.

$$B_{total} = \frac{\sum_{i=1}^{lifetime} (R(i)_{Annual}) - C_{Capital}}{lifetime} \tag{3.8}$$

In addition to the annual revenue, the capital cost of the BESS is also a fundamental part of the cost calculation. It consists of two separate parts: the battery and the inverter. These devices are taken into account by using a capacity factor $c_W = \left[\frac{\$}{Wh}\right]$ and a power factor $c_P = \left[\frac{\$}{W}\right]$. The general equation to calculate the capital cost is shown in Equation 3.9, where P_{max} stands for the power limit to charge / discharge the battery and W is the capacity of the battery.

$$C_{Capital} = c_P \, P_{max} + c_W \, W \tag{3.9}$$

A review of battery retail prices showed that the price does not just depend on the capacity rating. The maximum charge / discharge power also has an impact on its price. Therefore, the battery cost itself consists of both, a capacity coefficient c_W and of a power coefficient c_P. The power coefficient was also considered in the previous equation, but just for the inverter. This way of calculating the battery price is frequently used in the Literature [14, 19, 20]. The calculation of the parameters can be split up, as it is shown in Formula 3.10. It is assumed that the relation between the power and the price is linear, as well as the capacity and the price. The coefficients $d_{Battery}$ and $d_{Converter}$ are mentioned to consider a possible offset on the linear function.

$$C_{Capital} = (c_{P\,battery} + c_{P\,inverter}) \; P + c_{W\,battery} \, W + (d_{battery} + d_{inverter}) \tag{3.10}$$

The calculation of the cost coefficients is shown in the following paragraphs, which is split up into the coefficient for the battery and for the inverter part.

- Battery cost
  The prices used for the calculation of the battery factors are taken from the retailer *A123RC* [29]. To get a power factor, $c_{P\,battery}$, and a capacity factor, $c_{W\,battery}$, out of this data, different battery cells are taken into account to get different capacity and power ratings for the calculation. The basic condition for the considered cell types are the same manufacturer (*A123 Systems*

[30]) and equal chemical components. The chosen cell types are APR18650, ANR26650 and AMP20. The battery model used is based on the cell type *APR18650* from *A123 Systems*.
As there is no function describing the relationship between the technical details and the price of the chosen batteries, a function has to be fit into the manufacturer's listed data. There are three data sets available and just two parameters to identify[5]. This leads to an overdetermined equation system, which is solved by using the LMS [21]. The resulting parameters from the least square method are $c_{P\,Battery} = 1.79\,10^{-3}\,\$/W$ and $c_{W\,Battery} = 0.7533\,\$/Wh$. The calculation showed that there is no offset price necessary. If $d_{Battery}$ would be considered in the calculation it would result to a value of about four dollars, which is insignificant and can be omitted, therefore $d_{Battery} = 0$.

- Inverter cost
  The prices for the inverter cost are taken from the company SMA [31]. The inverter produced by this company is focused on PV applications, but the technology is the same as that used for battery charging. Therefore, it is reasonable to take prices from their products. The calculation of the parameters are again accounted with the LMS because of an overdetermined equation system. The results are: $c_{P\,inverter} = 0.31366\,\$/W$ and $d_{inverter} = 813.87\,\$$. In this case the offset has a considerable value and is considered in the cost calculation.

The values calculated above can now be combined into a new capital cost equation (Equation 3.11).

$$C_{Capital} = 0.31545\,P + 0.75331\,W + 813.87 \tag{3.11}$$

$[C_{capital}] = \$$

$[P] = W$

$[W] = Wh$

For the whole cost calculation, especially for the calculation of the benefit of the BESS, it is important to consider that the utility does not pay a customer money

[5]For this calculation it is assumed that there is no offset on the Battery price. Just the parameters c_P and c_W are calculated.

back if there would be a negative electricity bill. A negative bill could result from a high energy consumption at low prices in combination with a high amount of feed in at high prices. This case would be treated as a 0$ bill.

3.6 Simulation

The software product used for realizing the battery sizing strategy is MATLAB® (version R2008a). It uses double precision floating point numbers as the default data type and all computations are based on a numerical calculation, which makes it hard to deal with unknown variables and should be avoided.

MATLAB® offers different alternatives for the realization of a simulation. Here, a script file ("$m - file$"), which runs the simulation sequentially, line by line, is implemented, as it is shown in the flow chart in Figure 3.1.

Chapter 4

Implementation and verification of the proposed battery sizing strategy

The implementation and verification chapter includes a description of the chosen simulation scenario, the simulation results, and a discussion.

4.1 Simulation scenario

The chosen location for the simulation is Tallahassee, FL, USA and the necessary simulation data originates from this city to get a lifelike simulation results.

4.1.1 PV and load data

The simulation input data originates from a house in Tallahassee, which provides the raw data of their produced PV and their used load data online as download [24]. The characteristic of this data matches a residential character of power consumption, which has its power peak in the afternoon, which does not correlate well with the produced PV power (Figure 1.7). A commercial building / industry compared to the residential consumer usually has the power peak around noon which correlate better with the PV panel output power.

The peak power of this consumer load is $\hat{P}_{load} = 17.6\,kW$ and the installed PV system has a peak power of $\hat{P}_{PV} = 13\,kW$. These power ratings are much higher than an average residential customer. To get a realistic value, the downloaded data

is scaled with a factor of 0.4 for the PV power to get a value of $\hat{P}_{PV} = 5,2\,kW$ and a factor of 0.3 for the load data to get a load peak of $\hat{P}_{load} = 5.28\,kW$. The provided data is available in a time step of 1 minute. As the simulation time step is 15 minutes, this input data is averaged and scaled to get a time step of 15 minutes. As the customer started to record the data and provide it online at the end of December 2010 and the simulation was created in July 2011, there was just simulation data for half a year available. As the simulation is designed to use annual input data, the available data (Jan11 - Jun11) is taken, copied, flipped, and treated as a whole year (Jan - Jun : Jun - Jan). The PV and load power profiles used are shown in the Appendix in SectionA.1 and A.2.
The length of the simulation is defined by the battery life. The simulation data is considered to be the same for every year to be able to simulate for the whole battery lifetime which can be 10 years or longer, depending on the battery and the usage.

4.1.2 Temperature data

As the battery is considered to be stored underneath the house, the ambient air temperature is taken as the influencing temperature on the battery. This data originates from a meteorological homepage [32], which provides hourly historical temperature data. To have a consistent input data, the temperature is taken for the same period of time as the PV and the load data originates from.

4.1.3 Utility rate

The simulation uses the TOU and the RTP as utility rating system.

The time of use rate is taken from the Tallahassee Utility [25] with an off peak price of $7.536\,¢/kWh$ and an on peak price of $21.715\,¢/kWh$. On peak is between 7am and 7pm, whereas the off peak price is in remaining period.

The real time pricing rate is taken from the utility company ComEd [26]. This company is the only utility which offers this rate for residential usage. As ComEd is located in Illinois and the simulation location is in Florida, the electricity price has to be adapted to the applied region, which is taken from Reference [1]. The spreadsheet with the state-level energy prices is is shown in the Appendix in Section A.4. Electricity costs are mentioned in this paper as state-level prices and are quoted in $\$/(Million\,Btu)$. As ratings for both Illinois and Florida are given in this unit it

does not have to be converted and just the relation between these two values is taken to adapt the price from Illinois to Florida. Florida has an average electricity price of $21.47\,\$/(Million\,Btu)$ and Illinois has a price of $17.27\,\$/(Million\,Btu)$. Therefore, the downloaded RTP rate is adapted by scaling it with a factor of $\frac{21.47}{17.27}$.

The feed in tariff is treated in this simulation as $FIT = EP$, as it is accounted by the Tallahassee Utility. To get a comparable scenario the FIT for the RTP is also treated with this relation to reach a comparable rate.

4.1.4 Chosen depth of discharge

The chosen operation interval of the battery is between $15\,\% - 85\,\%$ SOC. The limitations are justified so that the battery is not damaged by a deep discharge and to make sure the battery is not overcharged. The DOD would be a variable parameter if the battery model would include a more accurate implementation of the cyclation based state of health, which is projected to work on that in the future. The current status of the implementation of the SOH_C includes just a linear relationship between the DOD and the lifetime, which is not accurate considering discharging down to almost $0\,\%$ SOC.

4.2 Simulation results

The simulation results are based on a comparison of a different utility rating (TOU and RTP) and comparing a simple battery model to the physical based battery lifetime model.

4.2.1 Different utility rate

- Time of use
  The trend of the PV-, grid-, load-, and battery power of 1 day of a whole lifetime simulation is shown in Figure 4.1. This day was chosen because in the morning and in the afternoon the PV is relatively low, whereas at noon it exceeds at least the load power which covers all considered cases for the EMS. The displayed example is for a power limit of $2.5\,kW$ and a capacity of $47.19\,kWh$. At the on peak time with the expensive prices, the load power

exceeds the PV power and the battery supports at least the load. At the PV surplus, the load demand is covered by the PV and the surplus energy is fed into the grid because the benefit is high at on peak times.

Figure 4.1: Power profile of P_{PV}, P_{load}, P_{grid} and $P_{battery}$

In Figure 4.2 is the difference between the grid power when using and not using a battery is demonstrated. The usage during off peak is higher with the battery, because the energy management strategy takes advantage of the cheap energy to charge the battery. During the on peak period and as long as the PV power does not exceed the load power, the battery energy is taken primarily to support the load energy and also to support the grid. As the PV power exceeds the load power, the battery is just in charging mode if the electricity price is low enough (this case is just important for the real time pricing, because the TOU rates usually have the high price during the day, where also the PV power has its peak at ideal weather conditions).

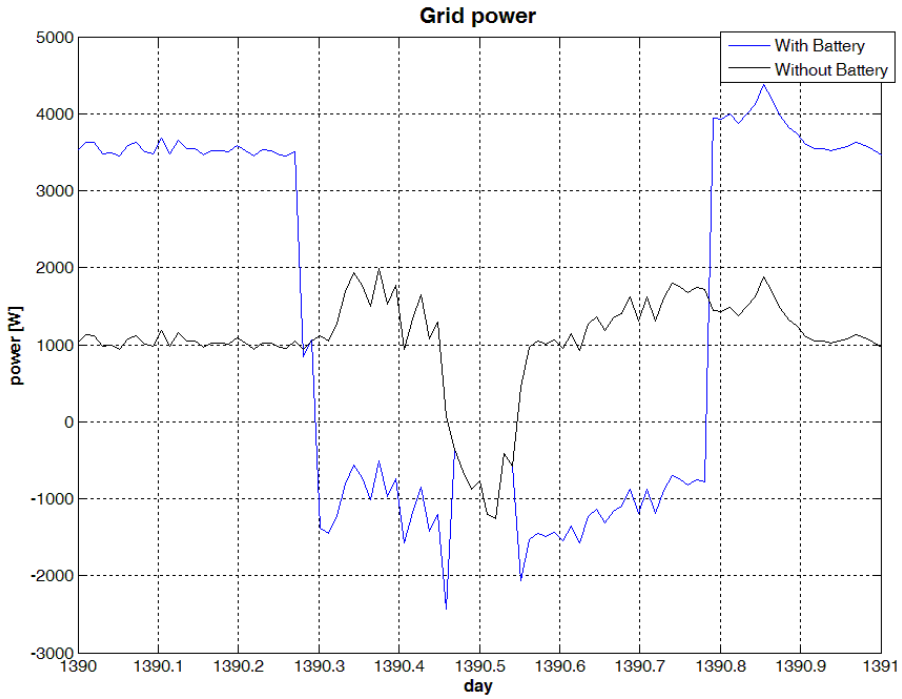

Figure 4.2: Grid power with / without using a battery

Figure 4.3 shows the annual profit after a whole battery life simulation. This profit depends on the maximum charge/discharge power and the capacity of the battery. The price consists the battery and the inverter part, as it was mentioned in Chapter 3.5.

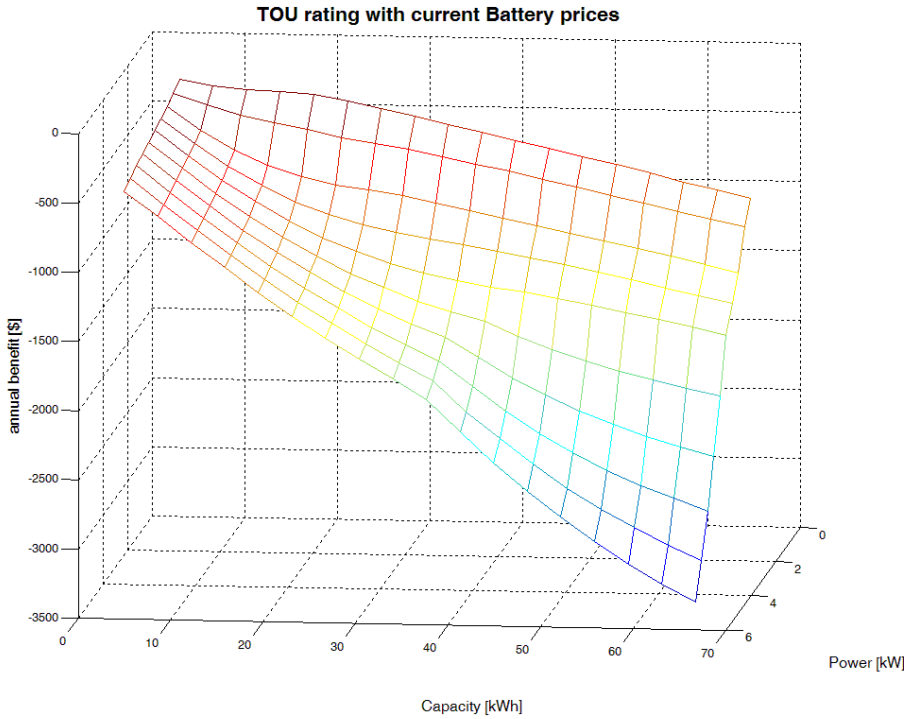

Figure 4.3: Annual profit of the BESS (with the current battery price)

It is evident, that there is no positive profit achievable with the BESS in this specified scenario. The reason for this negative profit is shown in Figure 4.4, which displays the capital cost of the battery system and the benefit of the electrical energy cost, depending on the capacity. The power limit for this graph is fixed to a value of $2.5\,kW$.

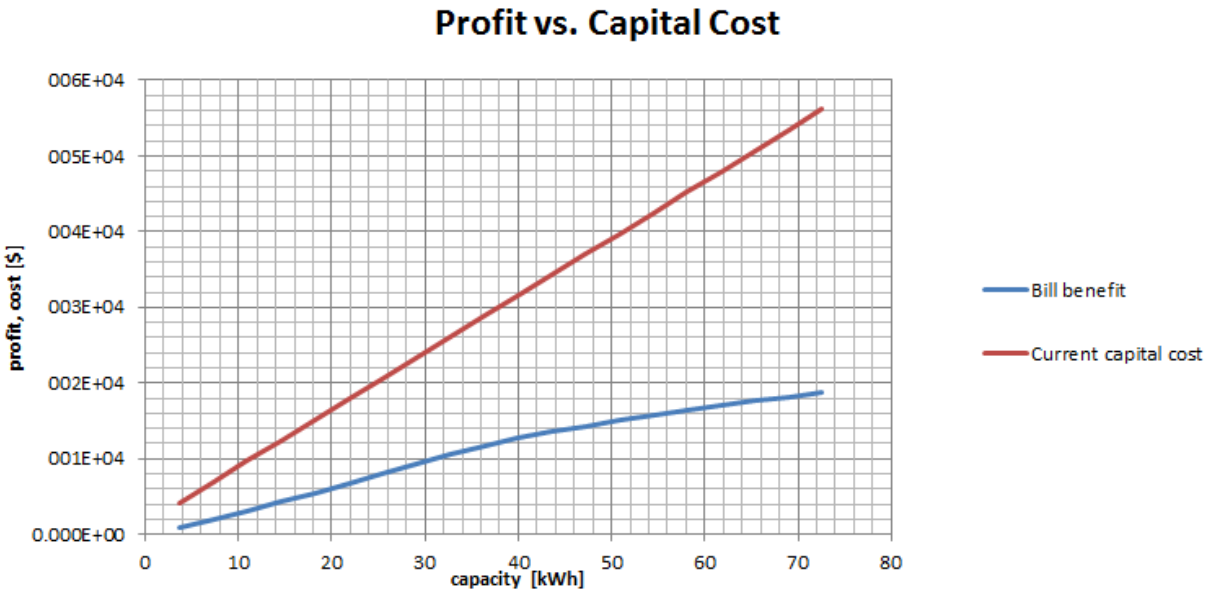

Figure 4.4: Capital cost and bill benefit with the current battery price

Since the capital cost is always higher than the benefit, it is not possible that the profit reaches a positive value. The used battery type (LiFePO4) is still a new technology which leads to a high price. Considering the price development of the Lithium Ion batteries for the used battery type the result would be different. The price of the Li-Ion batteries dropped in 5 years down to $\frac{1}{3}$, as it is shown in Figure 1.12 and already mentioned in Chapter 1. It is reasonable to apply this price development from the Li-Ion batteries to the LiFePO4 technology because the raw material for this battery type is very low and as this technology gets more popular the price will decrease. The price reduction is just considered for the battery part, because the used inverter technology is not a new invention and will stay about the same price. Applying the future price of $\frac{1}{3}$ to the battery a positive profit is gained out of the system, which is shown in Figure 4.5, as the bill benefit exceeds the capital cost.

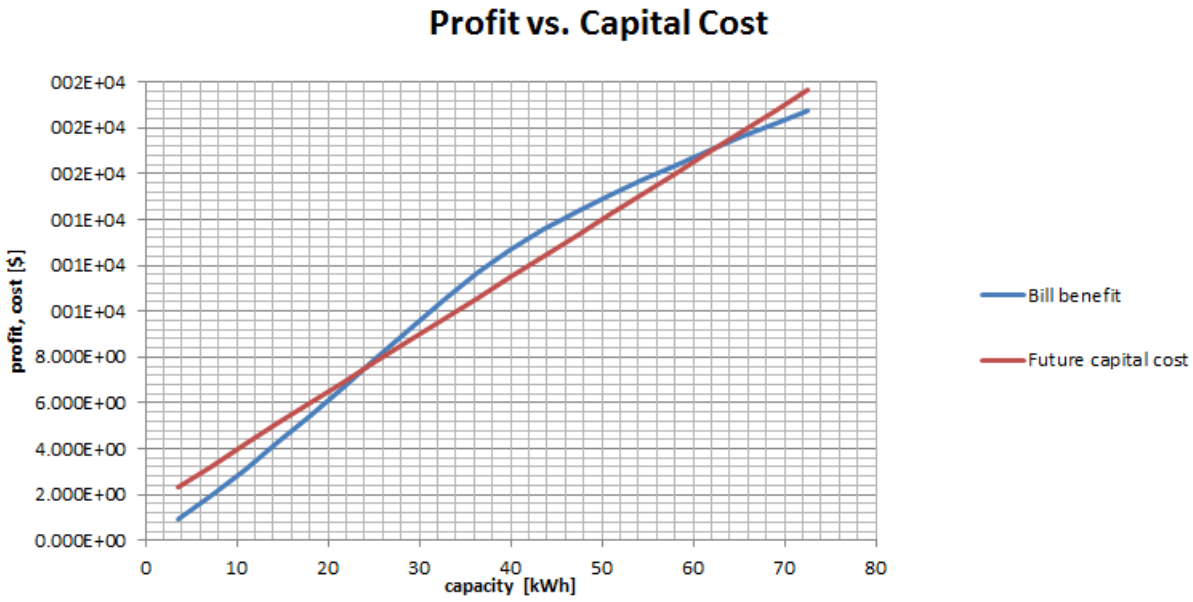

Figure 4.5: Capital cost and bill benefit with the future battery price

Executing the whole simulation considering the future price, Figure 4.6 shows the resulting profit, depending on the power limit and the capacity.

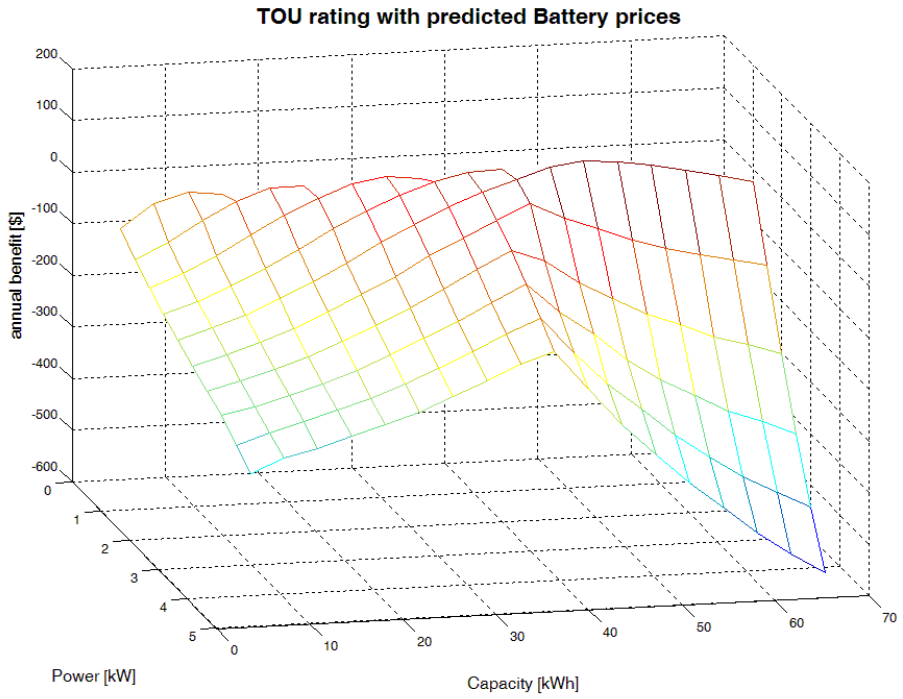

Figure 4.6: Annual profit of the BESS (considering the future battery price)

A global maximum of the annual profit is at a power limit of $P_{limit} = 2.5\,kW$

and at a capacity of $W = 47.19\,kWh$ which reaches a value of 121.1 \$. So it is economically reasonable to add a battery storage unit to a PV system. Also, in terms of supporting the grid, the energy storage system improves grid behavior and solves issues which occur through the rising penetration level of PV systems. Through the energy storage system the whole system can be seen as an assured energy source because if the PV does not produce energy then the energy is taken from the battery.

- Real time pricing
  The trend of the PV-, grid-, load-, and battery power of the same day as in Figure 4.6 for the time of use rate is shown in Figure 4.7 for the real time price rate.

Figure 4.7: Power profile of P_{PV}, P_{load}, P_{grid} and $P_{battery}$

It is apparent, that the use of the battery is rather low compared to the time of use which is founded in the electricity rate. The price rate for this day is shown in Figure 4.8, which explains the low use of the battery. The charge power follows a function depending on the current electricity price, depending on the daily average price for the electricity.

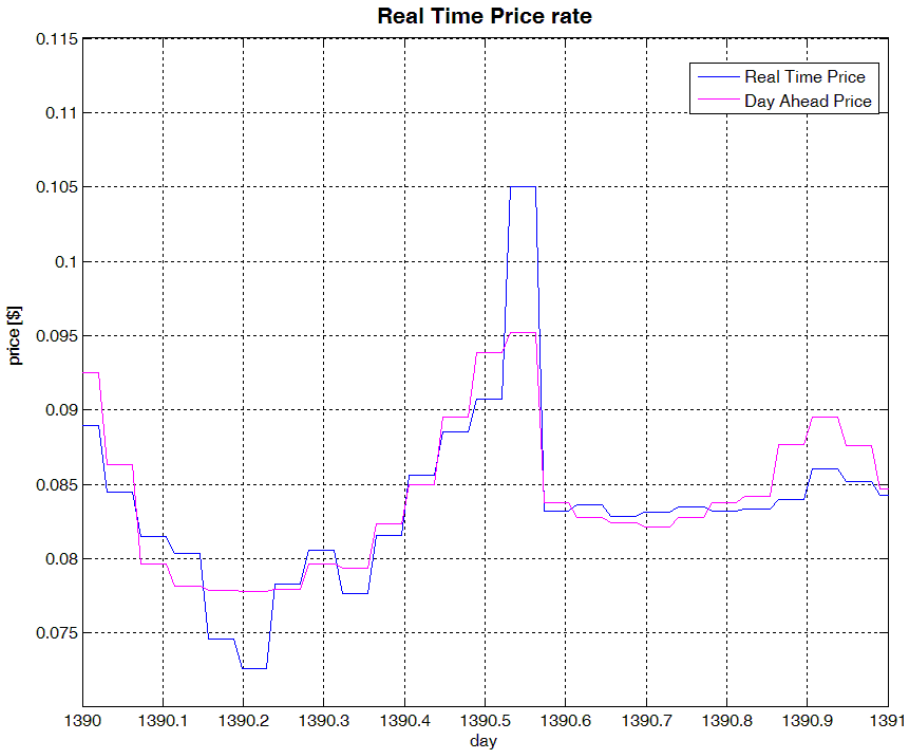

Figure 4.8: RTP rate (real price and day ahead estimation) [26]

So it is not profitable to use the battery because of low electricity prices during the day as the high peak just appears for $1.2\,h$ in this specific case. This assumption is confirmed by the simulation results, shown in Figure 4.9. There is no positive profit achievable, although the future price for the battery is used.

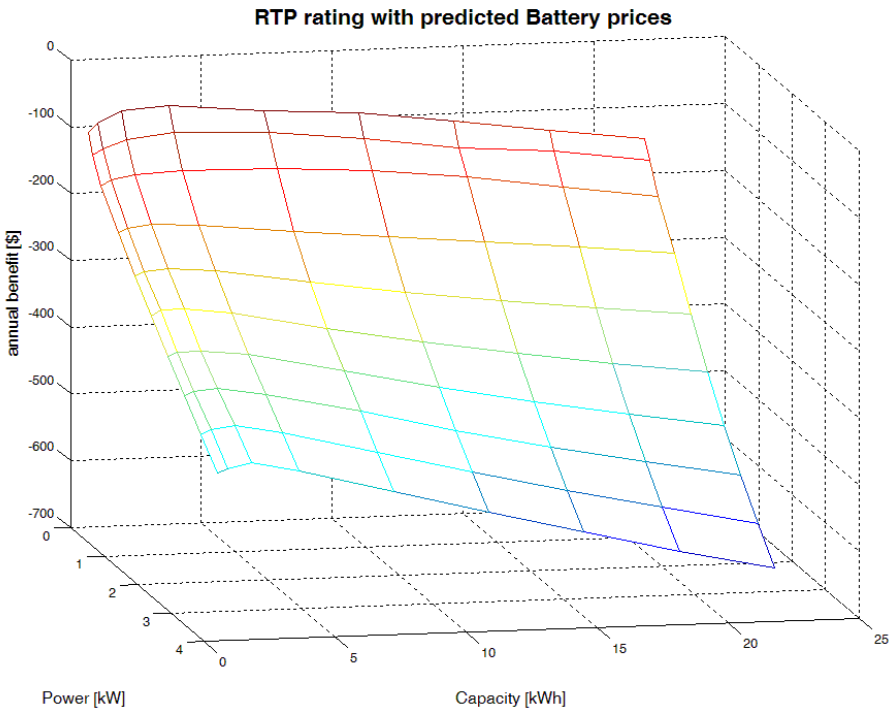

Figure 4.9: Annual profit of the BESS (considering the future battery price)

The main reason for the low profit originates from the low price and also from the short periods of the peak values. Another important reason for the bad result is the different predicted day ahead price. The energy management strategy calculates the appropriate charging curve one day ahead with the predicted day ahead price, whereas the charge power is calculated with the real price which differs a lot. The difference between the day ahead and the real time price is shown in Figure 4.8. To check the result of the simulation, assuming that the day ahead price is very accurate and the real time price is taken instead of the day ahead price, the resulting benefit is 34.12 % higher, compared to the result using the day ahead price. A better prediction of the utility would also improve the gained profit of the system.

4.2.2 Different battery model

Two simulations are compared, one using the physical based battery lifetime model and the other using a simple battery model. The used physical model is explained in Section 3.4. The simple battery model consists of a summation of the capacity and the efficiency is considered to be ideal. A lifetime simulation with a setting

of $P_{limit} = 2.5\,kW$ and $C = 47.19\,kWh$ using the TOU rate is accomplished. The results are shown in Figure 4.10 and 4.11, which shows the particular state of charge.

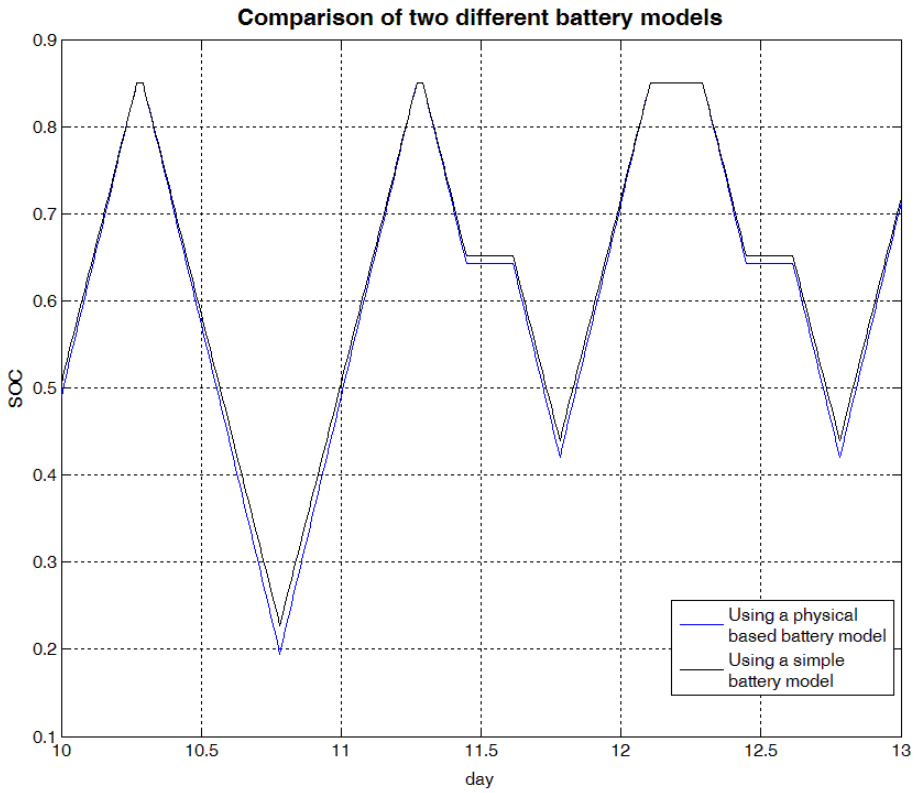

Figure 4.10: Comparison of 2 different battery models - day 10 - 13

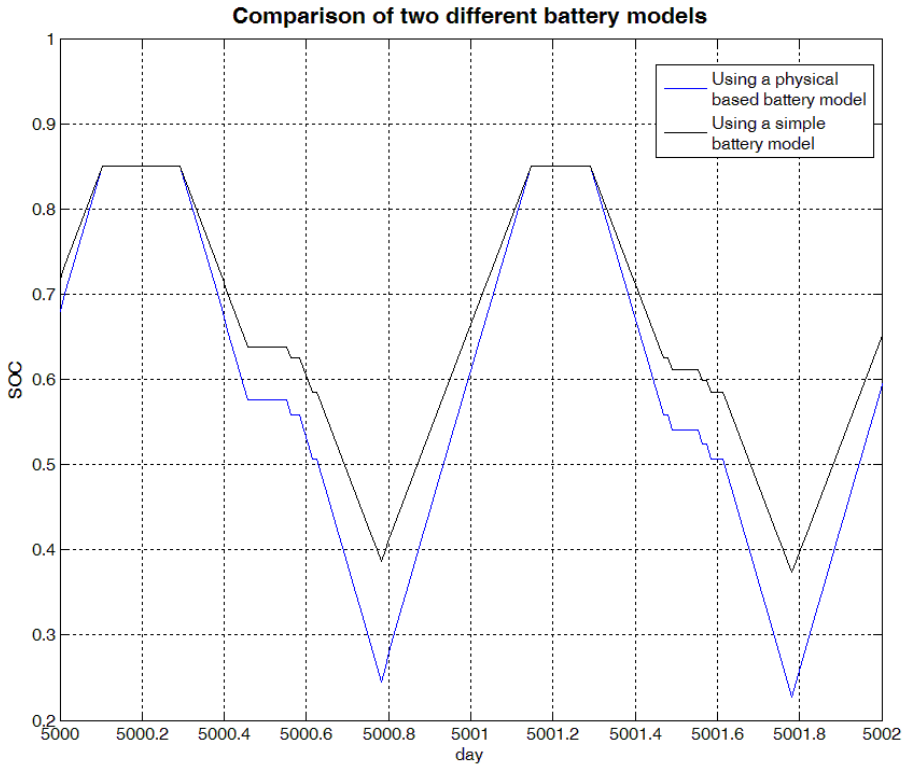

Figure 4.11: Comparison of 2 different battery models - day 5000 - 5002

Figure 4.10 shows the beginning of the simulation (from the 10th to the 13th day), whereas Figure 4.11 shows the result (between the 5000th to the 5002nd day) about the end of the 13th year of the simulation. The difference of using a physical based model and the simple one is not big in the beginning of the simulation as the battery is also not affected by the aging. The different slope of the state of charge is justified in the different effective amount of capacity which is added or subtracted from the battery originating from the physical parameters of the model. A mentionable difference in the SOC can be seen in Figure 4.11, which is caused by the capacity loss over the simulation time.

Chapter 5

Conclusion and future work

The two main objectives of this research are first to lower the electrical energy cost for the customer and second to support the electricity grid to solve problems that occur through the rising penetration level of PV systems.

The applied time of use rate achieves a cost saving for the customer of 121.1 $\$/year$ (Figure 4.6) if the future price for the battery is used in this simulation. Also, the grid is assisted through the energy storage system, as it is shown in Figure 4.1. With the application of the real time pricing rate, the grid was not well assisted by the storage system and through the low usage of the ESS, there was also less profit achieved. In this particular case, there was no positive profit (Figure 4.9). This is caused by the electricity pricing rate, as there are rather short periods with high and low values. Also the day ahead price of the RTP has a bad day ahead prediction. When the simulation was run with the real time price treated as the day ahead price, the whole system achieved a 34.12 % higher profit, which means that the achieved profit also depends on the accuracy of the prediction.

In summary it is not worth implementing the tested system with the RTP rating, whereas using the TOU rate it is profitable. As there would be different approaches of the real time pricing, like a more accurate electricity price prediction or a fixed price but still with the hourly change would be one possible further development. Disregarding from the application in this study, the real time pricing is still a new accounting method which has lots of advantages, but not useful for this application. If there are flexible high power loads, like a water heater(with a storage capacity that lasts longer than a day), energy costs can be optimized.

The result of the charge function, which is a part of the energy management strategy

also shows the influence on the profit just in case of the RTP.
In summary, a big benefit of this system is that the PV source can be seen as an assured energy source because of the energy storage backup for cloudy days, which supports the power grid. Therefore, non-renewable sources can be replaced through PV systems.

The battery type used is a new technology, which is still very expensive but has lots of advantages compared to older technologies, i.e. the Li-Ion and Lead - Acid batteries, because the material are more eco-friendly, safer, and the raw material is cheaper than for Li-Ion which will effect the future price. There is already at least one company which uses Lithium technology batteries for storage applications on the production - transmission - distribution and consumption (residential) level [28].

The described sizing technology for residential PV applications is a new methodology to calculate the optimum battery size for individual usage. Furthermore, a different energy management strategy can easily be implemented as well as a different battery model, as it is a modular system.

The future work for this project is to improve the accuracy of the battery model by executing more measurements on it. This developed model is in an early development stage and due to time issues, not every measurement could be executed, which is shown in Figure 5.1.

T [°C] \ SOC [%]	0	20	40	60	80	100
-30						X
-10						X
0						X
RT	X	X	X	X	X	X
20						X
40						X
80						X

Figure 5.1: Simulation matrix

Here the needed and the performed measurements are displayed. Measurements are executed at the places where an ”x“ is placed. At empty places, values are approximated. All measurements are currently just executed for 100 % of SOC and based

on this, the data is approximated for the other SOC values. It is also considered to make measurements, depending on the SOH, which makes the metering matrix 3-dimensional and therefore more time consuming to execute all these measurements.

Another important aspect to improve the sizing strategy is to detail financial aspects, like the inflation rate and the bank interest rate, because the simulation time is (in this case) longer than 10 years which makes it worth considering these economic factors.

As the goal for this sizing methodology is to make it as modular as possible, the changes for a different application area should be considered. Another important application area is for use on PV farms. The objective for this area is to improve the energy efficiency, to improve the grid quality, and use the battery as a backup for shady days, which is similar to the residential application but not identical. The focus on the residential application is to increase cost savings. The optimal battery size for PV farms depends on a compromise between an optimum calculated backup storage size and an economic factor. Also, the situation concerning the input data is different because for the residential application the input data (annual load profile) is treated as given, but for the PV farm application the load profile can not be treated as given because the profile depends on too many factors - probably just an average value can be assumed for the calculation which makes the result more inaccurate. This is one of the challenges of applying this method to a PV farm.

Bibliography

[1] Barbara T. Fichman, "Annual Energy Review 2009", U.S. Energy Information Administration, August 2010

[2] Tsung-Ying Lee, "Determination of optimal contract capacities and optimal sizes of battery energy storage systems for Time-of-Use rates industrial customers", IEEE Transaction on Energy Conversion, Vol. 10, No. 3, September 1995

[3] Chee Wei Tan, "A stochastic method for battery sizing with uninterruptible-power and demand shift capabilities in PV (photovoltaic) systems", ScienceDirect Energy Journal, September 2010

[4] C. Protogeropoulos, "Sizing and techno-echonomical optimization for hybrid solar photovoltaic/wind power systems with battery storage", International Journal of Energy Research, Vol. 21, 1997

[5] D.P. Jenkins, "Lifetime prediction and sizing of lead-acid batteries for microgeneration storage applications", IET Renewable Power Generation, Vol. 2, April 2008

[6] D. Manz, "Enhanced Reliability of Photovoltaic Systems with Energy Storage and Controls", NREL - National Renewable Energy Laboratory, Subcontract Report, February 2008

[7] Dan Ton, "Solar Energy Grid Integration Systems - Energy Storage (SEGIS-ES)", U.S. Department of Energy, May 2008

[8] Stan Mark Kaplan, "Smart Grid", TheCapitol.Net, ISBN 13: 978-1-58733-162-6, April 2009

[9] Sean Ong, "The Impacts of Commercial Electric Utility Rate Structure Elements on the Economics of Photovoltaic Systems",NREL - National Renewable Energy Laboratory, Technical Report, June 2010

[10] Younghyun Kim, Yanzhi Wang, "Maximum Power Transfer Tracking for a Photovoltaic-Supercapacitor Energy System", ISPLED'10, August 2010

[11] Michael Greenleaf, "Physical based modeling and simulation of LiFePO4 secondary batteries", Florida State University, October 2010

[12] Trannon Mosher, "Economic Valuation of Energy Storage Coupled wioth Photovoltaics: Current Technologies and Future Projections", Massachusetts Institute of Technology (MIT), June 2010

[13] Keith James Keller, "Fine-tuning TI's Impedance Track^{TM} battery fuel gauge with LiFePO4 cells in shallow-discharge applications", Analog Applications Journal, October 2011

[14] Weihao Hu, "Optimal Operation Strategy of Battery Energy Storage System to Real-Time Electricity Price in Denmark", Power and Energy Society General Meeting, IEEE, 2010

[15] Alireza Farman, "Erstellen eines messtechnisch gestützten Modells zur Berechnung der kalendarischen Alterung von LiFePO4-Batterien", Hochschule München, September 2010

[16] John Wang, "Cycle-life model for graphite-LiFePO4 cells", Journal of Power Sources, November 2010

[17] Andreas Jossen, "Moderne Akkumulatoren richtig einsetzen", ISBN-10: 3939359114, January 2006

[18] Andrzej Lasia, "Electrochemical Impedance Spectroscopy and its Applications", 1999

[19] Fouad Abou, "Impact of Energy Storage Costs on Economical Performance in a Distribution Substation", IEEE Transaction on Power Systems, Vol. 20, Nr. 2, May 2005

[20] Chin H. Lo, "Economic dispatch and optimal sizing of battery energy storage systems in utility load-leveling operations", IEEE Transaction on Energy Conversion, Vol. 14, No. 3, September 1999

[21] I.N. Bronstein: "Taschenbuch der Mathematik", 6. Auflage, Harri Deutsch Verlag, Frankfurt am Main 2005

Weblinks

[22] http://www.eia.gov/energyexplained/index.cfm?page=electricity_factors_affecting_prices, 08.26.2011

[23] http://www.sciencemag.org/content/315/5813/798.full, 08.25.2011

[24] http://egauge699.d.egauge.net/index.html, 09.01.2011

[25] http://www.talgov.com/you/energy/nw.cfm, 08.31.2011

[26] https://www.comed.com/sites/customerservice/Pages/realtimepricing_besh.aspx, 08.31.2011

[27] http://batteryuniversity.com, 09.04.2011

[28] http://www.saftbatteries.com/doc/Documents/stationary/Cube781/ESS_capa_en_1110_LD_protege.41b16288-5ba5-4480-b4ec-1738fd3ef94a.pdf, 09.12.2011

[29] http://www.a123rc.com, 09.07.2011

[30] http://www.a123systems.com, 09.07.2011

[31] http://sma-america.com/en_US.html, 09.07.2011

[32] http://wunderground.com, 09.01.2011

[33] http://www.atp.nist.gov/eao/wp05-01/append-3.htm, 09.27.2011

[34] http://www.mpoweruk.com/chemistries.htm, 11.19.2011

List of Abbreviations

BESS	Battery Energy Storage System
DOD	Depth of Discharge
DRES	Distributed Renewable Energy Source
EIS	Electrochemical Impedance Spectroscopy
EMS	Energy Management Strategy
EP	Electricity Price
FIT	Feed in Tariff
LSM	Least Square Method
PV	Photovoltaic
PCC	Point of Common Coupling
RES	Renewable Energy Source
RTP	Real Time Pricing
SOC	State of Charge
SOH	State of Health
TOU	Time of Use

List of Figures

List of Tables

Appendix A

A.1 PV power profile

The PV power data used and shown in this section originates from [24].

- **January**

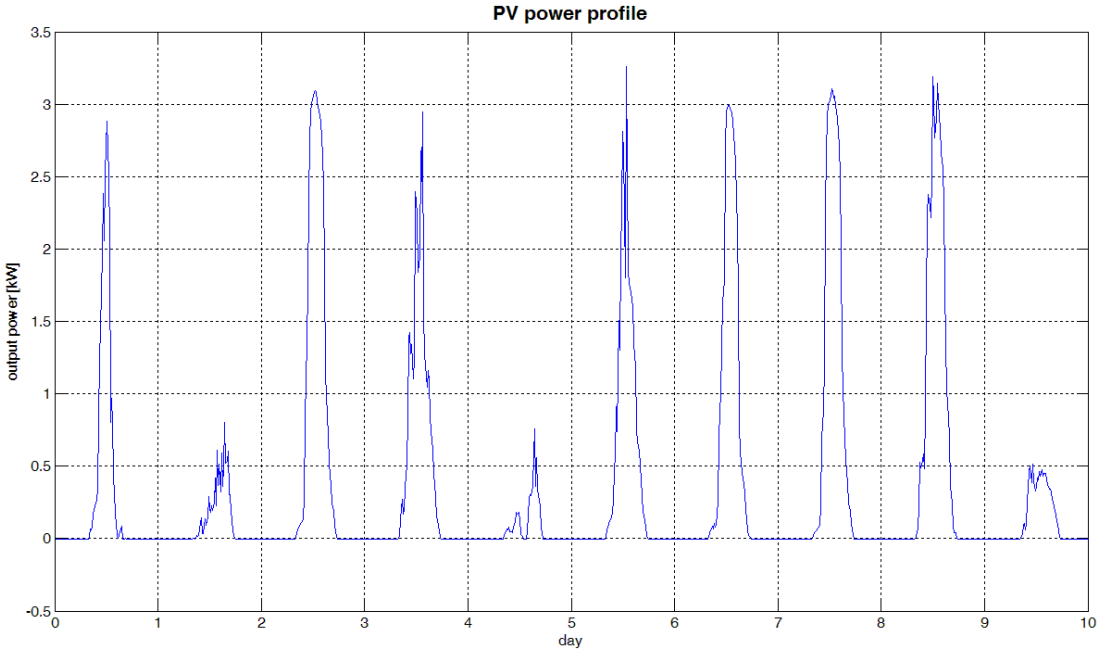

Figure A.1: PV power profile for: January 1st - 10th

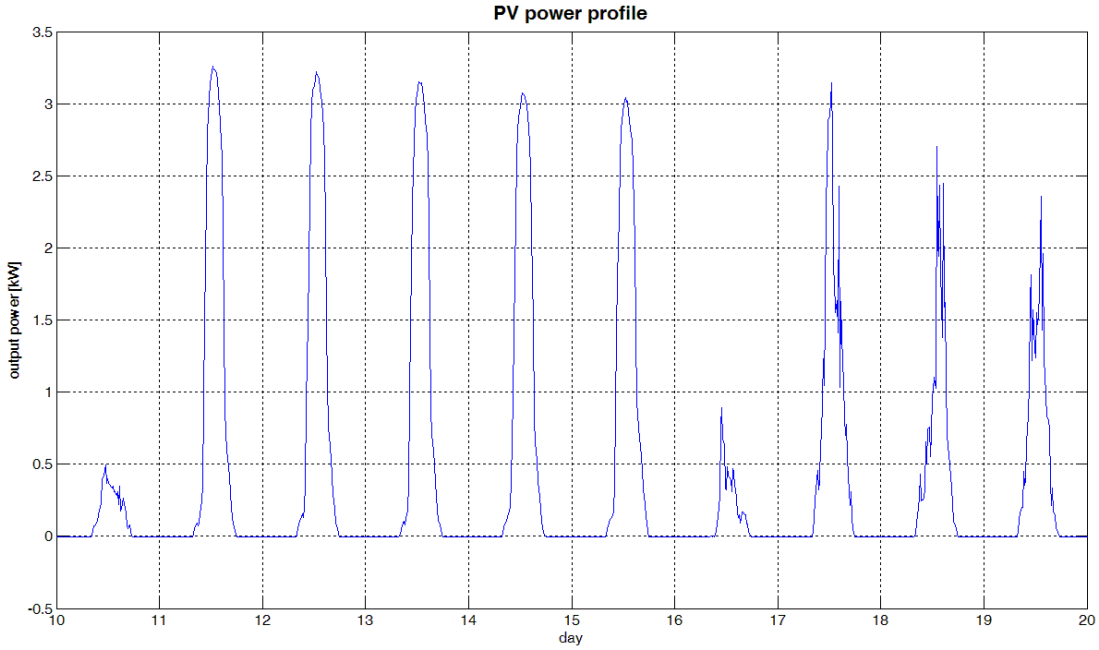

Figure A.2: PV power profile for: January 11th - 20th

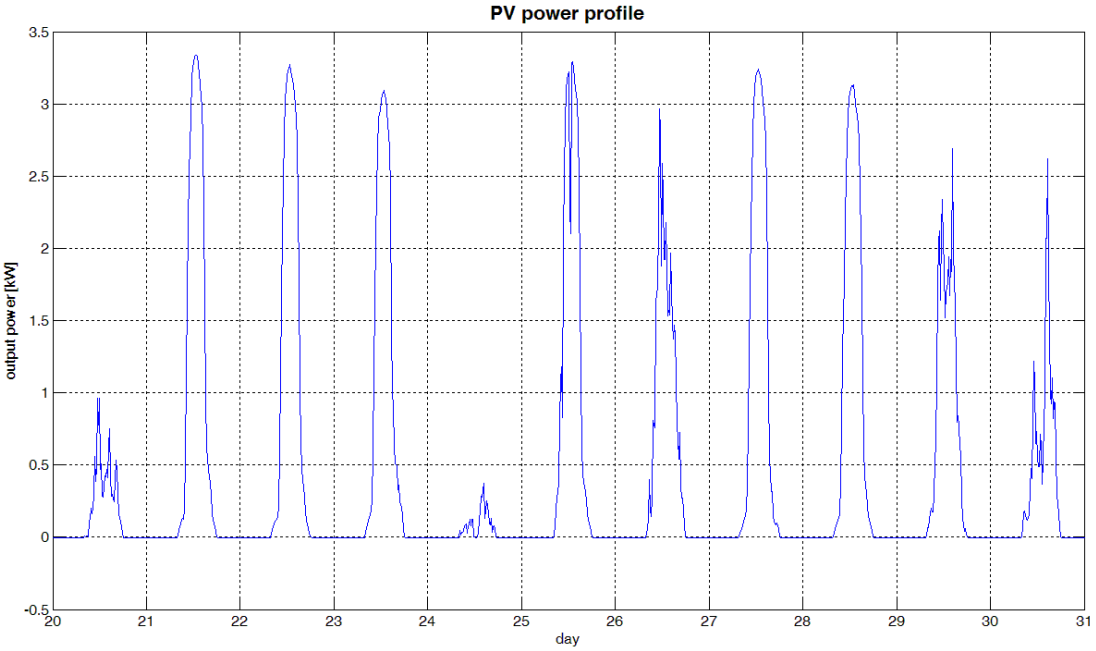

Figure A.3: PV power profile for: January 21st - 31st

- **February**

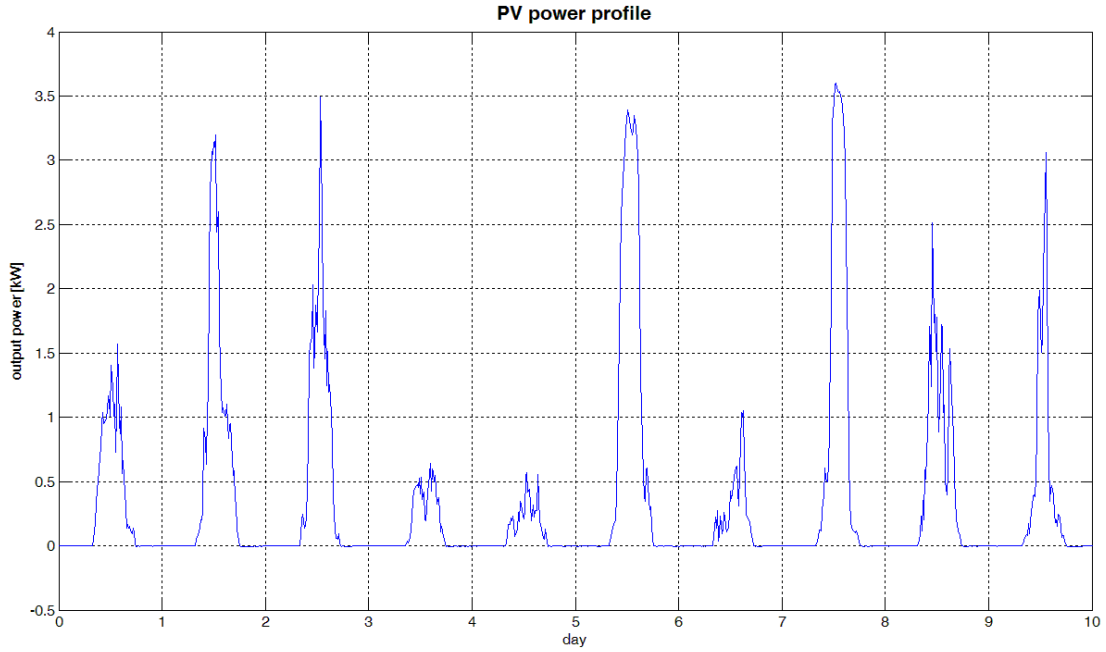

Figure A.4: PV power profile for: February 1st - 10th

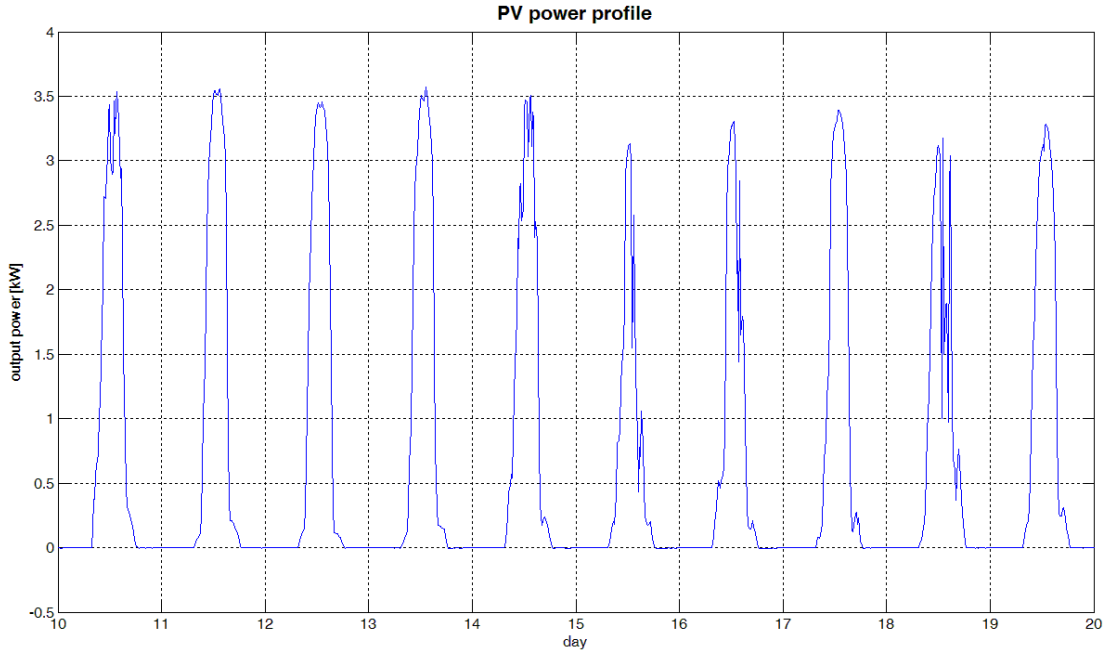

Figure A.5: PV power profile for: February 11th - 20th

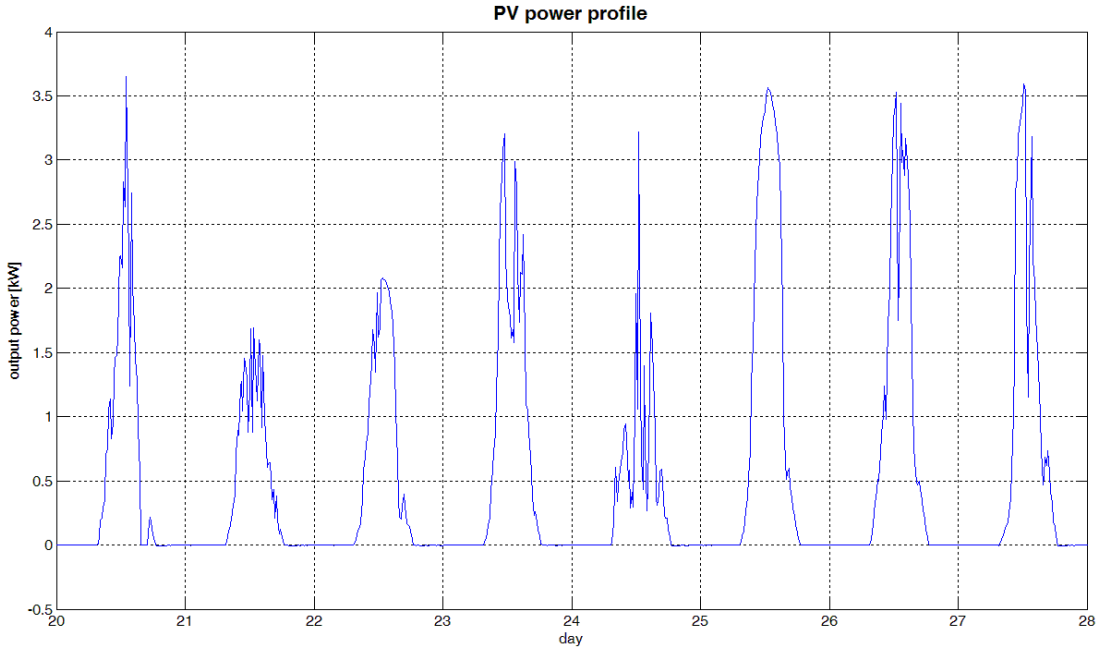

Figure A.6: PV power profile for: February 21st - 28th

- **March**

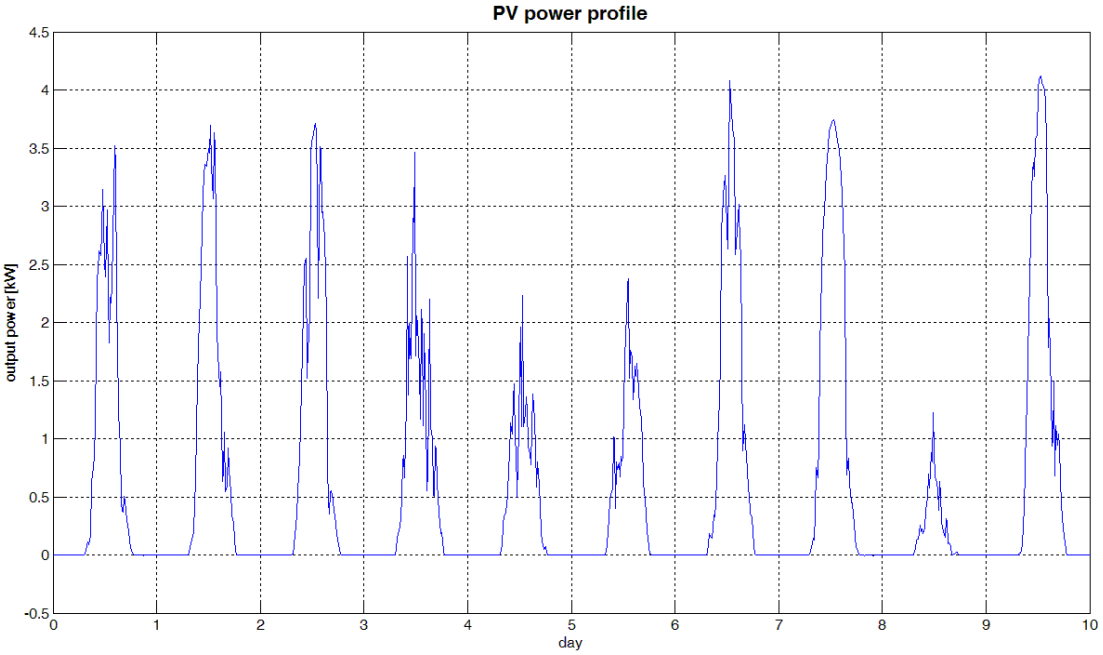

Figure A.7: PV power profile for: March 1st - 10th

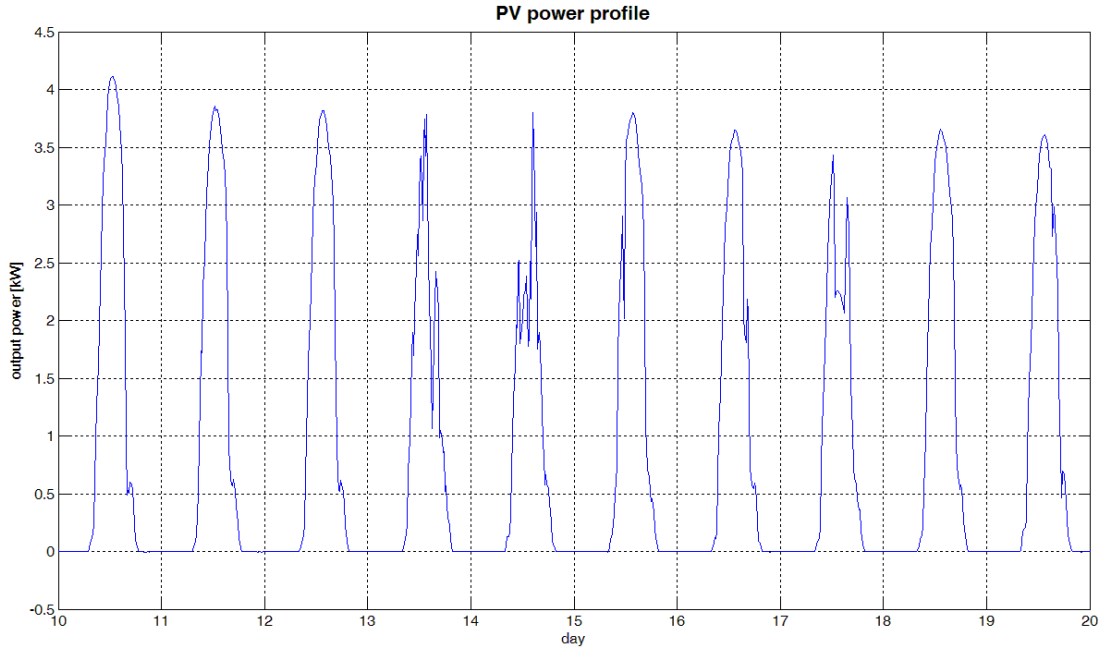

Figure A.8: PV power profile for: March 11th - 20th

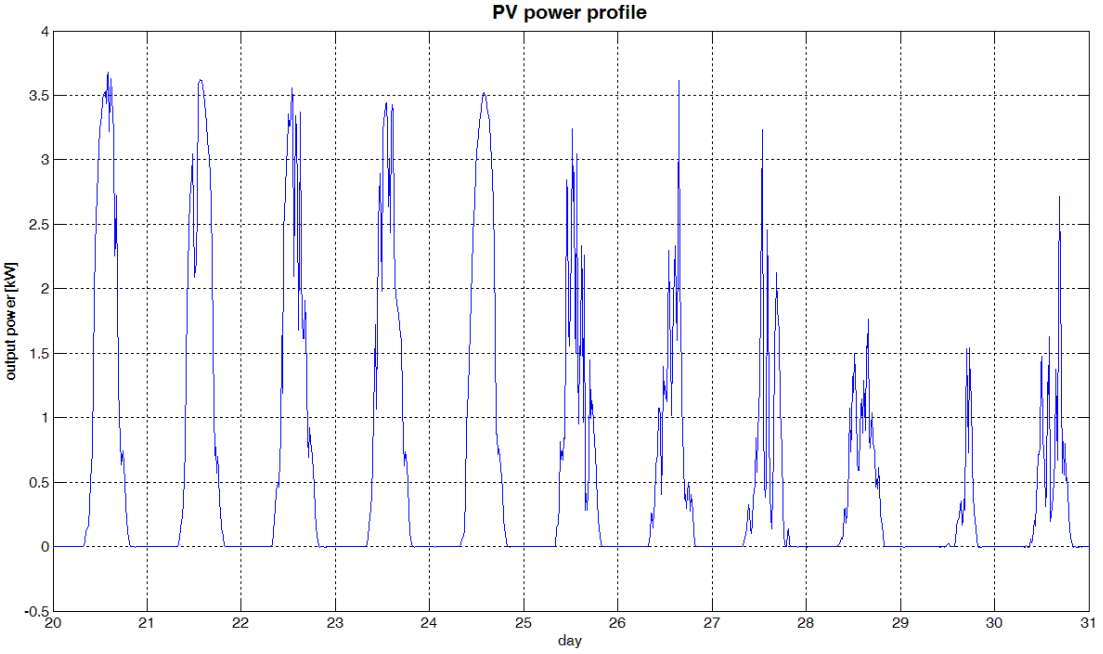

Figure A.9: PV power profile for: March 21st - 31st

- **April**

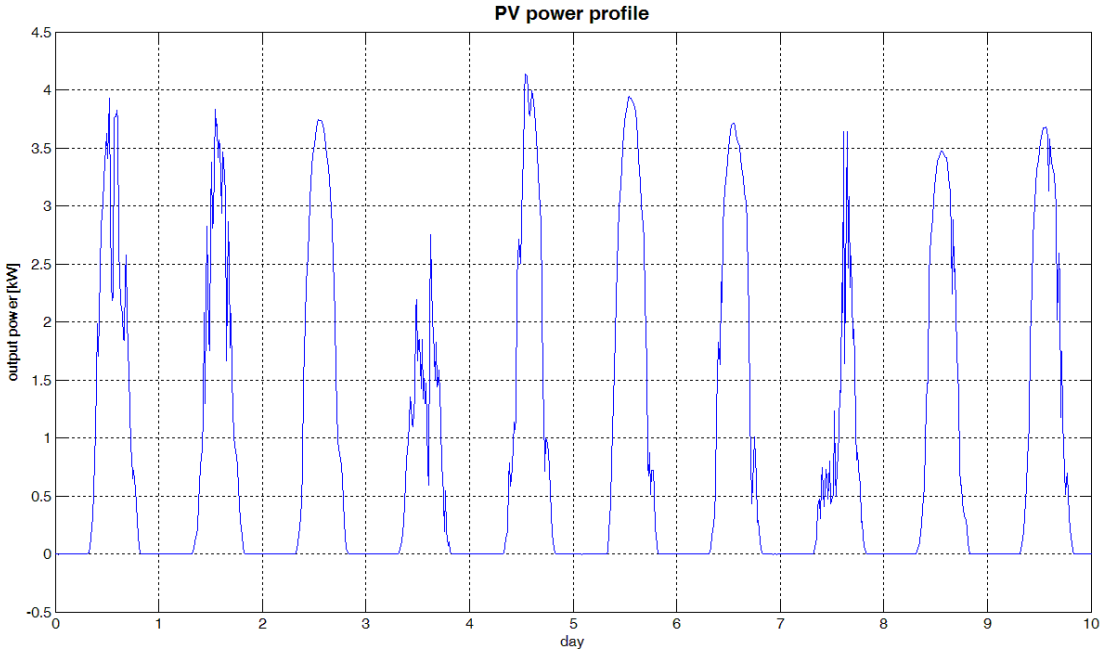

Figure A.10: PV power profile for: April 1st - 10th

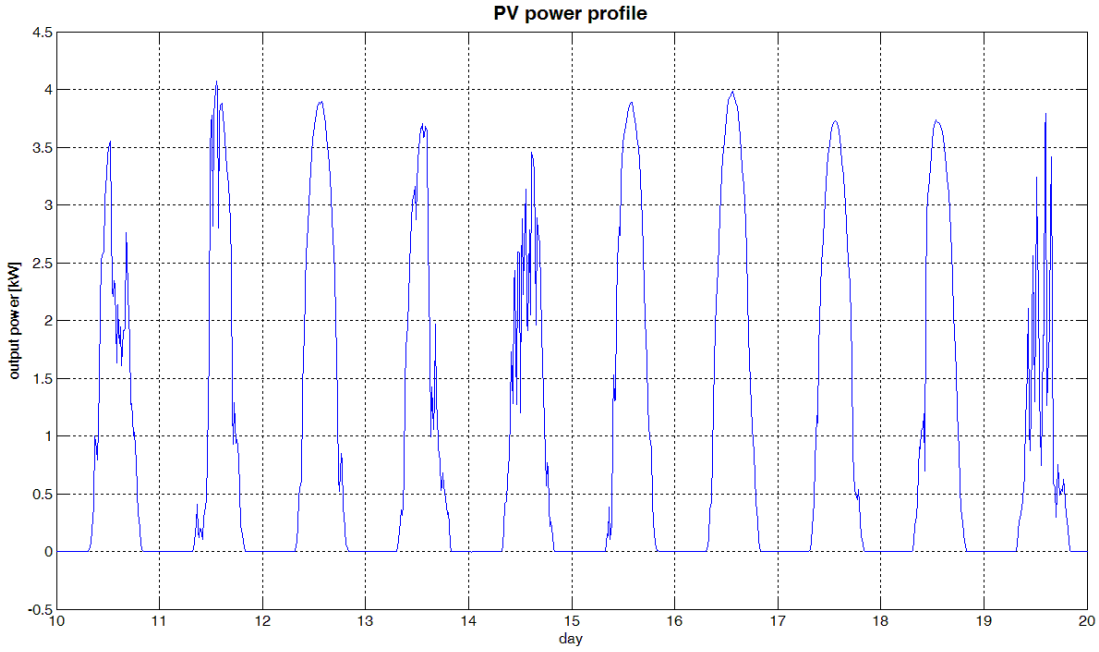

Figure A.11: PV power profile for: April 11th - 20th

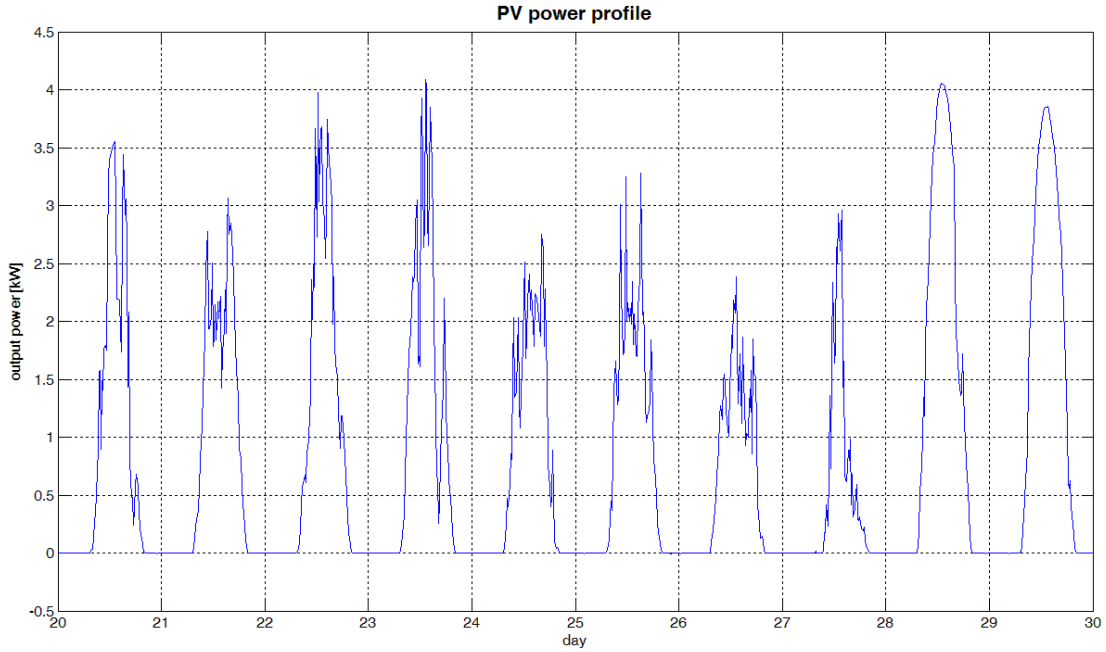

Figure A.12: PV power profile for: April 21st - 30th

- **May**

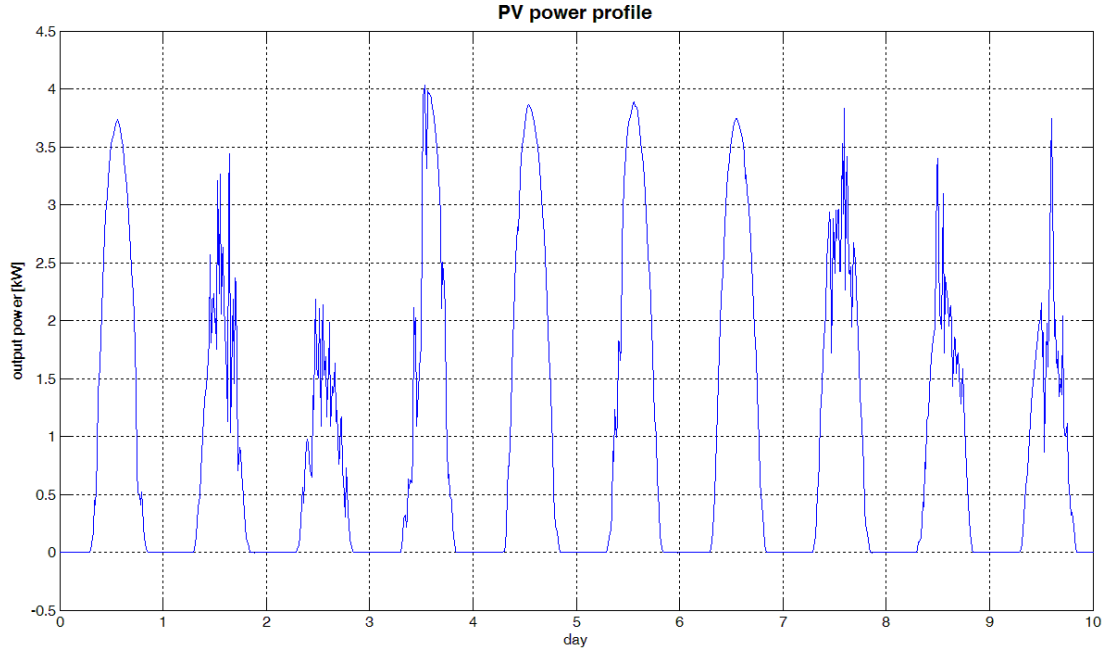

Figure A.13: PV power profile for: May 1st - 10th

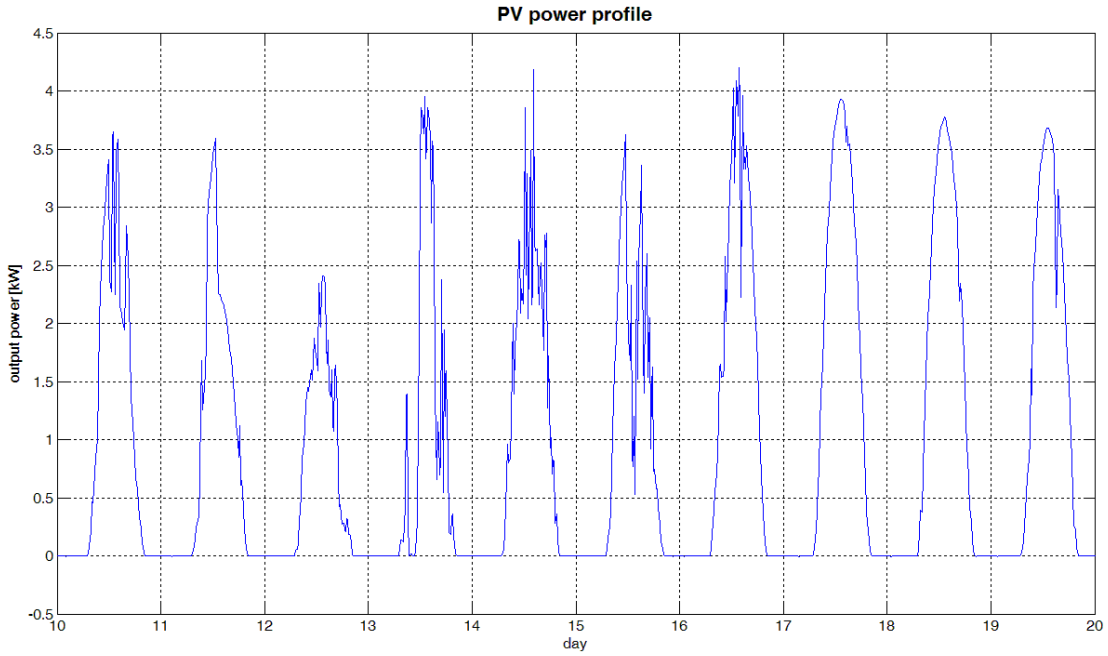

Figure A.14: PV power profile for: May 11th - 20th

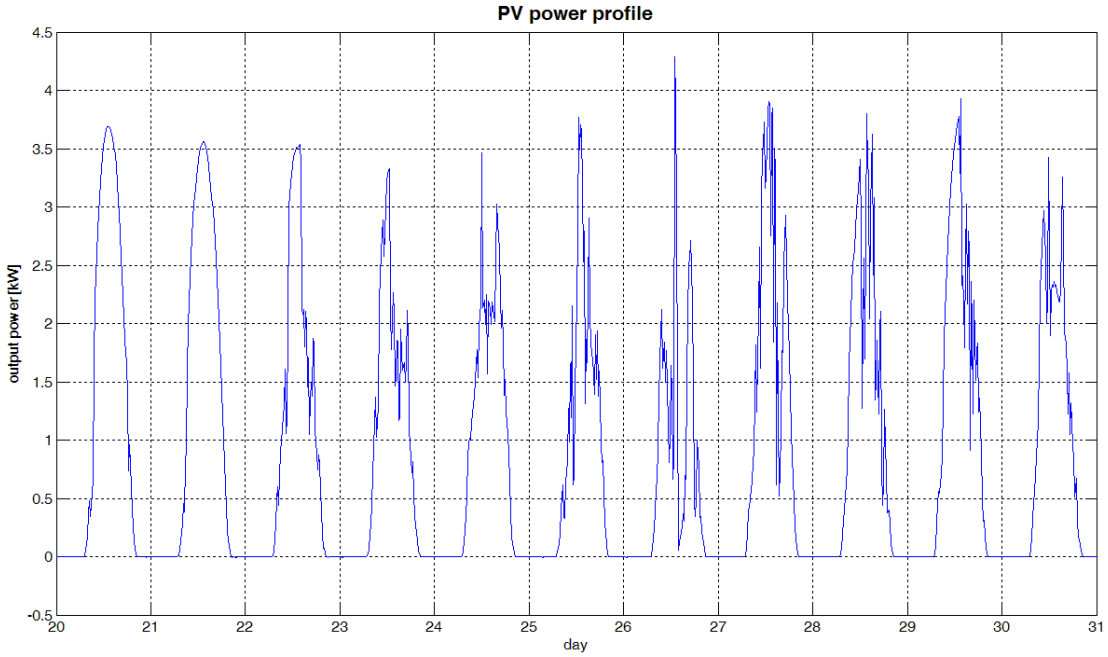

Figure A.15: PV power profile for: May 21st - 30th

- **June**

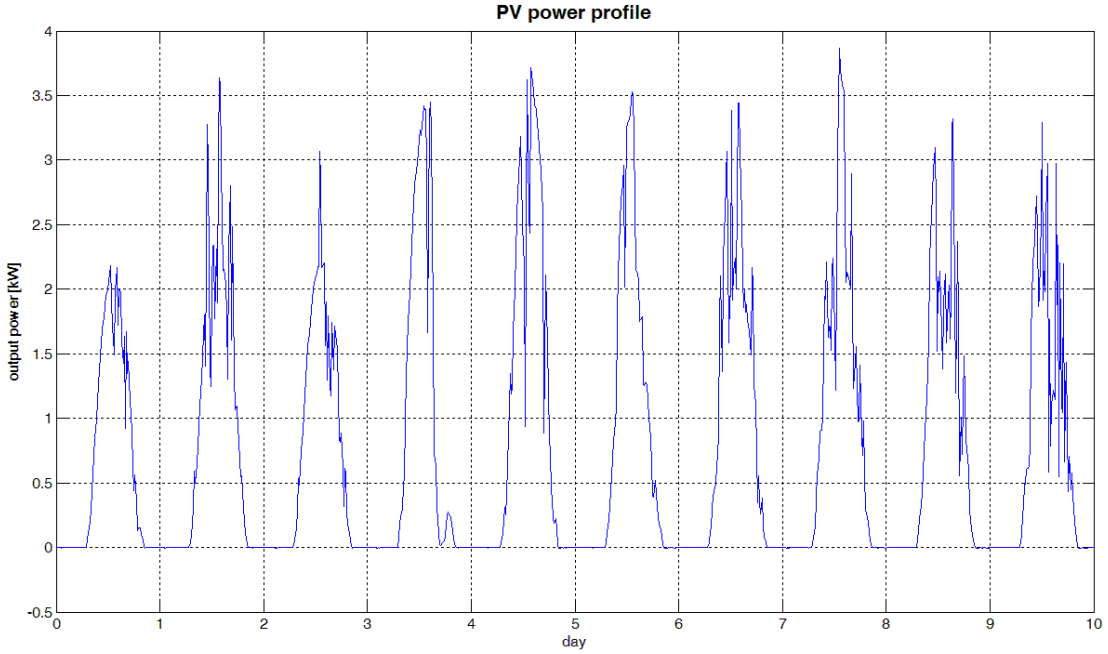

Figure A.16: PV power profile for: June 1st - 10th

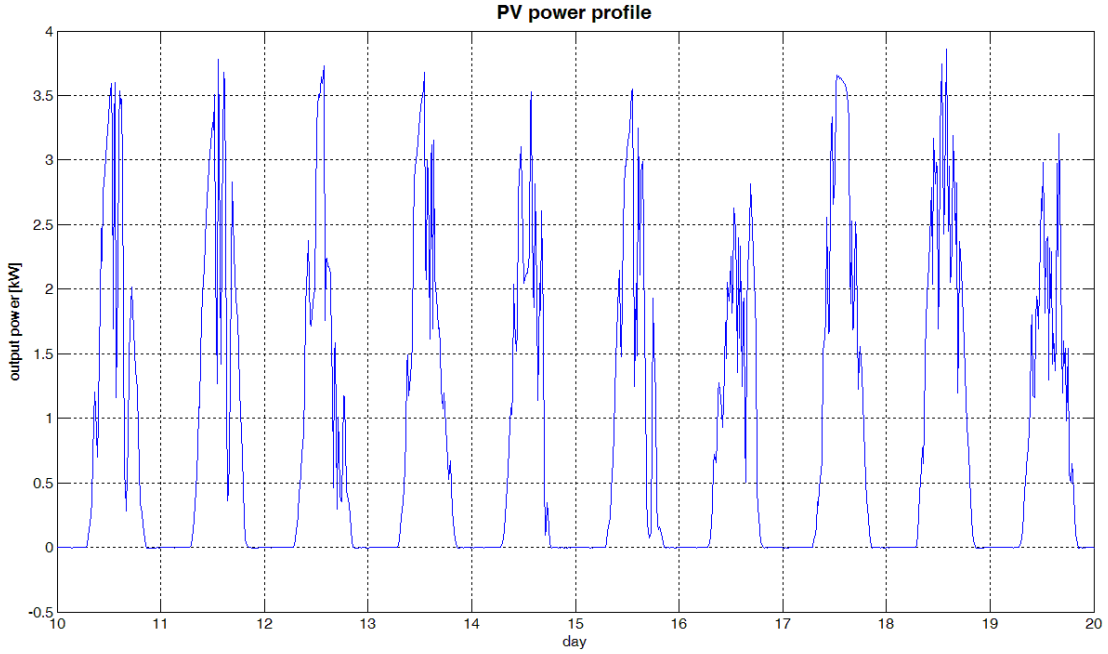

Figure A.17: PV power profile for: June 11th - 20th

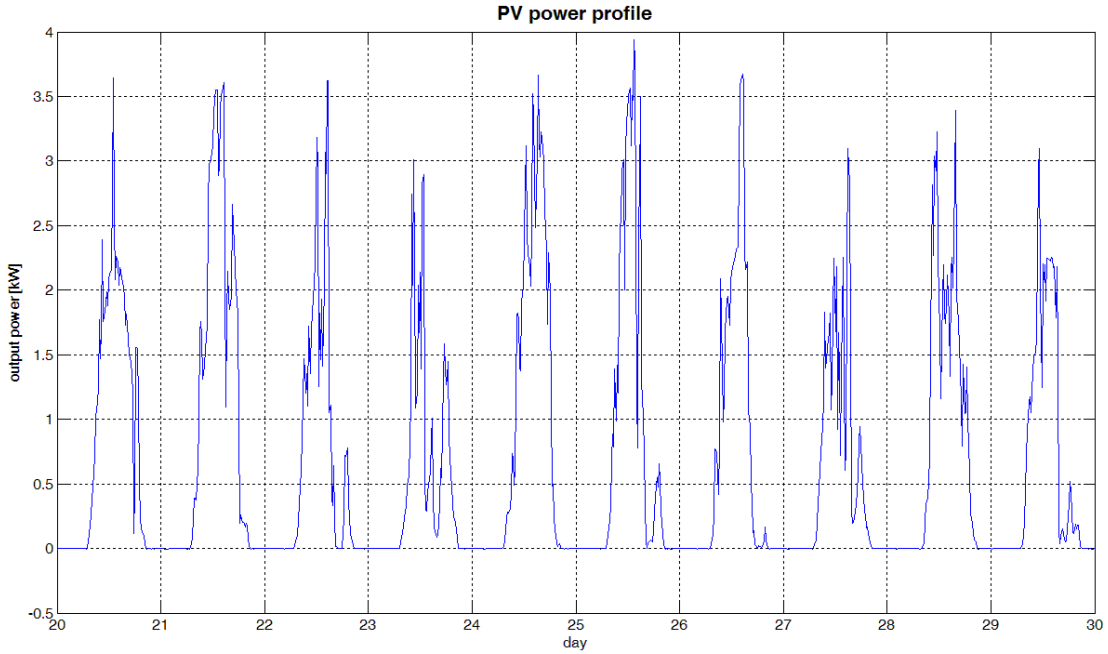

Figure A.18: PV power profile for: June 21st - 30th

A.2 Load power profile

The load power data used and shown in this section originates from [24].

- **January**

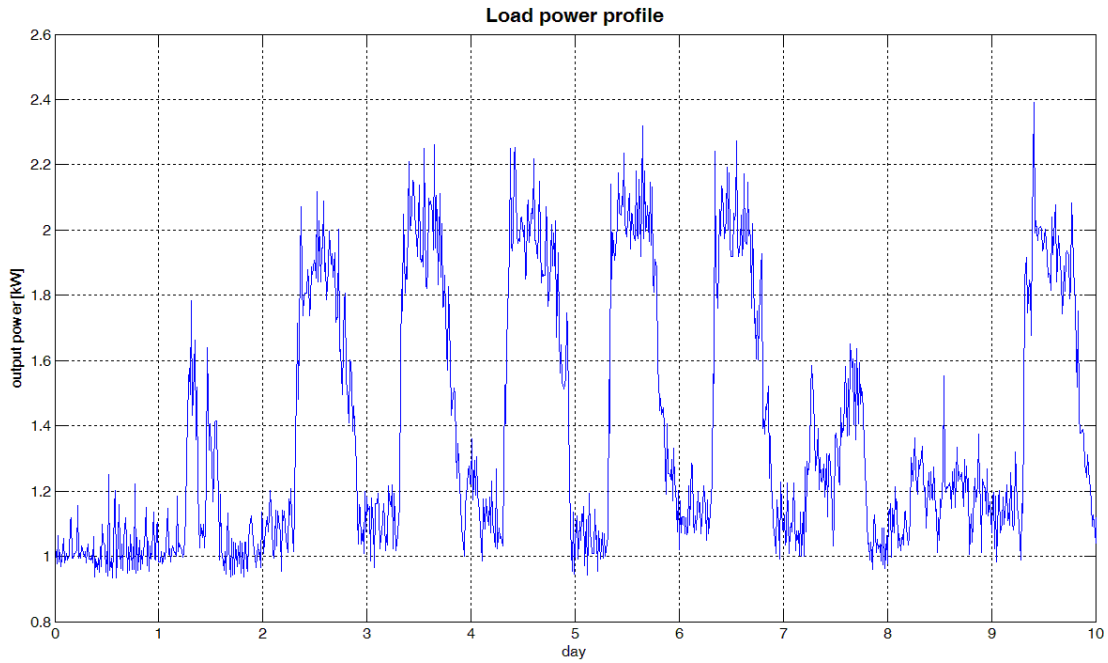

Figure A.19: Load power profile for: January 1st - 10th

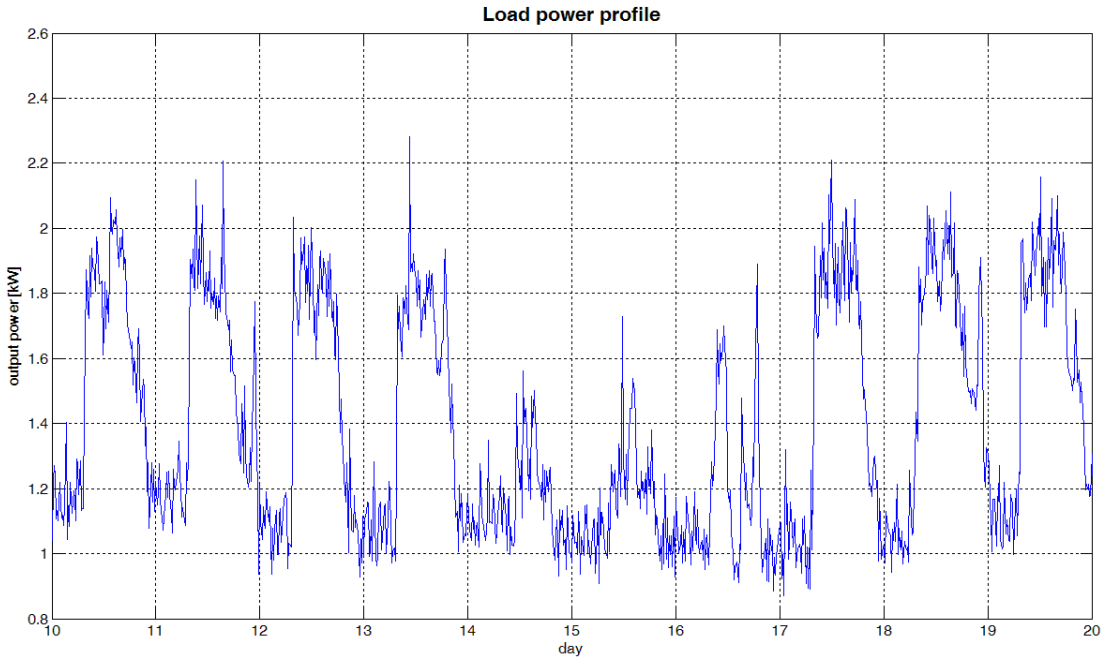

Figure A.20: Load power profile for: January 11th - 20th

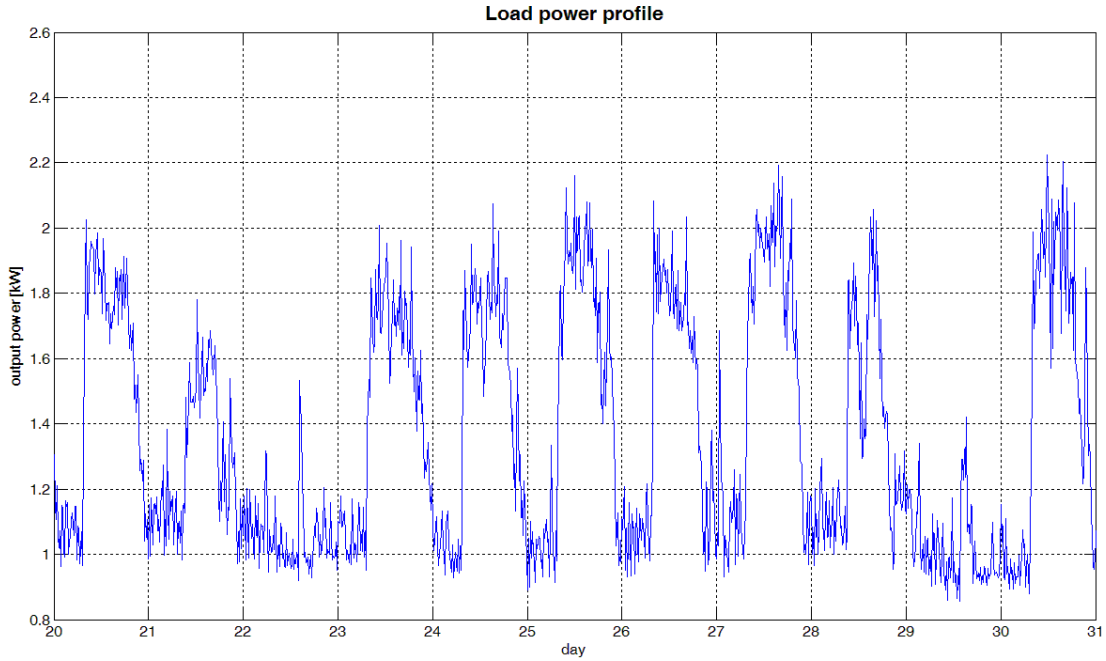

Figure A.21: Load power profile for: January 21st - 31st

- **February**

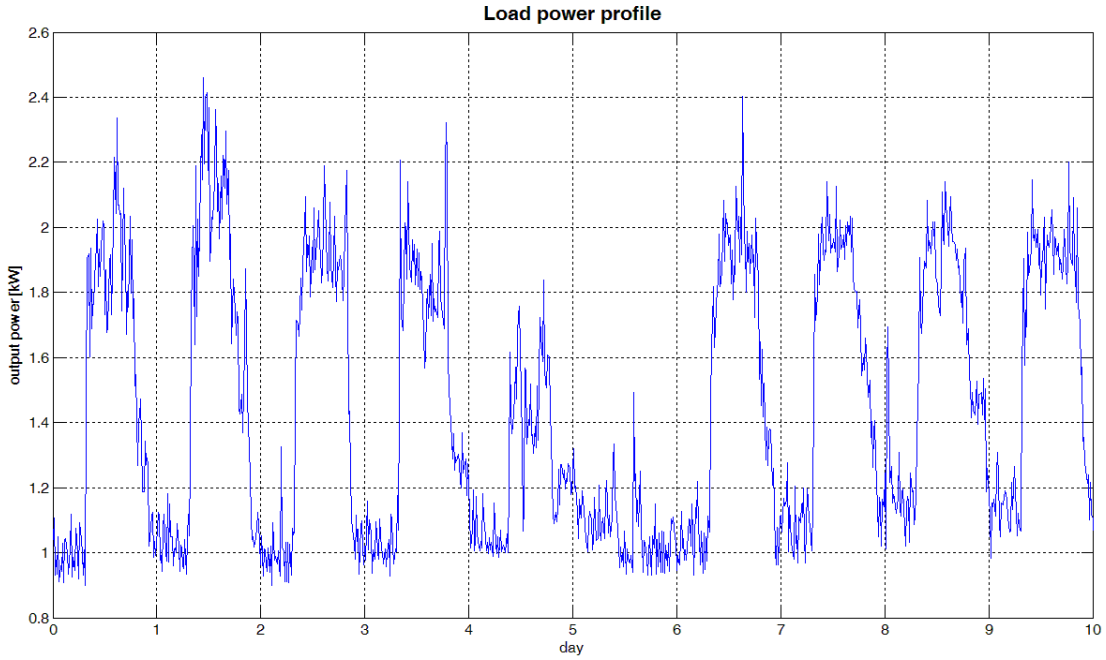

Figure A.22: Load power profile for: February 1st - 10th

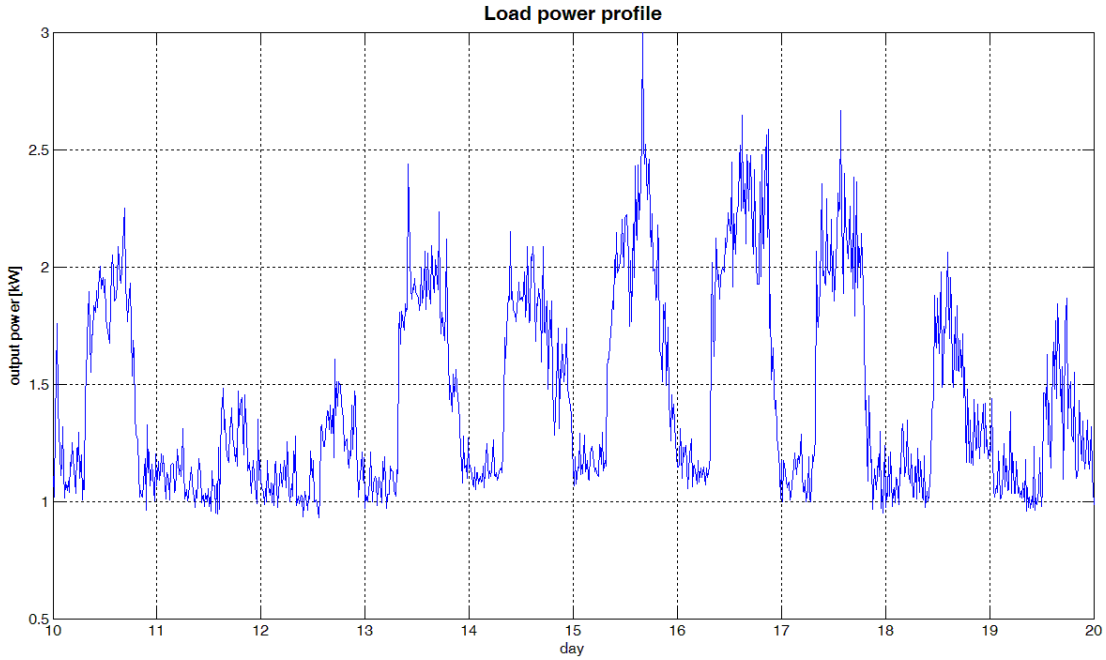

Figure A.23: Load power profile for: February 11th - 20th

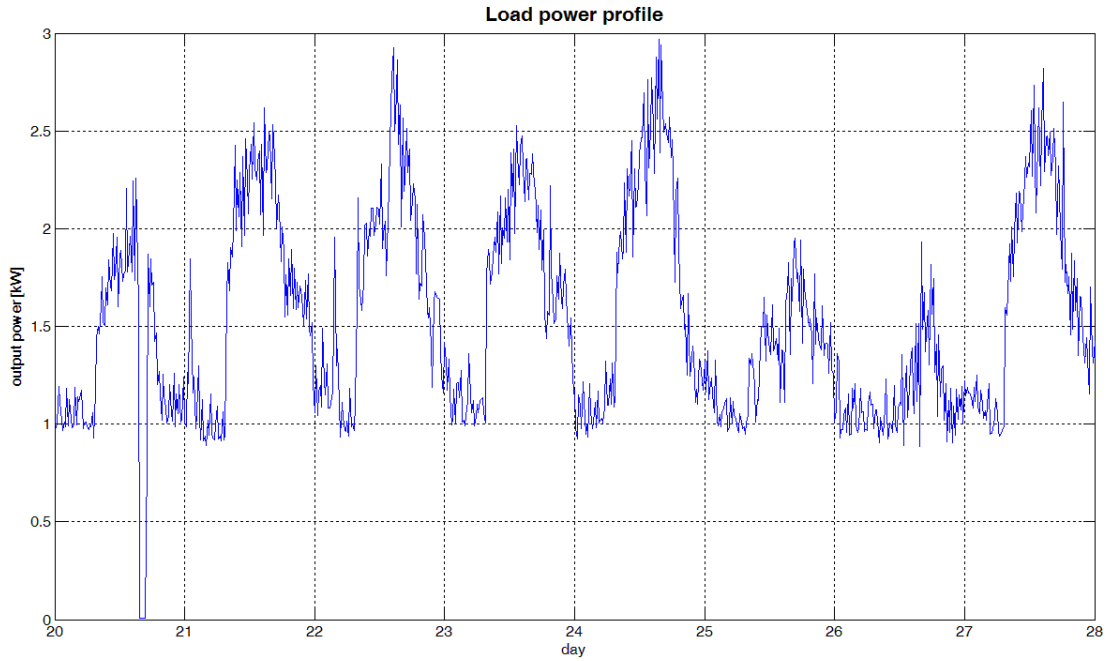

Figure A.24: Load power profile for: February 21st - 28th

- **March**

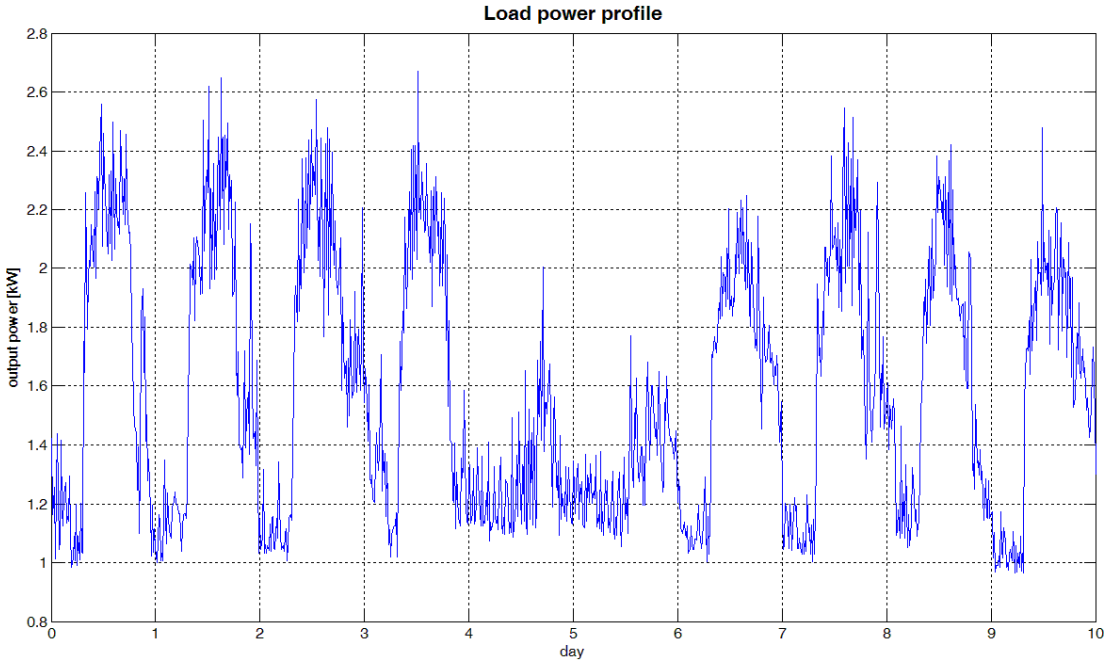

Figure A.25: Load power profile for: March 1st - 10th

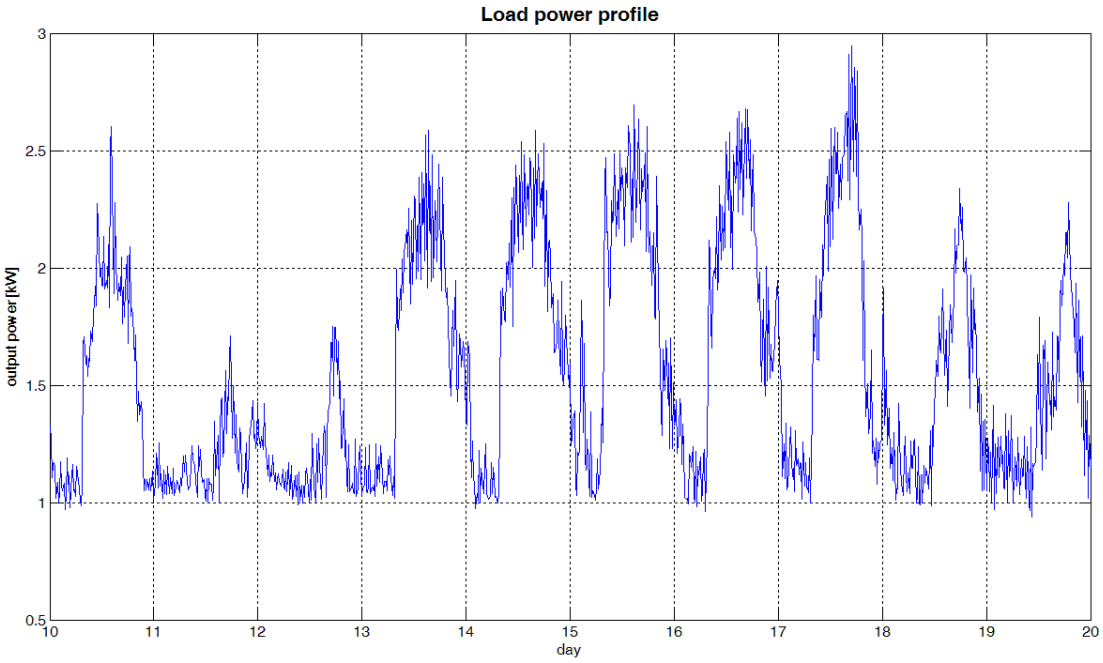

Figure A.26: Load power profile for: March 11th - 20th

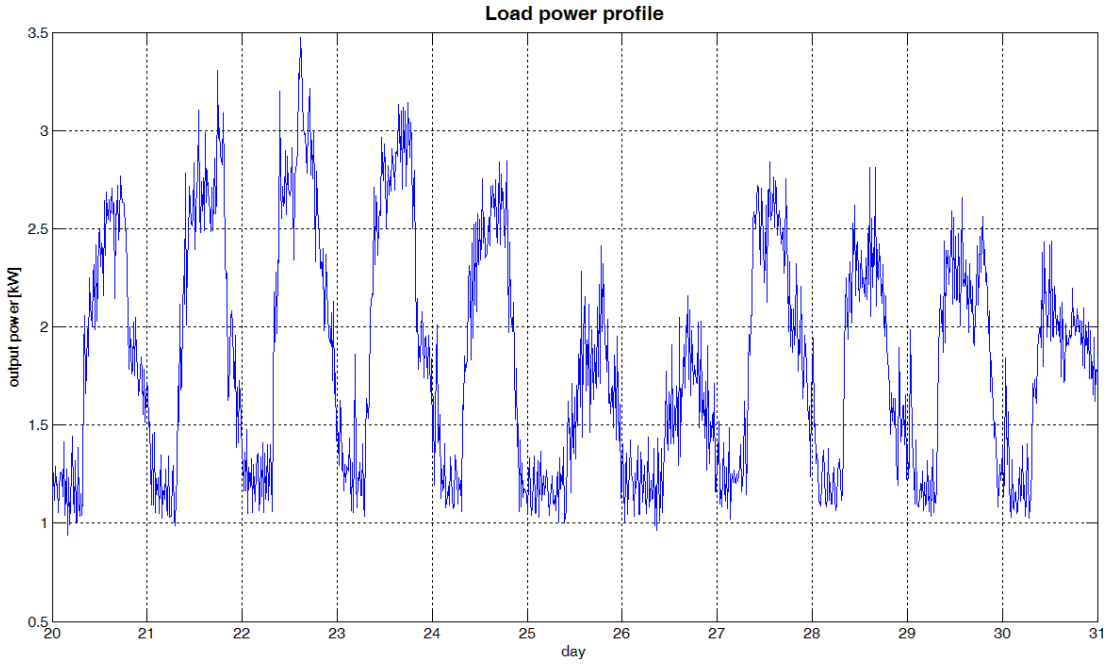

Figure A.27: Load power profile for: March 21st - 31st

- **April**

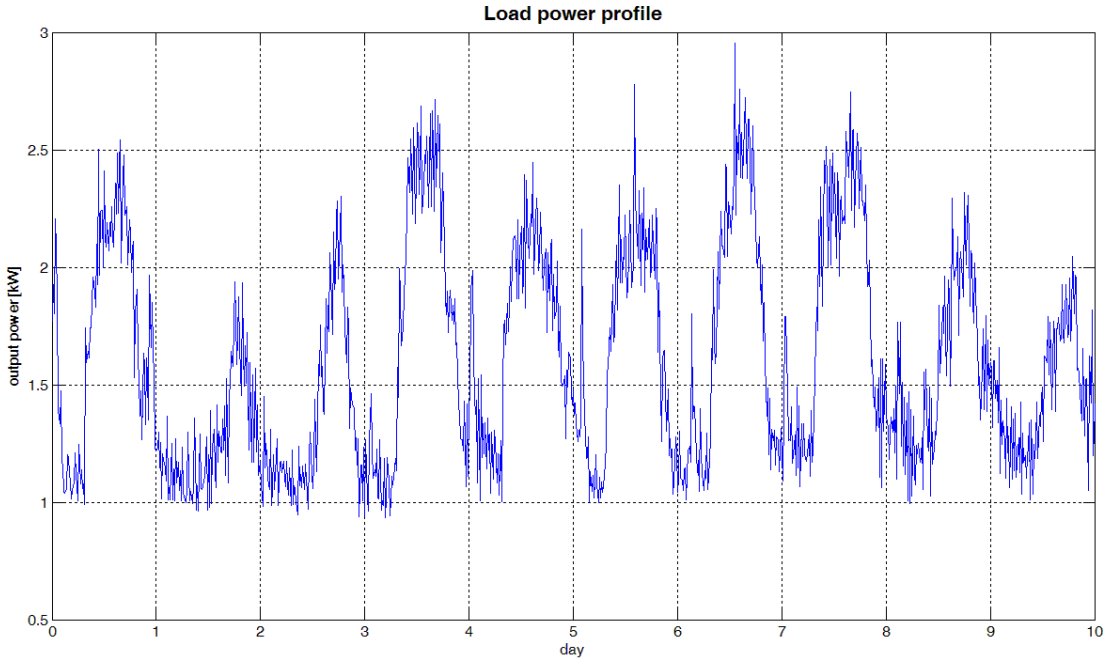

Figure A.28: Load power profile for: April 1st - 10th

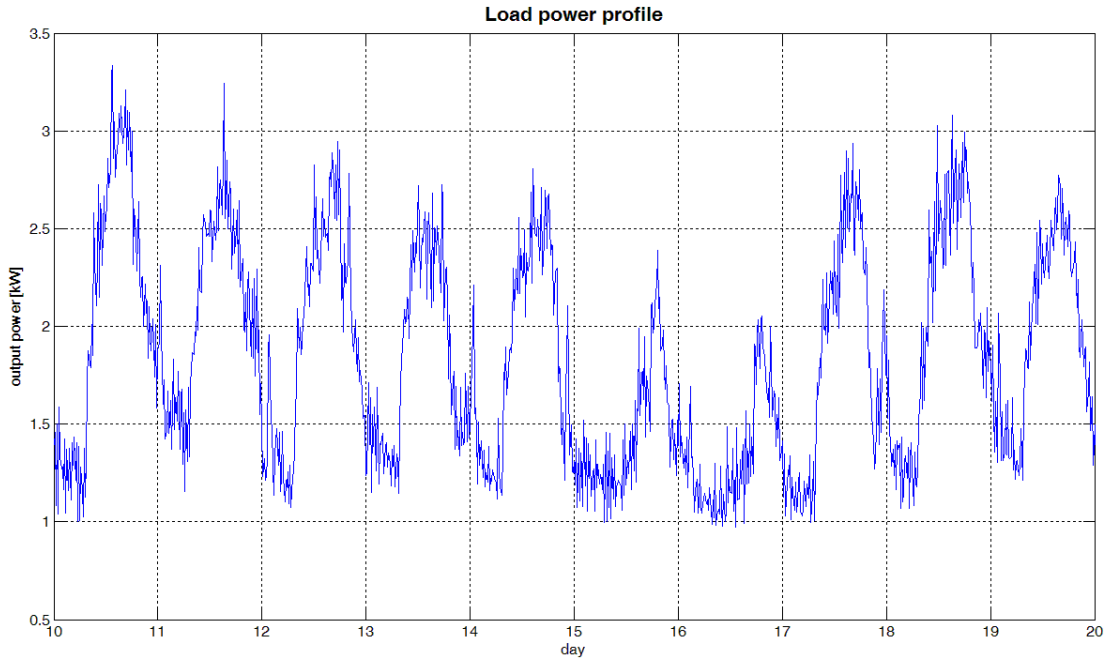

Figure A.29: Load power profile for: April 11th - 20th

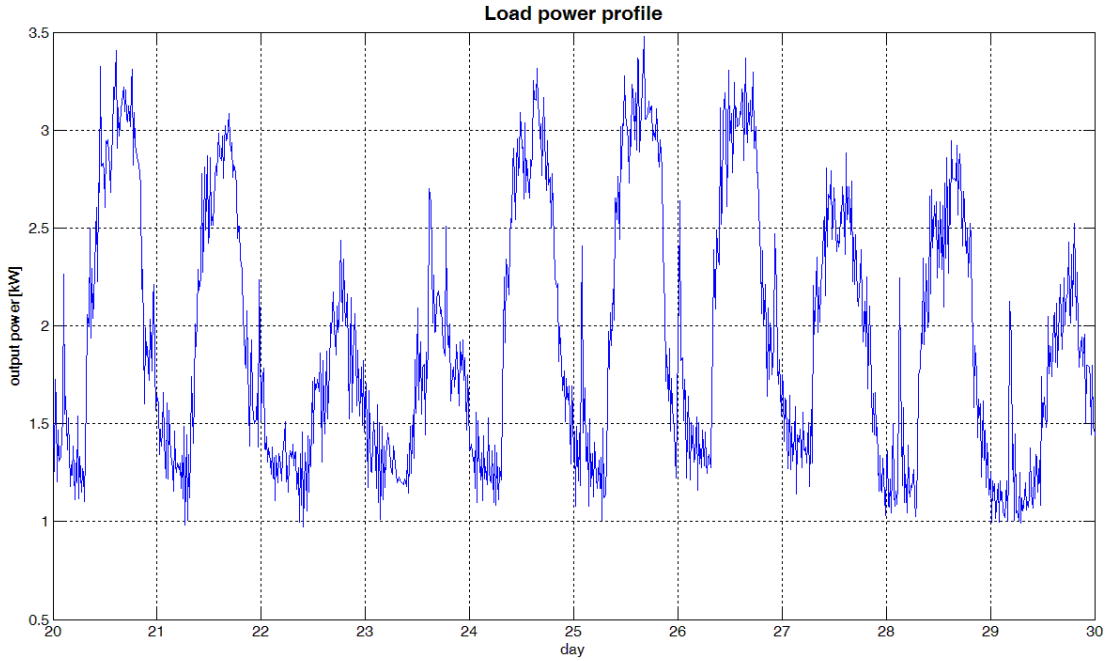

Figure A.30: Load power profile for: April 21st - 30th

- **May**

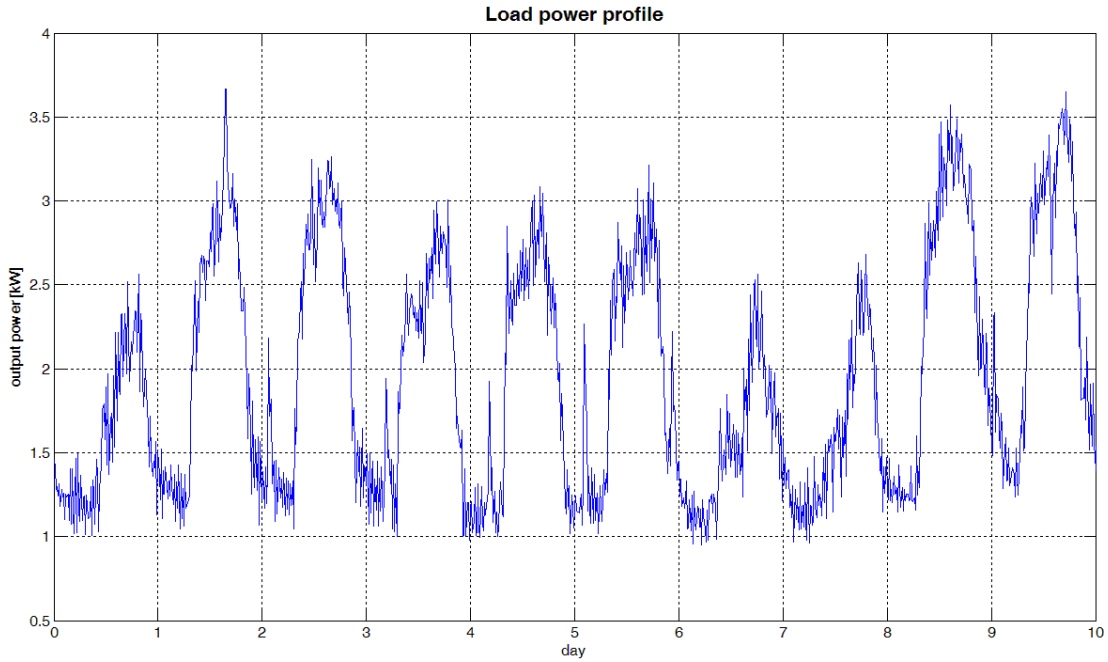

Figure A.31: Load power profile for: May 1st - 10th

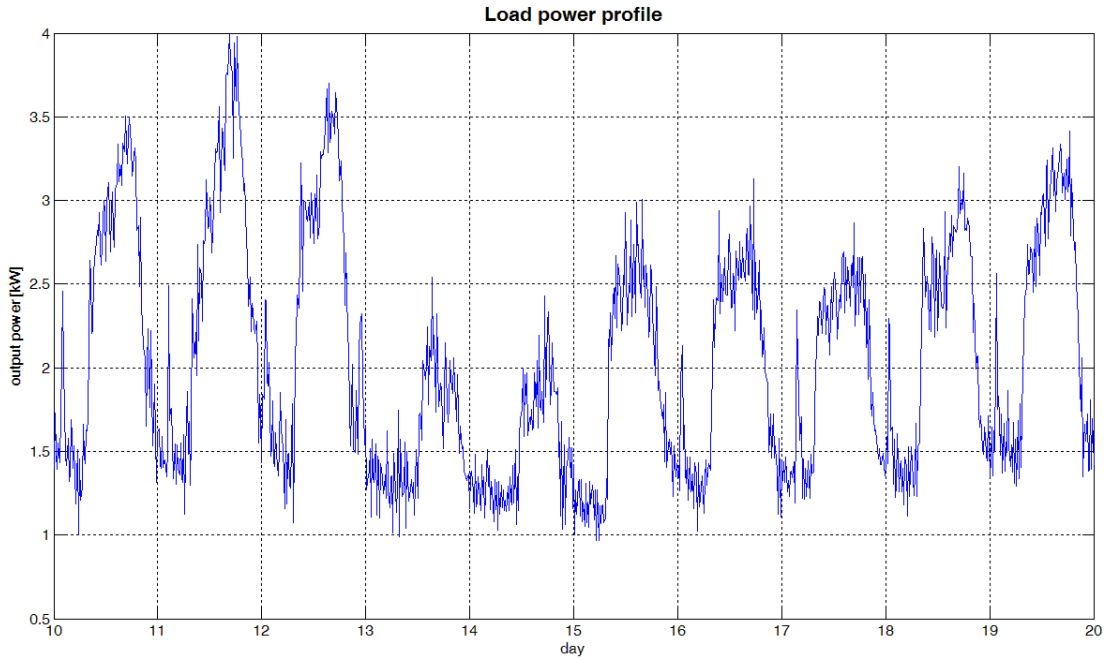

Figure A.32: Load power profile for: May 11th - 20th

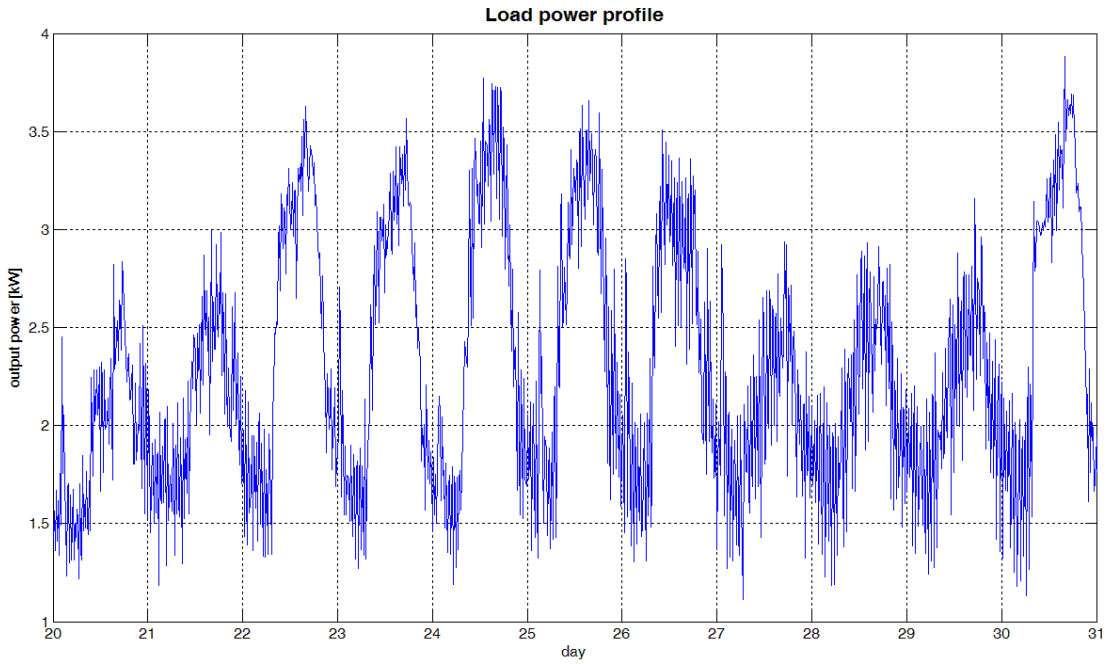

Figure A.33: Load power profile for: May 21st - 30th

- **June**

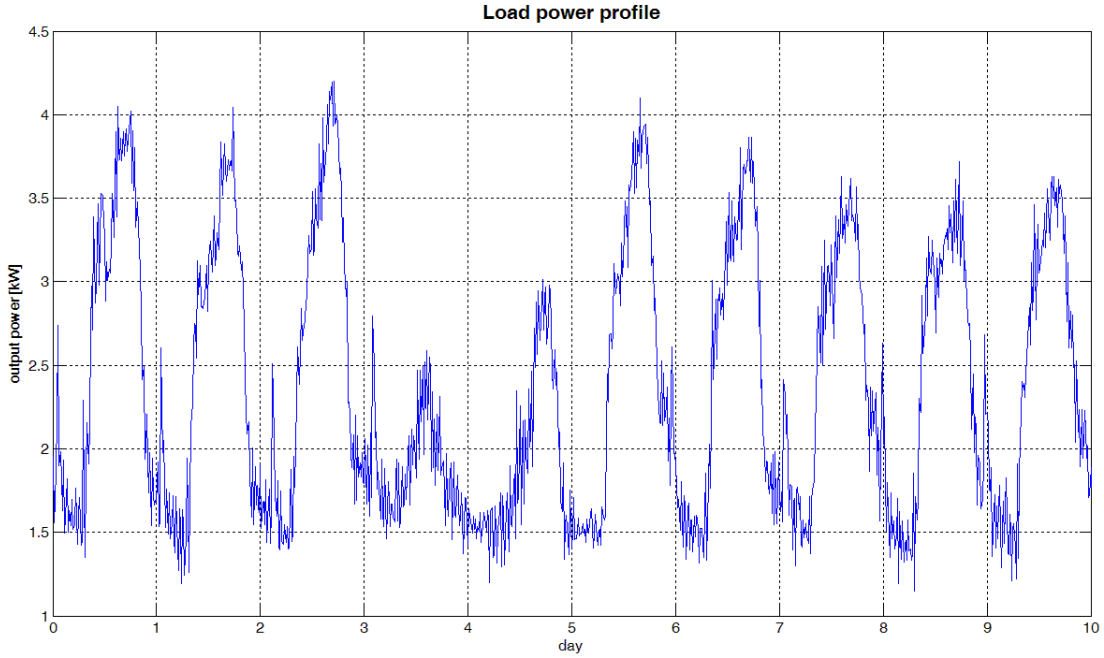

Figure A.34: Load power profile for: June 1st - 10th

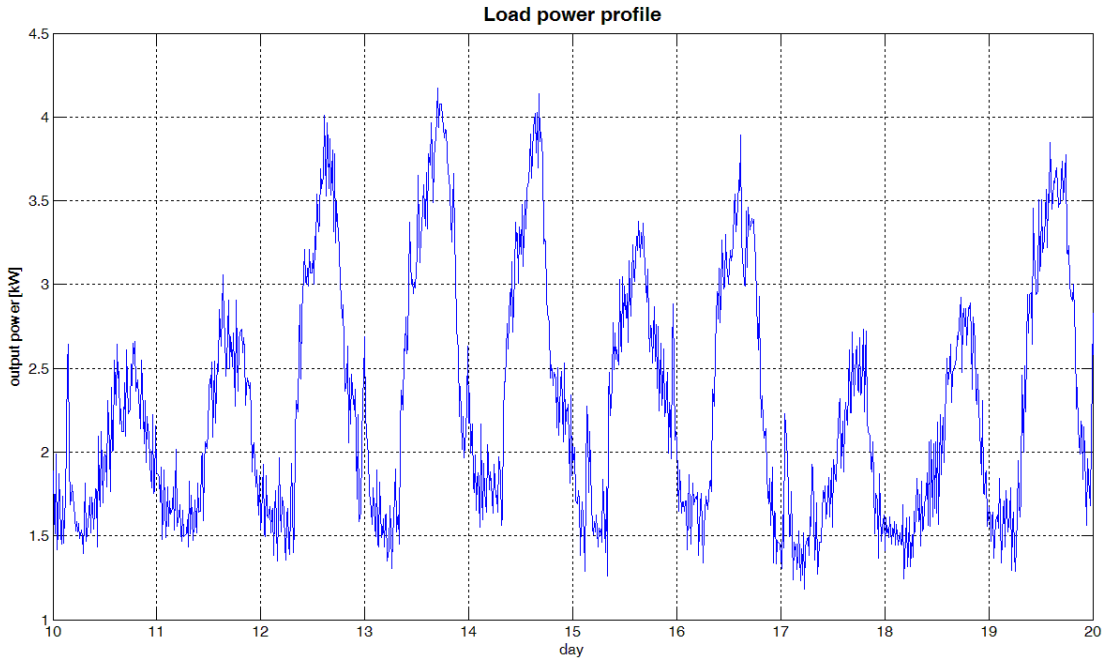

Figure A.35: Load power profile for: June 11th - 20th

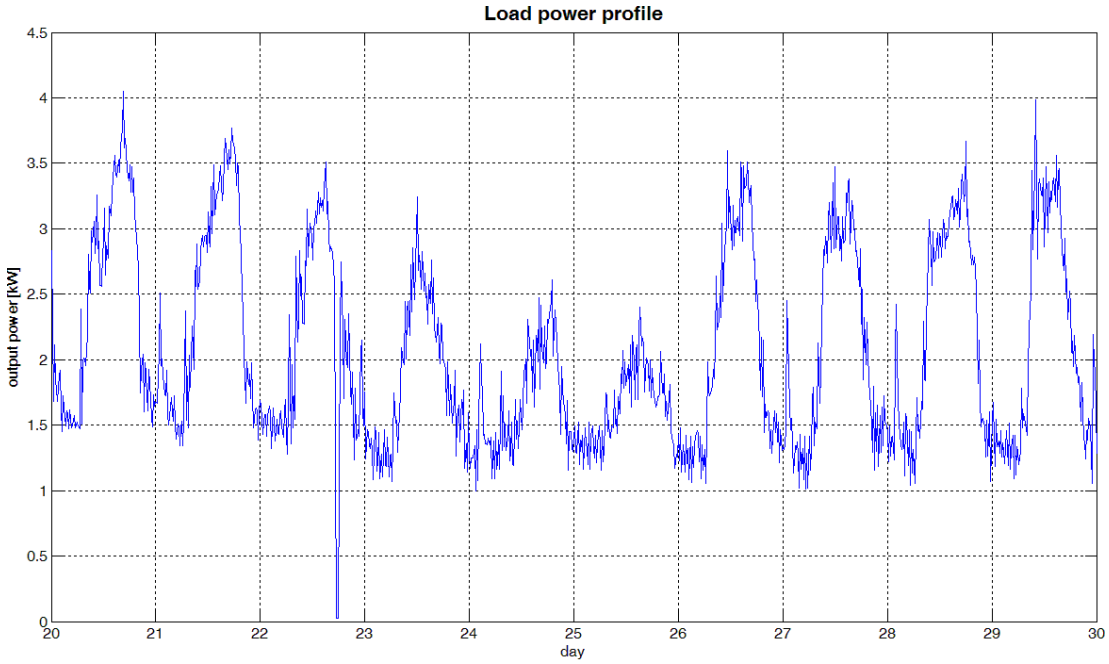

Figure A.36: Load power profile for: June 21st - 30th

A.3 Data sheet of the battery

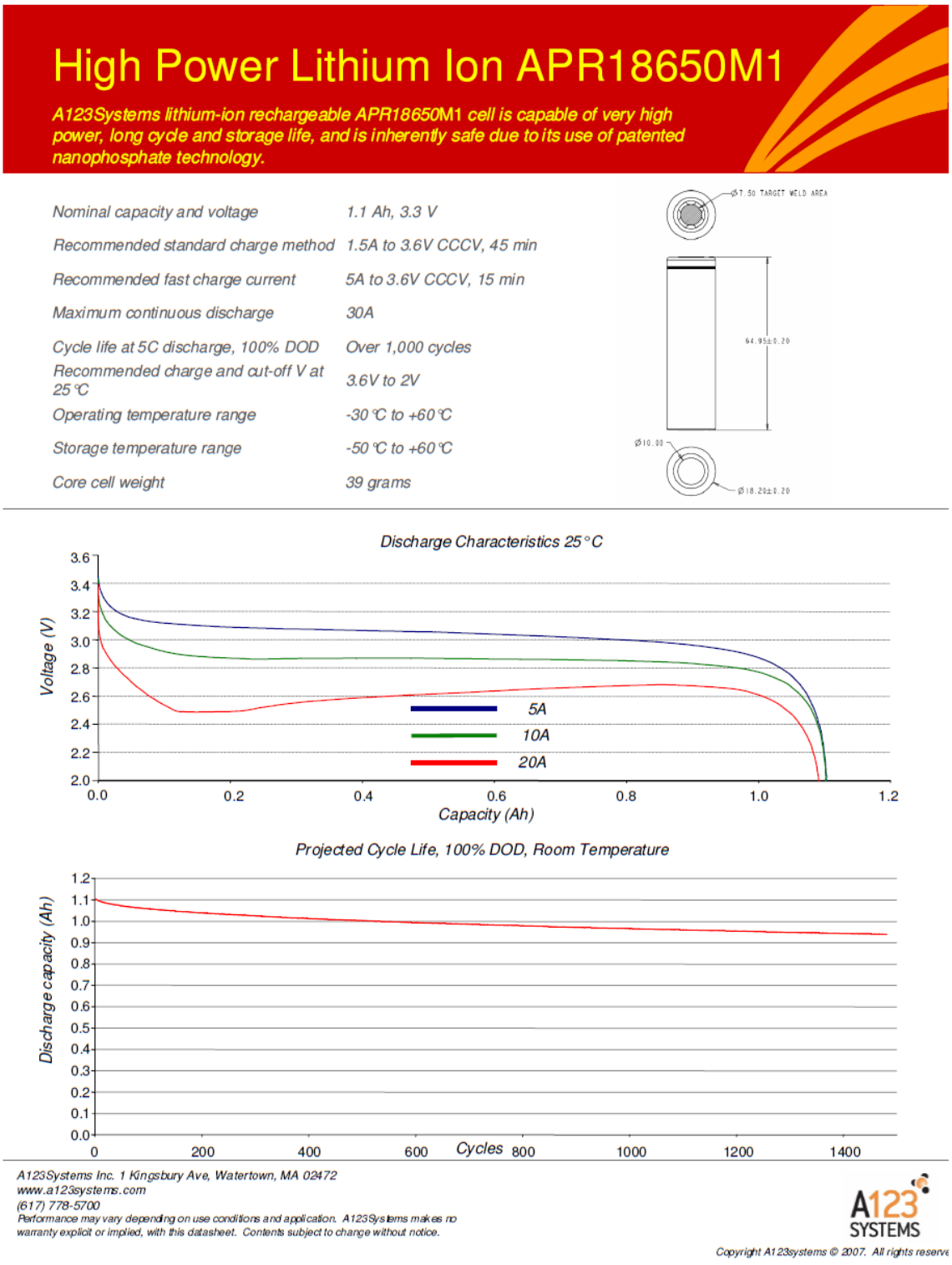

Figure A.37: Data sheet of the used LiFePO4 battery type APR18650 [30]

A.4 Data from the U.S. Annual Energy Review

Rank	Consumption	Trillion Btu	Consumption per Person	Million Btu	Expenditures [1]	Million Dollars [2]	Expenditures [1] per Person	Dollars [2]	Prices [1]	Dollars [2] per Million Btu
1	Texas	11,834.5	Alaska	1,062.3	Texas	140,651	Alaska	9,191	Hawaii	25.20
2	California	8,491.5	Wyoming	948.6	California	121,829	Wyoming	8,687	Connecticut	24.93
3	Florida	4,601.9	Louisiana	861.2	New York	63,642	Louisiana	7,688	District of Columbia	24.68
4	New York	4,064.3	North Dakota	671.1	Florida	60,747	North Dakota	6,442	Massachusetts	23.89
5	Ohio	4,048.9	Texas	496.3	Pennsylvania	49,301	Texas	5,899	New Hampshire	23.25
6	Illinois	4,043.2	Montana	483.1	Illinois	48,297	Montana	5,504	Vermont	22.90
7	Pennsylvania	4,006.2	Kentucky	477.5	Ohio	48,190	Maine	5,090	Rhode Island	22.72
8	Louisiana	3,766.2	West Virginia	469.9	New Jersey	39,609	Hawaii	4,833	New York	21.78
9	Georgia	3,133.0	Alabama	460.8	Michigan	36,882	Iowa	4,805	Maryland	21.60
10	Michigan	3,026.9	Indiana	458.4	Georgia	35,678	Kentucky	4,796	Florida	21.47
11	Indiana	2,904.0	Oklahoma	445.8	Louisiana	33,624	Oklahoma	4,719	Nevada	21.12
12	New Jersey	2,743.7	Mississippi	424.3	North Carolina	32,574	Alabama	4,670	Delaware	20.82
13	North Carolina	2,700.0	Iowa	414.0	Virginia	30,509	West Virginia	4,624	Arizona	20.72
14	Virginia	2,610.9	Kansas	409.1	Indiana	28,627	Kansas	4,610	California	20.12
15	Tennessee	2,330.5	Arkansas	406.1	Massachusetts	25,862	Mississippi	4,585	New Jersey	19.55
16	Alabama	2,132.0	Nebraska	391.6	Tennessee	25,462	New Jersey	4,577	Maine	19.17
17	Washington	2,067.2	South Carolina	384.2	Missouri	23,342	Indiana	4,518	North Carolina	19.17
18	Kentucky	2,023.0	Tennessee	379.0	Washington	23,224	South Dakota	4,506	New Mexico	19.05
19	Missouri	1,964.1	South Dakota	367.2	Wisconsin	22,455	Delaware	4,465	Pennsylvania	18.30
20	Minnesota	1,874.6	New Mexico	361.8	Minnesota	21,708	Nebraska	4,451	Oregon	18.23
21	Wisconsin	1,846.3	Minnesota	361.7	Alabama	21,606	Arkansas	4,428	Alaska	17.87
22	South Carolina	1,692.3	Idaho	354.0	Maryland	21,490	Connecticut	4,340	Wisconsin	17.84
23	Oklahoma	1,608.5	Ohio	352.8	Kentucky	20,316	Vermont	4,329	Missouri	17.73
24	Arizona	1,577.8	Delaware	350.4	Arizona	20,198	Ohio	4,199	Ohio	17.71
25	Massachusetts	1,514.6	Maine	346.3	South Carolina	18,130	Minnesota	4,189	Washington	17.63
26	Maryland	1,488.7	Virginia	339.1	Colorado	17,033	Tennessee	4,141	Texas	17.60
27	Colorado	1,479.3	Missouri	334.1	Oklahoma	17,027	Nevada	4,138	Virginia	17.58
28	Mississippi	1,239.5	Wisconsin	329.8	Connecticut	15,146	South Carolina	4,116	South Dakota	17.45
29	Iowa	1,235.2	Georgia	329.0	Iowa	14,334	District of Columbia	4,069	Michigan	17.37
30	Arkansas	1,149.3	Pennsylvania	322.6	Mississippi	13,392	New Hampshire	4,065	Illinois	17.27
31	Kansas	1,136.2	Washington	320.5	Oregon	13,175	Wisconsin	4,011	Montana	17.26
32	Oregon	1,108.2	District of Columbia	318.5	Kansas	12,803	New Mexico	4,010	Kansas	17.23
33	Connecticut	870.7	New Jersey	317.1	Arkansas	12,533	Massachusetts	3,998	Tennessee	17.19
34	West Virginia	850.5	Illinois	315.2	Nevada	10,571	Missouri	3,971	Mississippi	17.16
35	Utah	805.5	Colorado	305.5	Utah	8,739	Pennsylvania	3,969	Georgia	17.10
36	Nevada	777.4	Nevada	304.3	West Virginia	8,369	Virginia	3,963	South Carolina	17.04
37	Alaska	723.6	Utah	301.8	New Mexico	7,877	Maryland	3,825	Colorado	17.00
38	New Mexico	710.7	Michigan	301.2	Nebraska	7,877	Illinois	3,766	Minnesota	17.00
39	Nebraska	692.9	North Carolina	298.6	Maine	6,696	Georgia	3,746	Oklahoma	16.76
40	Idaho	529.6	Oregon	296.7	Alaska	6,260	Michigan	3,670	Nebraska	16.72
41	Wyoming	496.4	Hawaii	269.1	Hawaii	6,174	Idaho	3,621	Arkansas	16.66
42	Montana	462.1	Maryland	265.0	Idaho	5,418	North Carolina	3,603	Utah	16.44
43	Maine	455.6	Vermont	261.2	New Hampshire	5,335	Washington	3,601	Iowa	16.12
44	North Dakota	428.1	Florida	252.9	Montana	5,265	Oregon	3,527	Alabama	16.01
45	Hawaii	343.7	Connecticut	249.5	Wyoming	4,546	Colorado	3,517	Kentucky	15.99
46	New Hampshire	314.2	Arizona	248.3	North Dakota	4,110	Rhode Island	3,387	Idaho	15.92
47	Delaware	302.0	New Hampshire	239.5	Delaware	3,849	California	3,349	West Virginia	15.28
48	South Dakota	292.2	Massachusetts	234.2	South Dakota	3,585	Florida	3,338	Wyoming	14.81
49	Rhode Island	217.6	California	233.4	Rhode Island	3,567	New York	3,276	Indiana	14.41
50	District of Columbia	187.2	New York	209.2	Vermont	2,687	Utah	3,274	Louisiana	14.19
51	Vermont	162.1	Rhode Island	206.6	District of Columbia	2,392	Arizona	3,179	North Dakota	13.22
	United States	[3,4]101,468.0	**United States**	336.8	**United States**	[5]1,233,058	**United States**	[6]4,093	**United States**	18.23

[1] Prices and expenditures include taxes where data are available.
[2] Prices are not adjusted for inflation. See "Nominal Dollars" in Glossary.
[3] Includes 25.2 trillion Btu of coal coke net imports and 378.0 trillion Btu of energy losses and co-products from the production of fuel ethanol that are not allocated to the States.
[4] The U.S. consumption value in this table does not match those in Tables 1.1 and 1.3 because it: 1) does not include biodiesel; 2) does not incorporate the latest data revisions; and 3) is the sum of State values, which use State average heat contents to convert physical units of coal and natural gas to Btu.
[5] Includes $347 million for coal coke net imports, which are not allocated to the States.
[6] Based on population data prior to revisions shown on Table D1.
Note: Rankings based on unrounded data.
Web Page: For related information, see http://www.eia.gov/emeu/states/_seds.html.
Sources: **Consumption:** U.S. Energy Information Administration (EIA), "State Energy Data 2007: Consumption" (August 2009), Tables R1 and R2. **Expenditures and Prices:** EIA, "State Energy Data 2007: Prices and Expenditures" (August 2009), Table R1. "State Energy Data 2007" includes State-level data by end-use sector and type of energy. Consumption estimates are annual 1960 through 2007, and price and expenditure estimates are annual 1970 through 2007.

Table A.1: State-Level Energy Consumption, Expenditures, and Prices, 2007 [1]